ISBN 0-7743-7584-1
0-7743-7589-2

MODELS FOR LONG-RANGE AND MESOSCALE TRANSPORT AND DEPOSITION OF ATMOSPHERIC POLLUTANTS

PHASE I: MODELING SYSTEM DESIGN

VOLUME III

August 1982

ARB-39-82-AQM

Prepared for

ONTARIO MINISTRY OF THE ENVIRONMENT
AIR RESOURCES BRANCH
880 Bay Street, 4th Floor
Toronto, Ontario M5S 1Z8 Canada

Prepared by

Environmental Research &
Technology, Inc.
696 Virginia Road
Concord, MA 01742, USA

Meteorological and Environmental
Planning Limited
850 Magnetic Drive
Downsview, Ontario
M3J 2C4, Canada

DISCLAIMER

This report was prepared by consultants under contract to the Air Resources Branch, Ontario Ministry of the Environment. The views and findings expressed herein and the quality and accuracy of the text are the sole responsibilities of the contractor. Opinions and recommendations expressed are those of the contractor and should not be construed to represent policy of the Ministry of the Environment or the Government of Ontario. Mention of specific brand or trade names does not constitute an endorsement by the Government of Ontario.

Table of Contents

LIST OF TABLES

LIST OF FIGURES

LIST OF FIGURES (continued

INTRODUCTION

The MOE Long Range Transport and Mesoscale Model Design components carried out by MEP included the overall Model Operating System and the Wind Field Model. This report presents the design framework for these components, and provides details for the principal procedures and system programs which will need to be developed and implemented on the MOE computer.

Section 1 details the Model Operating System and the data base structure. Anticipated data requirements are discussed, and data analysis and gridding procedures defined.

Section 2 presents the results of a review of current wind field procedures used for long-range transport modeling.

Section 3 details the approach adopted for the Wind Field Model and the procedures which will be required for an operational Wind Field Model.

1. MODEL OPERATING SYSTEM

The development and operation of the proposed long-range and mesoscale transport models will require the capability of assembling and maintaining a large number of diverse data sets which are required for driving the models, as well as maintaining control over the large number of model output files generated in the modeling process.

In order to provide the required facilities in a form which would allow a non-specialist user to carry out routine modeling, a comprehensive operating system has been designed. The system will provide a controlled user environment which will allow the user to:

- archive all pertinent data sets and retrieve selected data as required
- produce gridded fields for model input
- set-up and monitor a model run
- analyze and display model output results
- assemble and maintain the various models which form part of the system

The objective of this section is to outline the proposed system structure and facilities and discuss the implementation requirements. In addition to the system level detail, some of the data gridding functions are described at the procedure level in Section 1.5 . The wind field model is described in depth in Sections 2 and 3 .

1.1 Scope of System

The Model Operating Environment is configured as a system which allows the non-specialist user to define his modeling requirements interactively and provides the environment for assembling the necessary model input data, initiating and monitoring the model run, and analyzing and displaying the model results. The implementation of this system will provide a number of advantages:

a) the data management components of the system facilitate the archiving and data preparation functions for the large amount of data of various types required in long-range transport models,

b) the system facilities for labelling, archiving, and retrieving results out of model runs can save a great deal of time, as well as eliminating data losses which necessitate costly reruns,

c) the data management and supervisory facilities allow for efficient set-up and execution of model runs with minimum involvement by scientific and modeling staff,

d) the system is ideal for the developmental stage of advanced models, since it provides the facilities necessary to test modifications in an efficient and systematic fashion.

The system structure is fully modular, allowing direct updating of modeling capabilities in the future, as new information warrants replacement of existing model components. This ensures that the overall model system with all sub-systems can be preserved through all modifications, and that future models can be accommodated within the existing system.

In order to accomplish the modularity and interchangeability objectives, the system incorporates standardized procedures and modules wherever practical. Similarly, an integrated nomenclature for procedures and data files is adopted to facilitate integration of the system, as well as future modifications to the system.

The interactive specification of modeling and data requirements is integral to the system, and allows the system to pace the user through the model run process. This necessitates a computer facility which allows for interactive access, at least for part of the model operation. It is, however, possible to set-up the system so that the model run is carried out on a batch system on a large machine, with the rest of the system being resident on a different machine with an interactive operating system.

A functional description of the system is provided by Figure 1.1 . In order to improve system efficiency, the overall system is composed of six integral components:

MOE - MAINSYS - maintains control of the system and provides a controlled user environment

SUBSYS1 - performs all archiving functions for model input and output data

SUBSYS2 - generates interpolated, gridded fields of emissions, physical data and meteorological fields

SYBSYS3 - assembles model input files and initiates and monitors model runs

SUBSYS4 - provides facilities for the analysis and display of model results

SUBSYS5 - provides facilities for assembling models from stored module components, and for maintaining an archive of such models.

MAIN SYSTEM COMPONENTS OF MOE (MODEL OPERATING ENVIRONMENT)

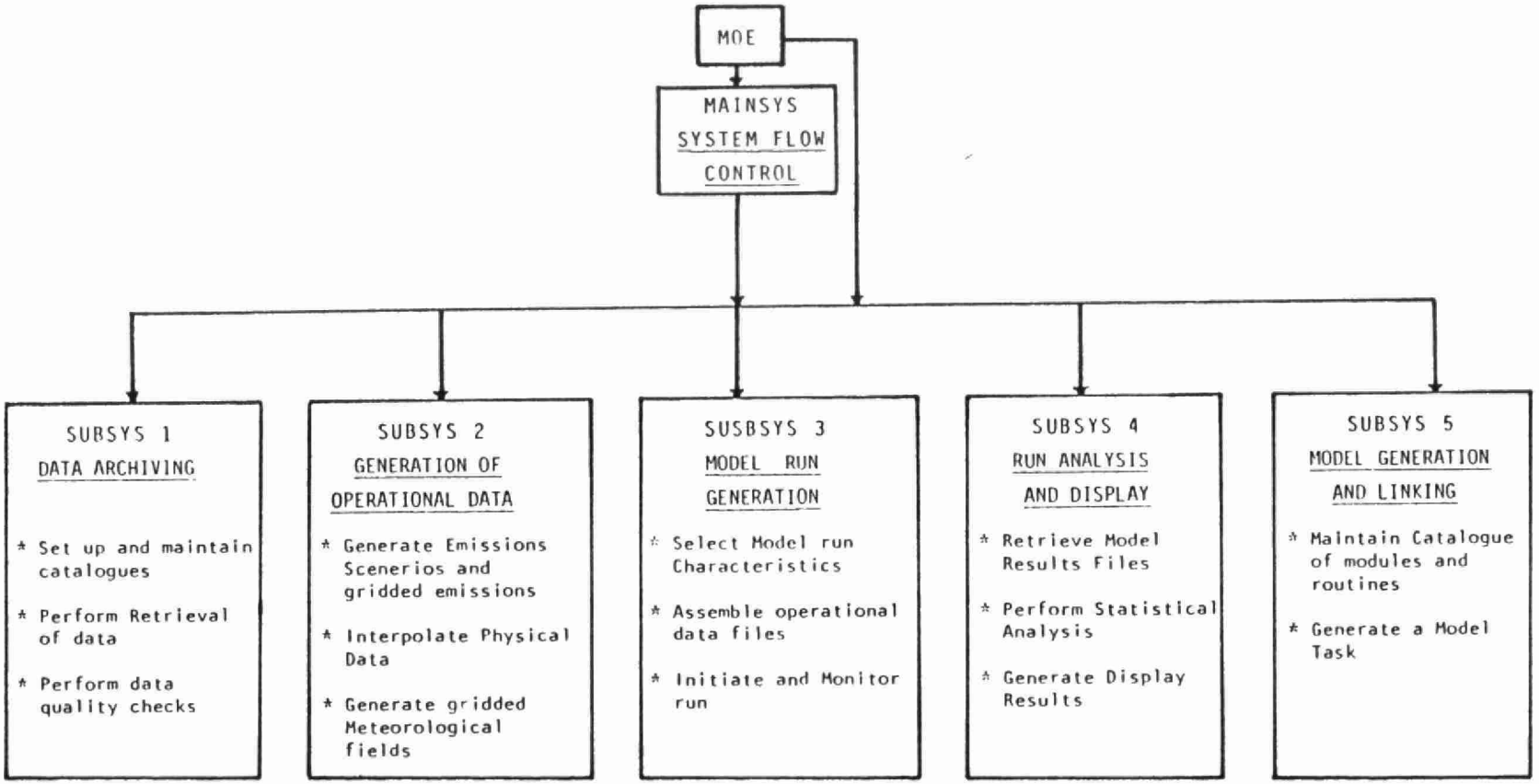

Figure 1.1 Functional System Description

Each subsystem is an interactive system which provides a controlled user environment for performing the specific function. Control is relinquished by MAINSYS to each subsystem, with the control reverting to MAINSYS following completion of the task.

The design approach has been to assume that the computer storage resources are limited. As far as possible, the online storage requirements are minimized, by providing an efficient data cataloguing and retrieval system. In a typical model run situation, only the essential operational data files are brought on-line for the intended procedure. As the procedure is completed, result files are either used in a subsequently initiated procedure or backed-up to tape for subsequent processing. The backing up process involves a cataloguing step, with most of the catalogue information supplied by the generating procedure automatically.

Provision has also been made in the system design to allow several users to carry out simultaneous operations. This allows non-interfering operations such as archiving, model running, model results display and analysis to be carried out on the system in parallel, resulting in greater flexibility and efficiency. This capability is made possible through the subsystem approach, and the segregation of files for the various subsystems.

Although the system provides a menu-driven and paced environment for the standard operations, it also provides override capabilities which allow access at will to all parts of the system. This provision is necessary for system maintenance operations, and will normally be used by the system supervisor to modify or update modules, or to incorporate new modules for new models or enhanced system capabilities.

1.2 System Components

The following sections detail each of the major subsystems and their interlinking facilities.

1.2.1 System Flow Control (MOE-MAINSYS)

System entry is through the interactive procedure MOE (Model Operating Environment) which serves to apprise the user of system status and to activate the appropriate subsystem as required for the user intended operation. (Figure 1.2)

MOE invokes the procedure DSTAT which displays on the terminal the current status of the system. This is accomplished by reading from the disk resident file SYSTAT which is automatically updated by the various subsystems as they are invoked or terminated. The status information consists of the following:

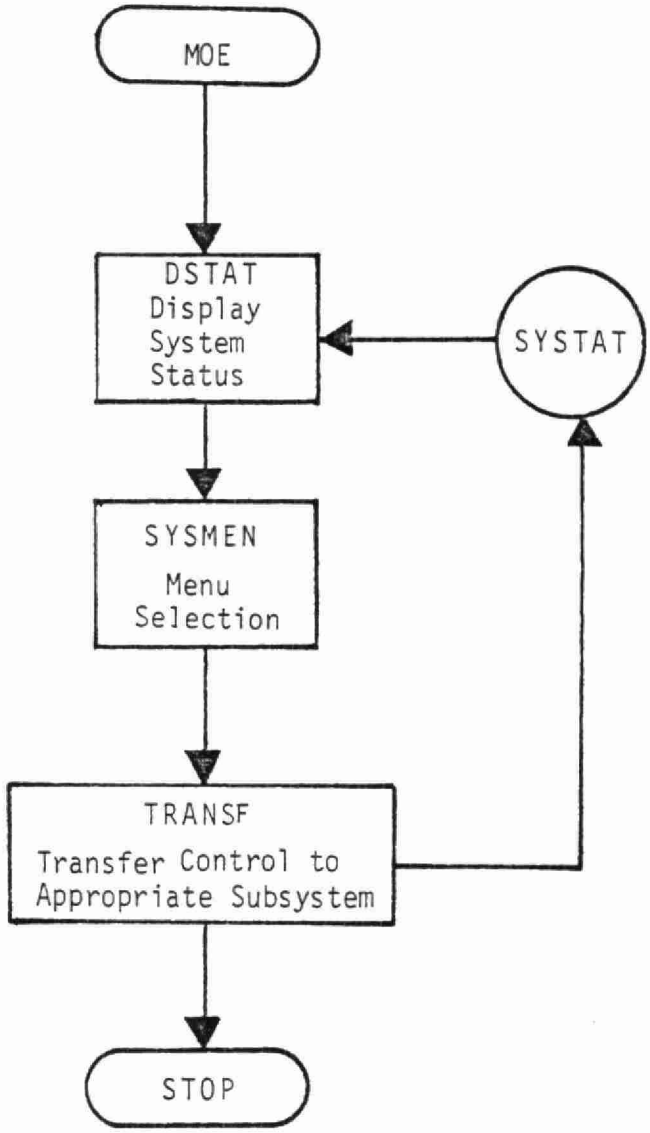
MOE
DSTAT
Display
System
Status
SYSTAT
SYSMEN
Menu
Selection
TRANSF
Transfer Control to
Appropriate Subsystem
STOP

Figure 1.2

File: SYSTAT

Attributes: Direct Access, Shared Use

Contents:

1. Number of Users - users active on the system at present
2. Subsystems in Use - list of subsystems in current use (encoded bit information reset each time the status changes)
3. Latest Model Run number - identifying model run number encoded by MAINSYS (CRUN)
4. Date and Time - start date and time of latest model run number

On the basis of the displayed system status, the user is given the option of proceeding into one of the available subsystems, or of exiting by terminating the session. The SYSTAT file is updated with information on the selected subsystem and transfer is made into the appropriate subsystem.

At this point MOE exits and is available to another user.

If the user intends to carry out a model run or initiate new model information, he must enter the system through MAINSYS . For other

operations, the appropriate subsystem may be entered directly.

MAINSYS provides the controlled environment for carrying out model runs (Figure 1.3) . This is accomplished through the MODSTAT (model run status) file and a number of procedures for updating the file. The file attributes include the following:

File: MODSTAT

Attributes: Direct Access, Shared Use

Contents:

1. Current model run number - sequentially assigned identifier used for monitoring and labelling

2. Model run start date and time

3. Procedures run previously - ordered list of procedures carried out under the current number

4. Model used - identifying number for model type and version number

The procedure MSTAT is invoked by MAINSYS to generate the model status information, through one of three possible channels:

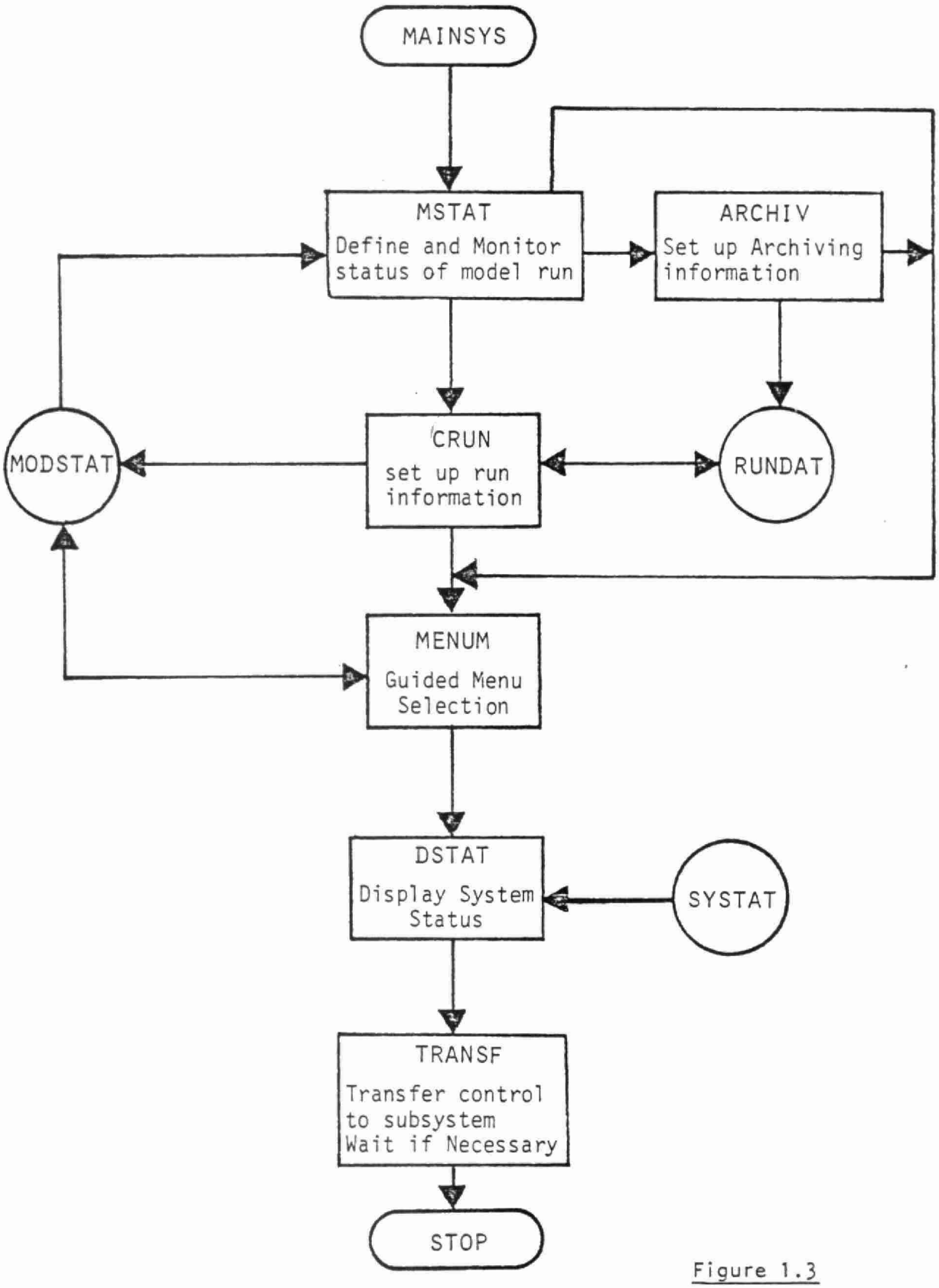
MAINSYS
MSTAT
Define and Monitor status of model run
ARCHIV
Set up Archiving information
MODSTAT
CRUN
set up run information
RUNDAT
MENUM
Guided Menu Selection
DSTAT
Display System Status
SYSTAT
TRANSF
Transfer control to subsystem Wait if Necessary
STOP

Figure 1.3

1. A new run is being initiated: in this case the procedure CRUN is invoked to generate all the necessary information to code the run files. A new entry is made into the file RUNDAT which maintains in consecutive records the full information to all previous runs, and the MODSTAT file is initiated. Control is then transferred to MENUM which provides a guided menu selection process.

2. A continuation of on-going model run: this is signalled by MAINSYS, which would be initiated from another sub-system. In this case control is transferred to MENUM directly. Appropriate update information is written to MODSTAT .

3. A previously uncompleted model run is to be continued: in this case the user must supply the required run number. CRUN retrieves the model run information from RUNDAT file and recreates the MODSTAT file. Control is then transferred to MENUM .

The procedure MENUM determines current model run status from MODSTAT and provides the user with alternative options for the next step. After testing system status, control is transferred to the appropriate subsystem and MAINSYS exits. Control from the subsystem reverts to MAINSYS upon completion. When the full run has been completed, an entry is made to RUNDAT by ARCHIV and MAINSYS exits.

1.2.2 Data Archiving (SUBSYS1)

SUBSYS1 is a menu-driven cataloguing, archiving and data retrieval system. Primary control is through the procedure MENUS1 which allows the user to perform the following functions (Figure 1.4):

1) Catalogue Primary Data Sets (CP)
2) Catalogue Derived Data Files (CD1)
3) Catalogue Gridded Fields (CD2)
4) Catalogue Operational Data Files (CM)
5) Extract Primary Data (EXTP)
6) Store Working Files on Tape (STOR)
7) Retrieve Stored Data from Tape (RESTOR)

In order to permit multiple users on the system, and to control the operating environment, all control information is passed between

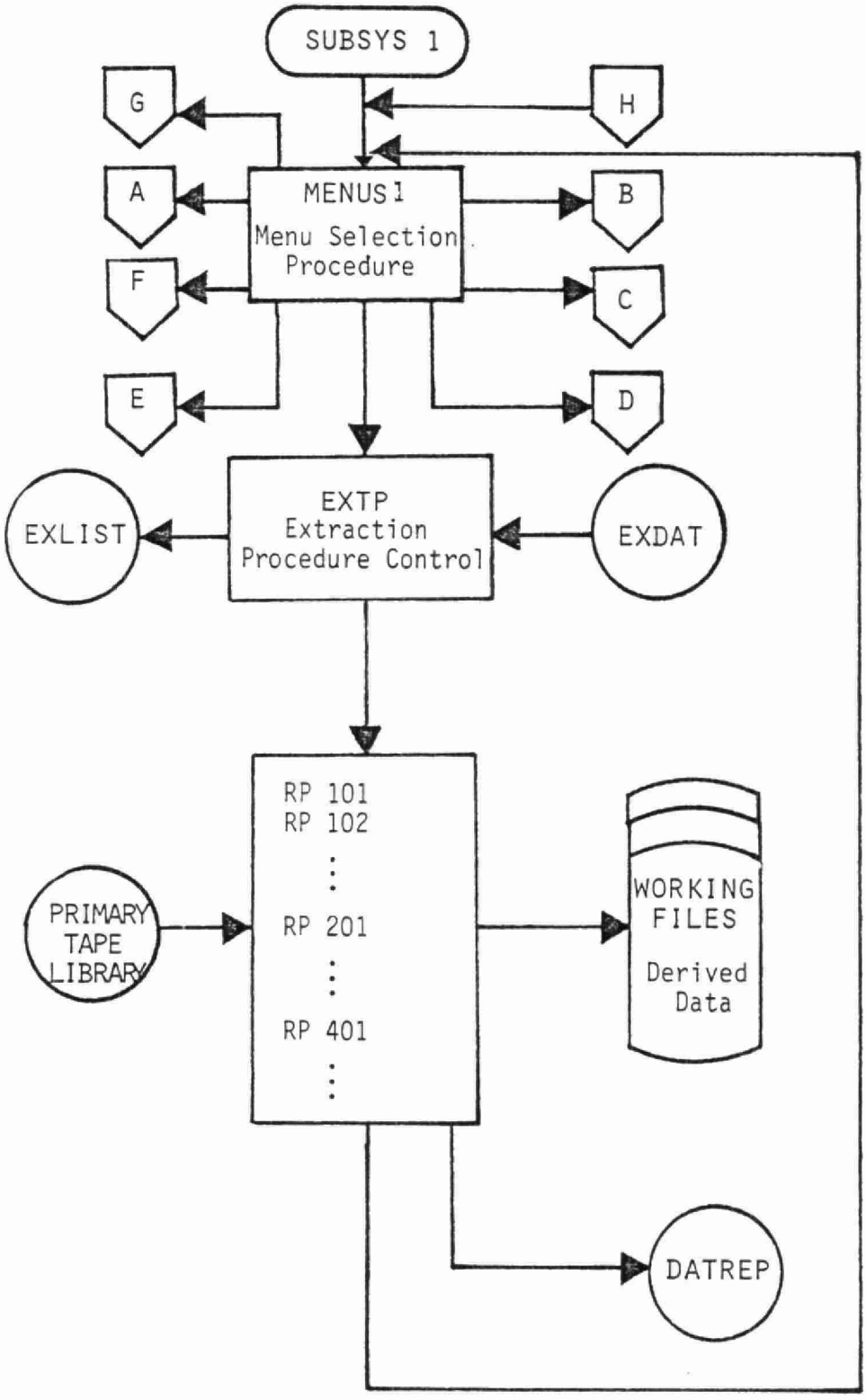
SUBSYS 1
G
H
A
MENUS1
Menu Selection
Procedure
B
F
C
E
D
EXLIST
EXTP
Extraction
Procedure Control
EXDAT
RP 101
RP 102
RP 201
RP 401
PRIMARY
TAPE
LIBRARY
WORKING
FILES
Derived
Data
DATREP

Figure 1.4

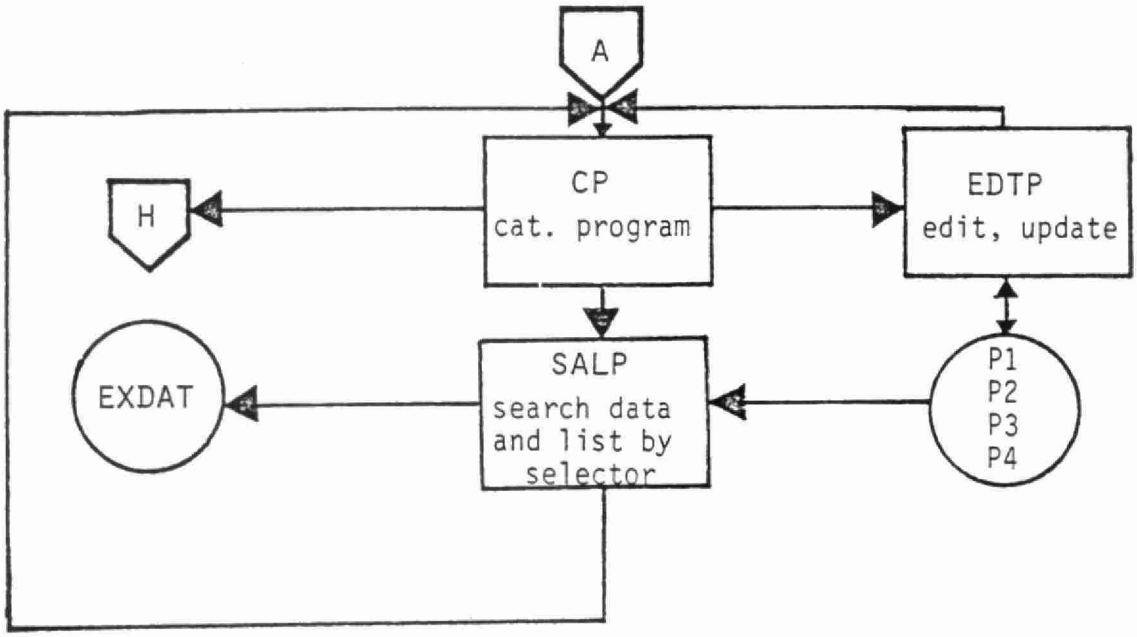

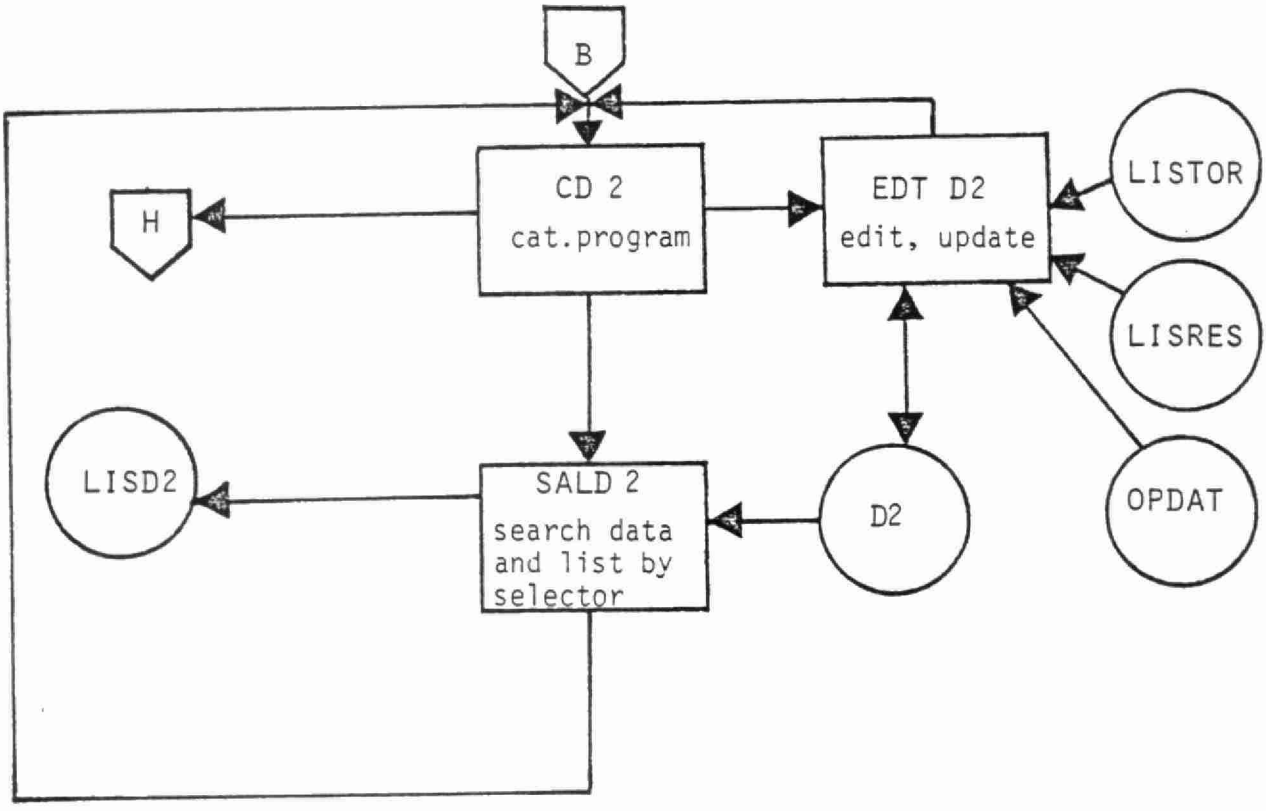

Figure 1.4 Cont'd.

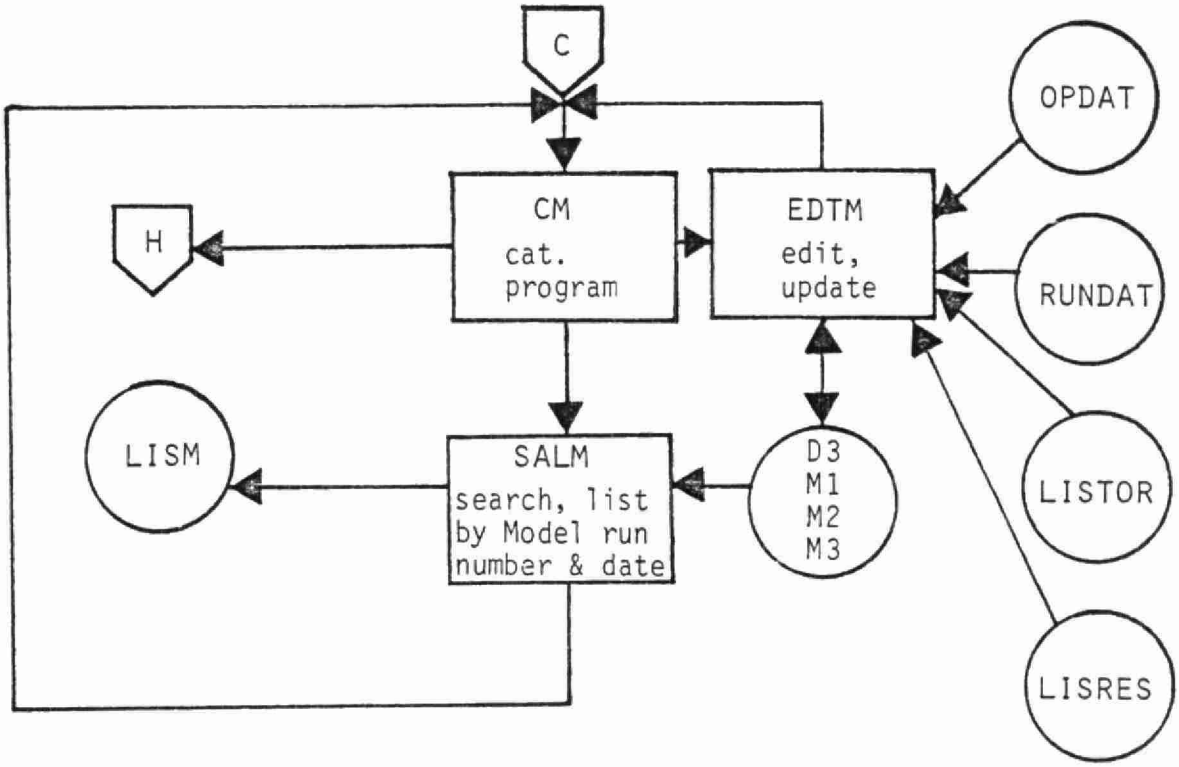

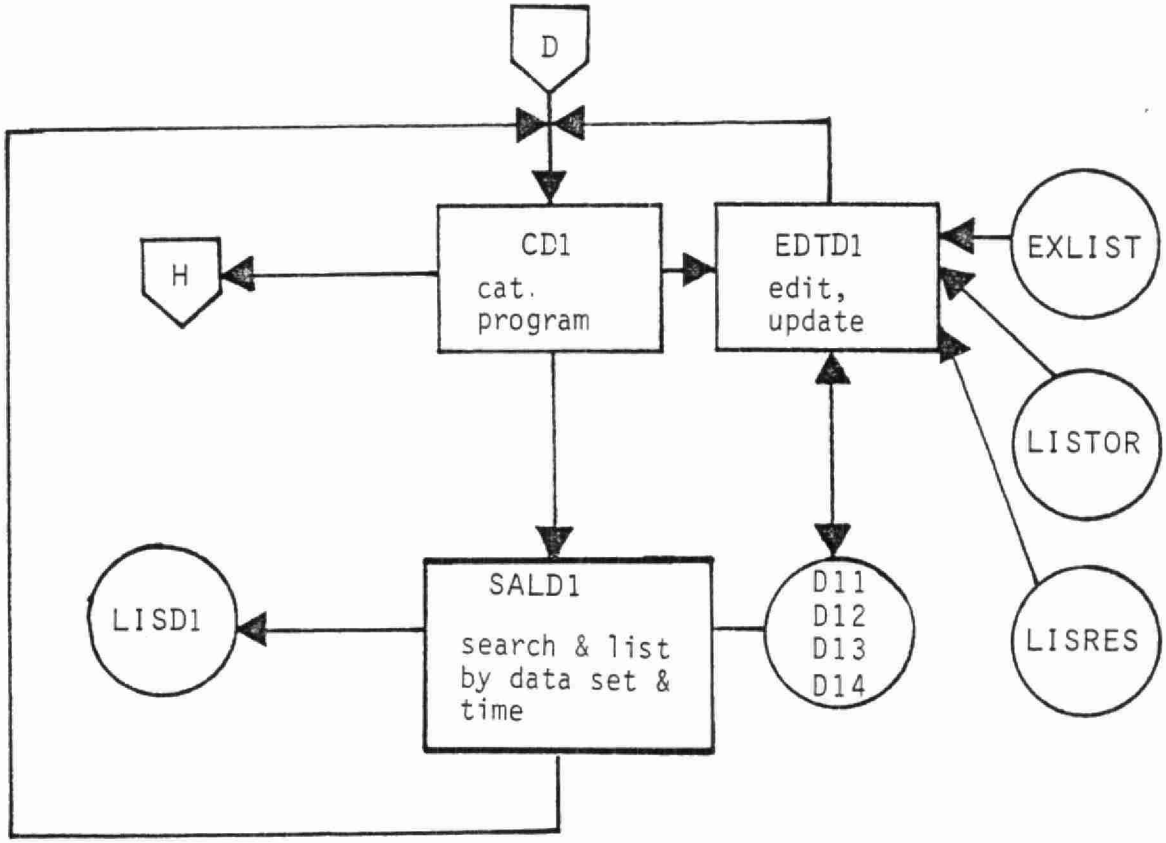

Figure 1.4 cont'd.

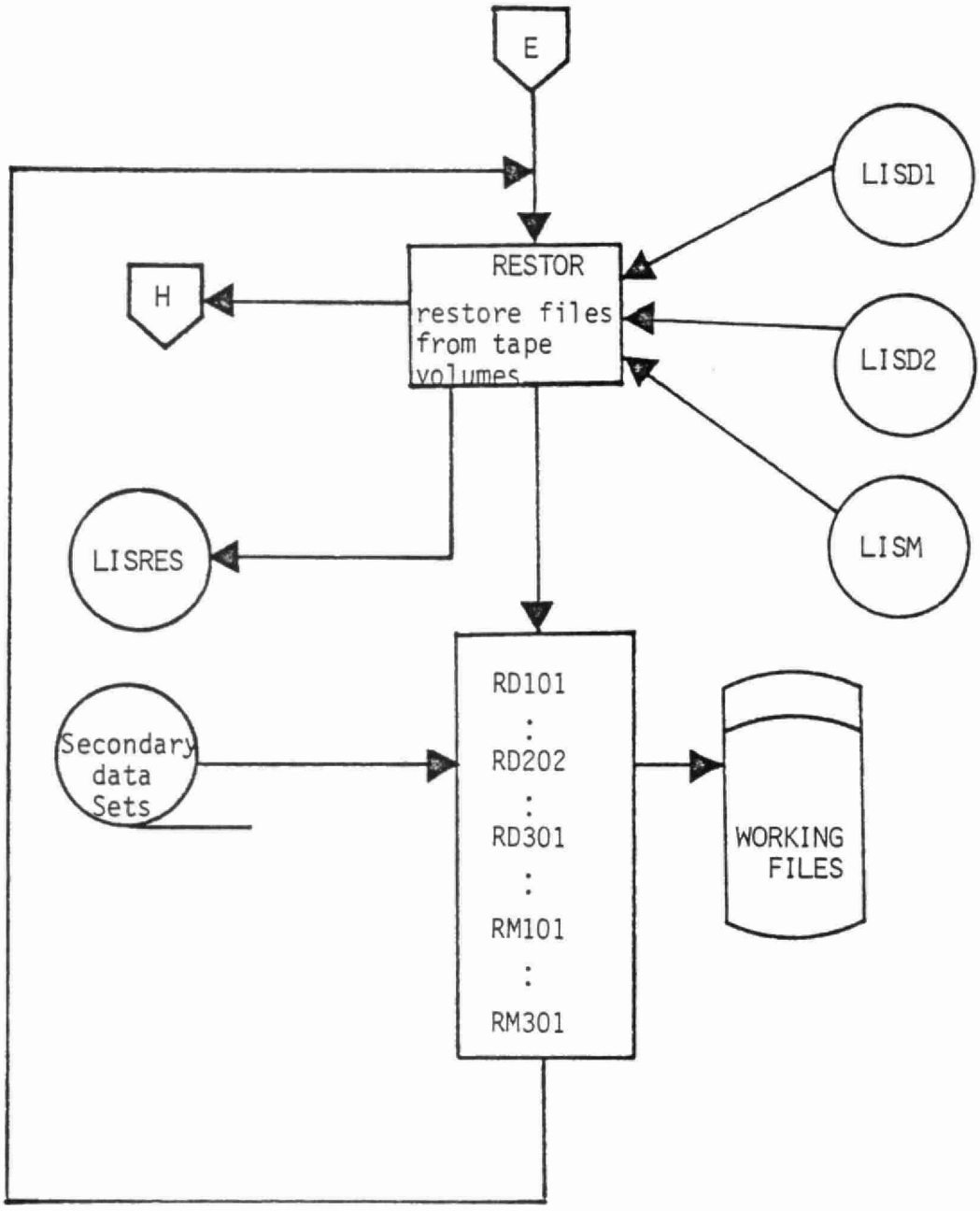

Figure 1.4 cont'd.

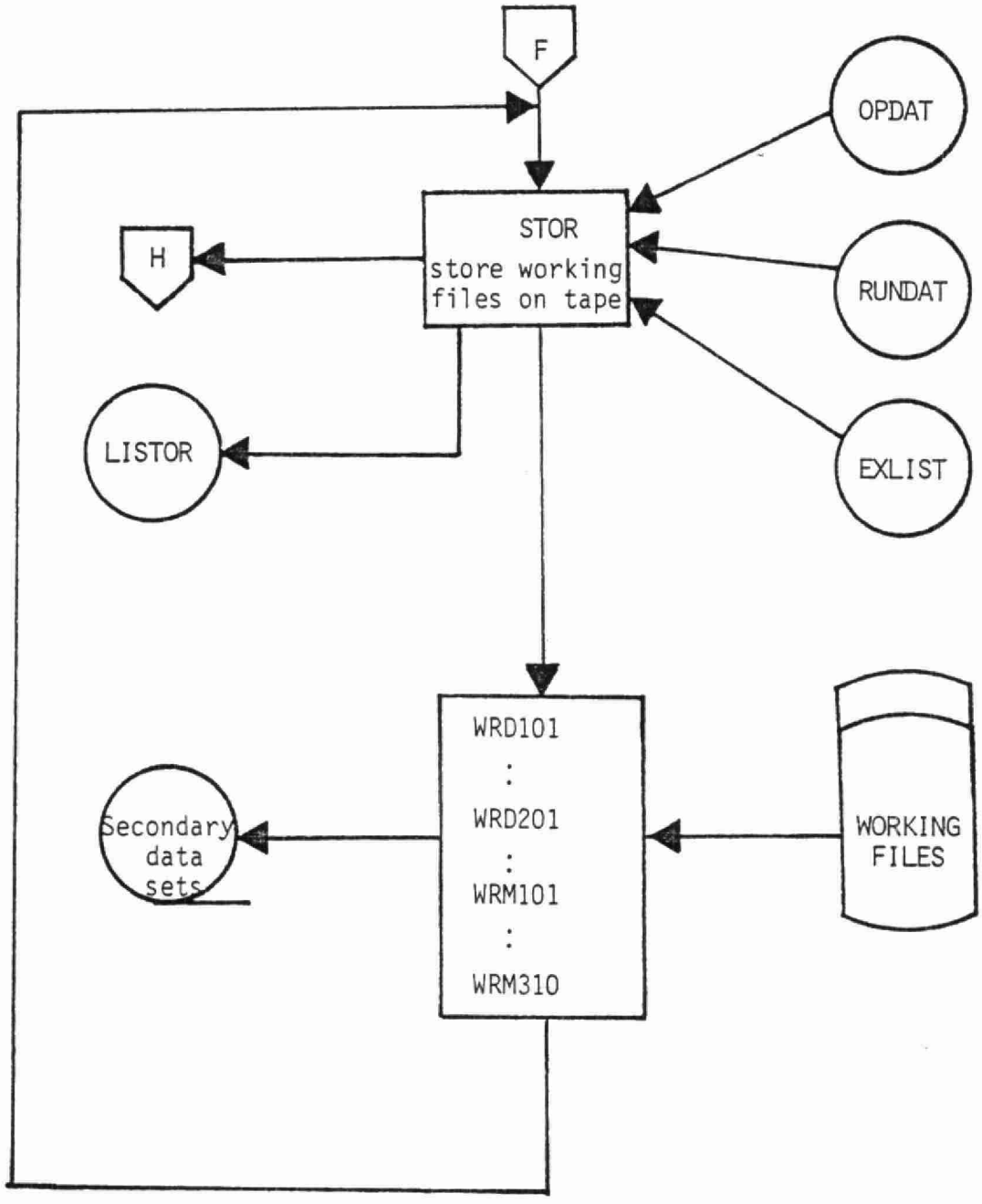

Figure 1.4 cont'd.

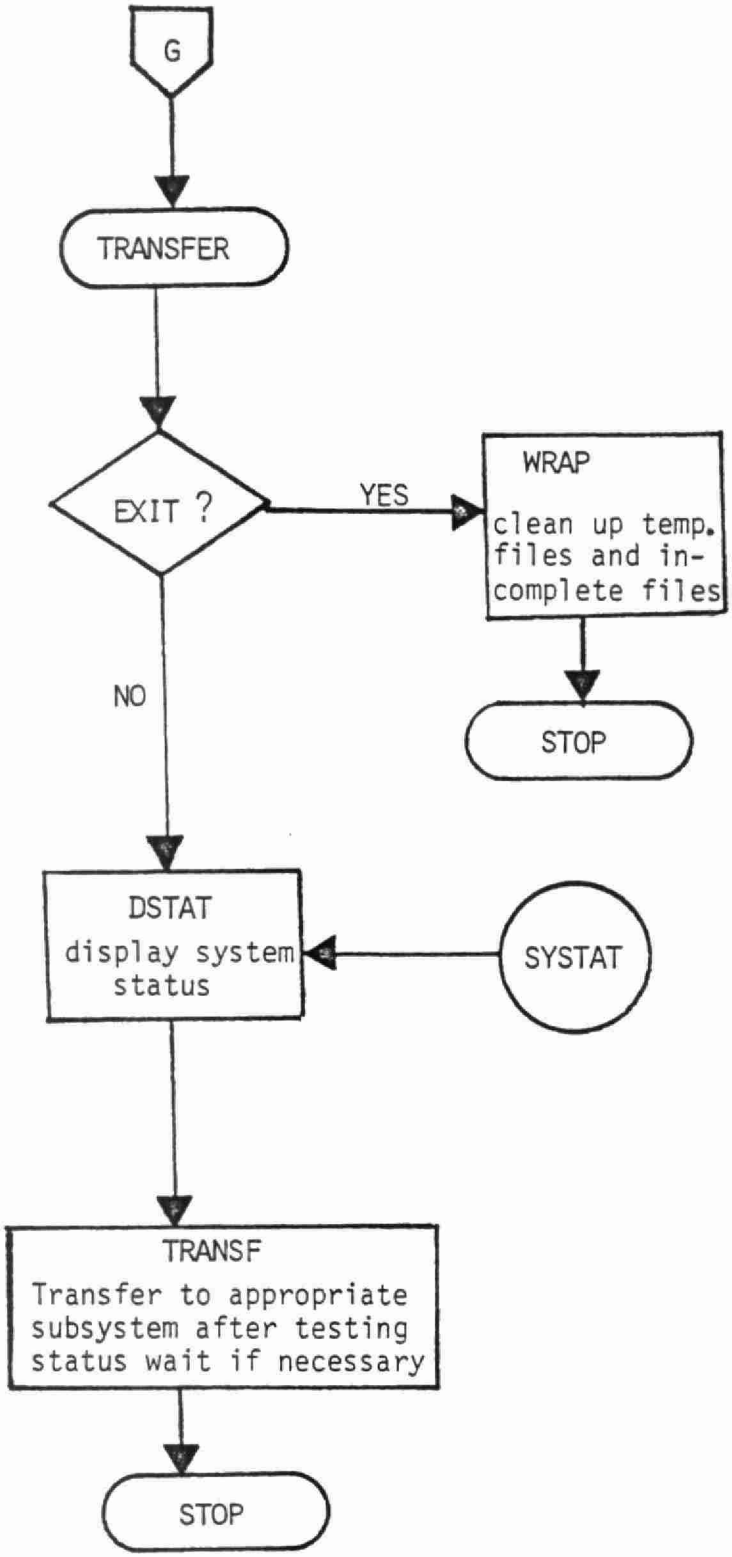

Figure 1.4 cont'd.

programs by means of status and intermediate files, rather than by internally stored data. Each of the above functions is a separate procedure (or linked sequence of procedures) as detailed in Figure 1.4 . The following sections describe the principal features of the component functions.

1. Catalogue Primary Data Sets (CP)

   This cataloguing procedure consists of four catalogues, as well as editing/updating and search functions. The four catalogues contain information on the primary data sets maintained in the model operator tape library:

   P1 - Primary Emissions Data

   P2 - Primary Physical Data

   P3 - Air Quality and Precipitation Chemistry Data

   P4 - Meteorological Data

   The catalogues are maintained on-line, and can be searched by SALP and edited by EDTP . Table 1.1 shows the contents of each record in the catalogue files. Where possible, standardized nomenclature and procedures are incorporated. Thus, a coded list of elements is used in all references to specific parameters, and requisite read programs are specified to facilitate retrieval.

Table 1.1

PRIMARY DATA CATALOGUES

P1, P2, P3, P4

FIELD		DESCRIPTION
DSN	-	data set number; sequentially assigned within each type of data P1, P2, P3, P4
ELT	-	element identifier standardized over all data sets
	1	SO_2 emissions
	2	SO_4 emissions
	3	NO_x emissions
	4	TSP emissions
	5	HC emissions
	6	Elevation
	7	Land Boundary
	8	Land use classification
	10	SO_2 Conc'n - air
	11	SO_4 Conc'n - air
	12	NO_x Conc'n - air
	⋮	
	20	SO_4 conc'n - precip
	21	NO_2 conc'n - precip
	⋮	
	40	Upper Air Wind
	41	Upper Air Temp

PRIMARY DATA CONT'D

42 Upper Air Dewpoint

43 Surf. Wind

44 Surf. Temp

45 Precipitation

46 Insolation

47 Surf Pressure

48 Upper Air Pressure

49 Cloud Information

TYPE - specification of data type; different for the different data sets where applicable

P1 - source type: utility, industrial, area, all, etc

P4 - raob, surface synoptic, surface other, climatological, gridded NWP product

RGN - region represented in the data: coded information on area covered, centered, etc.

FD,LD - first and last dates contained within the data set, where applicable

SFILEID - site file identifier; identifies a file which contains location information for the network, where needed

FREQ - data frequency, if applicable

RDPROG - identifier for reading program: standardized reading programs to simplify integration of system

NT - number of tapes in the data set

LBL1, LBL2 LBNT - NT labels of the tapes in the data set

The search program SALP allows the user to specify his data requirements in terms of data type, period of coverage, area covered. SALP creates an output list EXDAT containing the catalogue entries which fit the selection criteria. The list is then made available to EXTP which prompts the operator for the appropriate tape labels during the extraction process.

2. Catalogue Derived Data Files (CD1)

This cataloguing procedure is similar to CP, but is used for derived data files, these being extractions from the primary data files. The edit/update function EDTD1 obtains information through EXLIST (a list file produced by EXDAT) and LISTOR and LISRES (list files generated by the store and retrieve operations STOR and RESTOR) and updates the catalogues D11, D12, D13, D14 which are corresponding catalogues to the primary date catalogues P1, P2, P3, P4 .

The search procedure SALD1 generates the list file LISD1 which can subsequently be used by RESTOR to guide retrieval operations.

3. Catalogue Gridded Fields (CD2)

Gridded fields of emissions, surface characteristics, and meteorological parameters generated by the wind field model are archived and catalogued separately from the primary or derived data. Table 1.2 shows the contents of each record of D2 . The edit/update program EDTD2 uses the list files LISTOR and LISRES, as well as the permanent file OPDAT to update the catalogue D2 . The search program SALD2 creates the list file LISD2 used by the STOR and RESTOR procedures.

4. Catalogue Operational Data Files (CM)

Assembled model input files for a given run, as well as model output files are stored for subsequent access and catalogued by CM . This program maintains four catalogues:

D3 - Assembled Model Input Files

M1 - Primary Model Output Files

M2 - Model Display Files

M3 - Evaluation Statistics

The catalogue record contents are described in Table 1.3 . The edit/update program EDTM uses list files LISTOR and

Table 1.2

DERIVED GRIDDED DATA CATALOGUE D2

DFN	-	data file number; sequentially assigned within the catalogue sequence
DFC	-	data file code: internal system code based on creating program and writing program
ELT	-	element identifier - same as P1 to P4 and D11 to D14
TYPE	-	specification of data type
RGN	-	region represented in the data: coded information on area covered, centered, etc.
FD,LD	-	first and last dates contained within the data set, where applicable
SFILEID	-	site file identifier; identifies a file which contains location information for the network, where needed
FREQ	-	data frequency, if applicable
RDPROG	-	identifier for reading program; standardized reading programs to simplify integration of system
NT	-	number of tapes in the data set
LBL1 LBL2, ... LBLNT	-	NT labels of the tapes in the data set
CRDAT	-	creation date
CRPROG	-	creating program
VGRID	-	vertical grid level or levels to which data applies
NGRID	-	grid size - number of rows, columns
GRIDS	-	grid spacing (intervals)

Table 1.3

OPERATIONAL AND MODEL RESULTS CATALOGUES

D3, M1, M2, M3

DFN	-	data file number; sequentially assigned within the catalogue sequence
DFC	-	data file code: internal system code based on creating program and writing program
ELT	-	element identifier - same as P1 to P4 and D11 to D14
CRDAT	-	creation date
CRPROG	-	creating program
MRUN	-	run number used for retrieving complete data by run number
DISPN	-	disposition of computer file: keep, keep/catalogue/ delete (scratch)
VOLUME	-	volume of residence
DIRECTORY	-	addressing information to file

LISRES as well as the permanent file RUNDAT to update the appropriate catalogue. The search program SALM creates the file LISM which is used by RESTOR to retrieve off-line data.

5. Extract Primary Data (EXTP)

The procedure EXTP is an interactive command procedure which allows the operator to extract required data from the primary data sets. It uses the file EXDAT created by CP to prompt for the appropriate tape labels to read the tape and create a working file on disk. EXTP also writes the file EXLIST which allows cataloguing and storage of the extracted files.

The read procedures produce the report DATREP which provides data quality information on the transferred data.

6. Store Working Files on Tape (STOR)

The Procedure STOR allows the user to store off-line any of the derived or model result files. It uses the files EXLIST , RUNDAT , OPDAT as appropriate to invoke the appropriate write routine. The file LISTOR is created to allow the cataloguing procedures to update the appropriate catalogue entry.

7. Retrieve Stored Data From Tape (RESTOR)

   RESTOR allows retrieval of tape files. The list files LISD1 , LISD2 , LISM generated by the catalogue programs are used to initiate the appropriate read program and prompt for the required tape label. The file LISRES is generated to allow the cataloguing procedures to update the appropriate catalogue entry.

1.2.3 Generation of Operational Data (SUBSYS2)

SUBSYS2 is a menu-driven system which interacts with the user through MENUS2 to perform the following functions (Figure 1.5):

1. Retrieve Stored Data from Tape Files (RESTORD)
2. Generate Gridded Emissions Data (EMIS)
3. Generate Gridded Physical Data (GROUND)
4. Produce Wind Fields and Gridded Meteorological Fields (MENUW)

MENUS2 allows the user to transfer into SUBSYS1 in order to search the derived data catalogues (CD1) and generate the list file LISD1 . (Within SUBSYS1, a check can be made for the required operational files through CD2) .

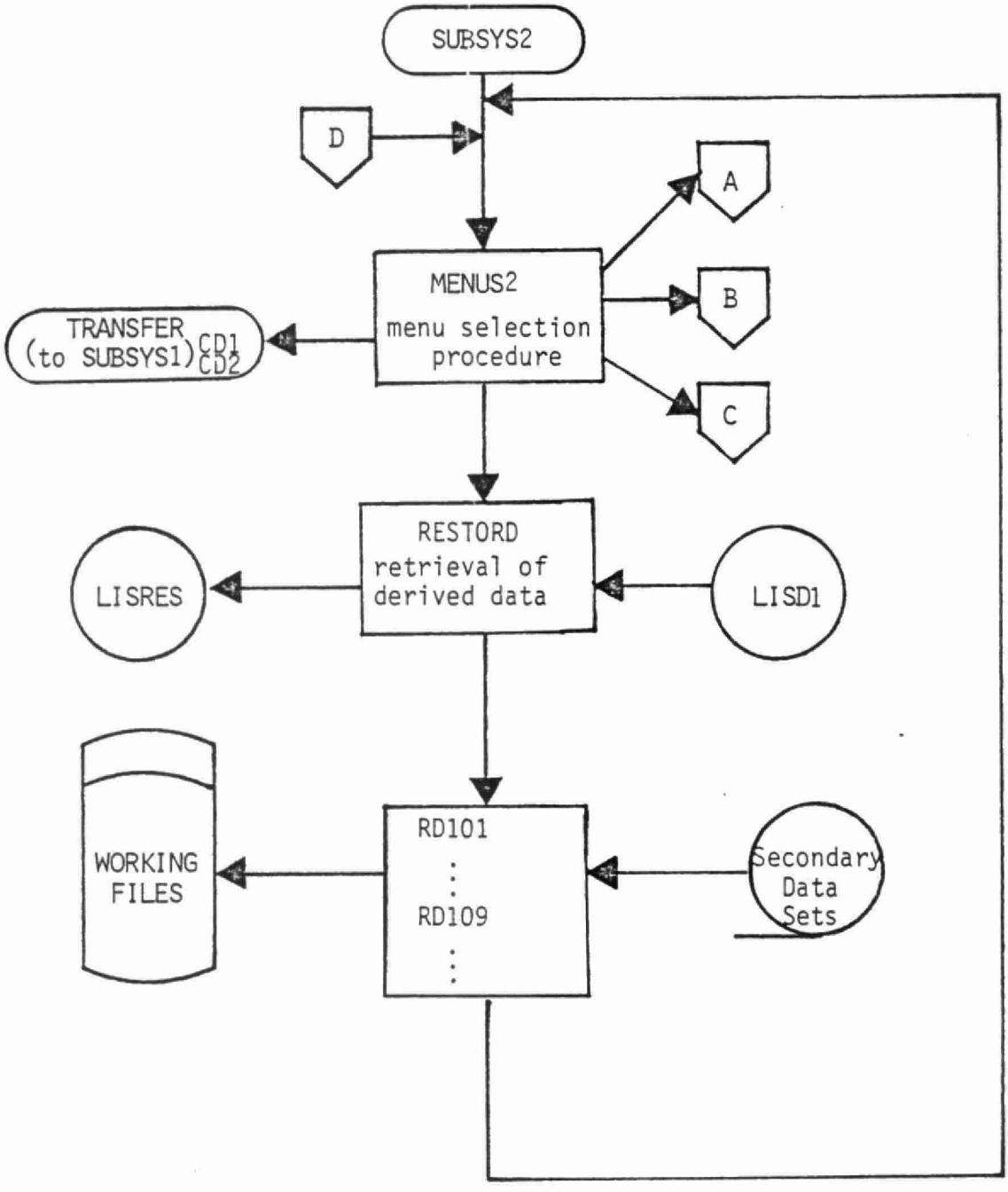
SUBSYS2
D
A
MENUS2
menu selection procedure
B
TRANSFER (to SUBSYS1) CD1 CD2
C
RESTORD
retrieval of derived data
LISRES
LISD1
WORKING FILES
RD101
RD109
Secondary Data Sets

Figure 1.5

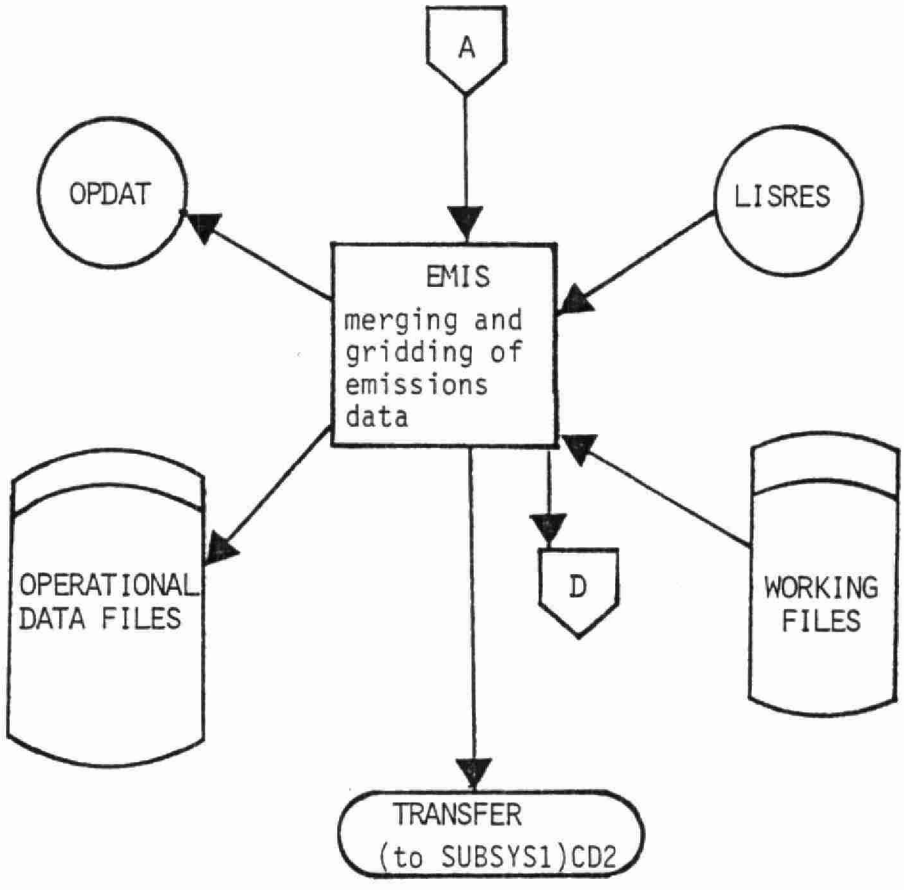

Figure 1.5 cont'd.

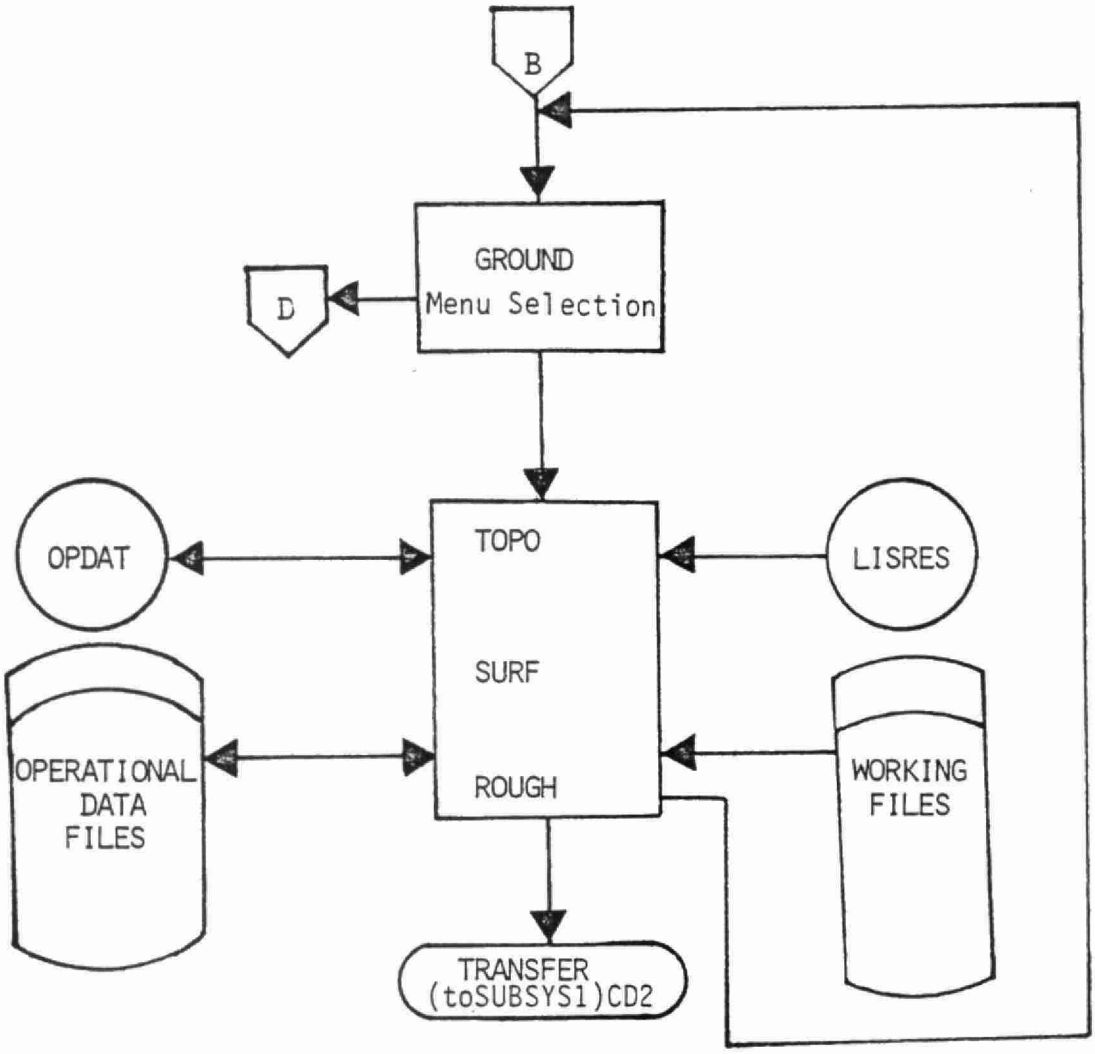

Figure 1.5 cont'd.

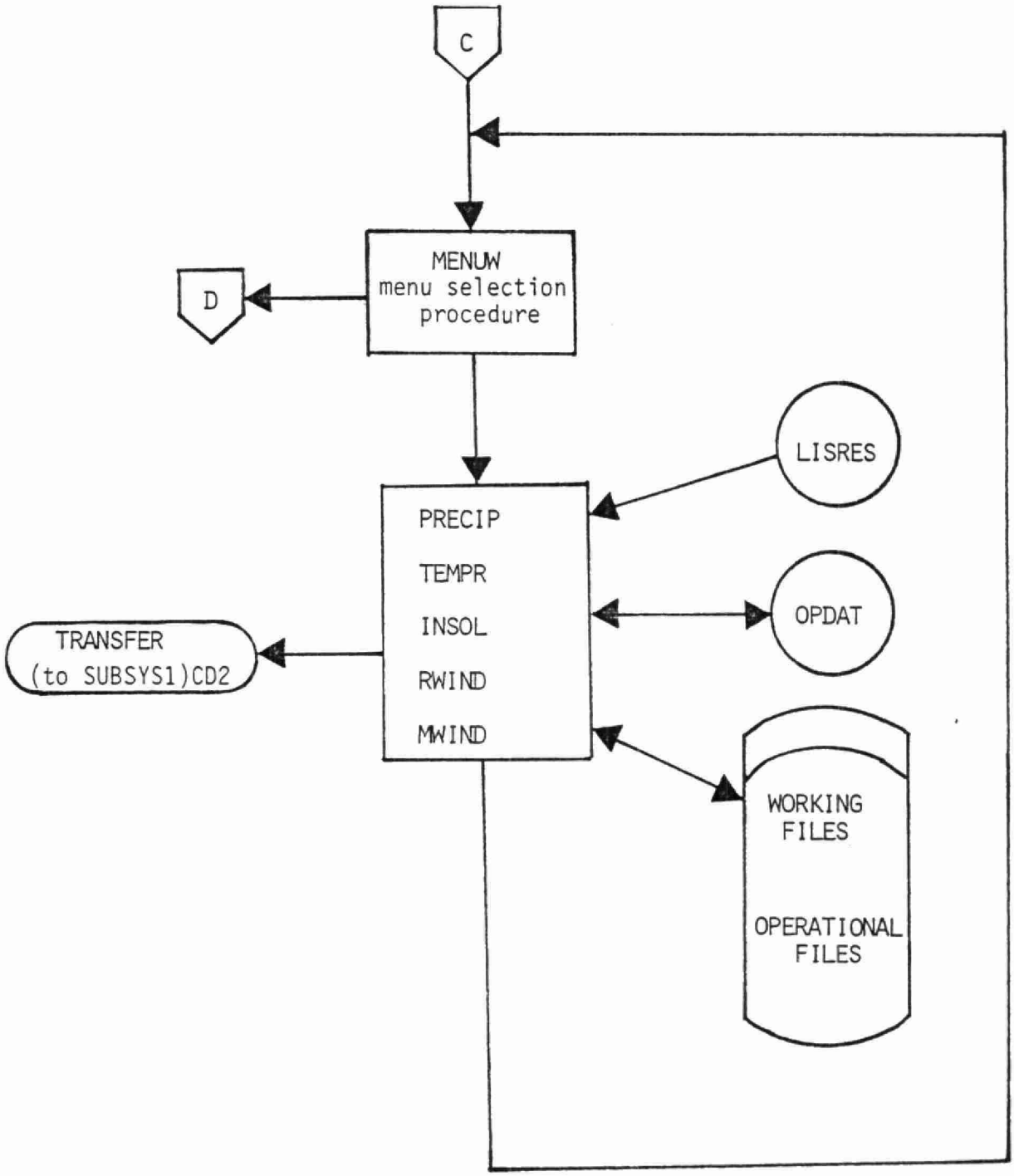

Figure 1.5 cont'd.

1. Retrieve Stored Data (RESTORD)

This procedure is a scaled down version of the RESTOR procedure in SUBSY1, which is used only for derived data files. The use of a separate retrieval procedure for operational file generation will greatly reduce contention for SUBSYS1 availability, allowing for more convenient multi-user operation.

2. Generate Gridded Emissions Data (EMIS)

EMIS is the controlling program for generating emissions scenarios and gridded emissions under control of the user who is required to specify:

- element or elements of interest
- region to be considered
- particulars of grid to be generated
- temporal resolution
- restriction on source category, emitting region, etc.
- restriction on source of data.

This process may require several transfers to SUBSYS1 in order to produce the proper subselection of the primary data sources. EMIS reads the file LISRES to define the location of the specific files required in the gridding process. The gridding

process writes the gridded operational data files and makes the appropriate entry to OPDAT file. A transfer can be made (optionally) to SUBSYS1 to catalogue the gridded data files (CD2) . The OPDAT file contains a listing of operational data files generated by the current run process.

3. Generate Gridded Physical Data (GROUND)

GROUND is a specification and menu selection program which initiates the following operations:

TOPO - extract topographic information for the required region, interpolate to the appropriate grid, perform appropriate smoothing, and write the operational data file.

SURF - generate gridded land cover map for the region for the appropriate season from map data or pre-gridded fields.

ROUGH - using surface and land coyer gridded data, generate grid of roughness length.

After writing the operational data, transfer can be made to SUBSYS1 for cataloguing procedures. The operational programs are described in greater detail in another section.

4. Produce Wind Fields and Gridded Meteorological Fields (MENUW)

MENUW controls the operation of meteorological parameter gridding and wind field generation. The principal procedures are:

PRECIP - produce gridded precipitation fields for selected periods and grid characteristics. Also produces an intermittency factor on the basis of nearby stations.

INSOL - estimate insolation to specified grid location and period on the basis of cloud cover information.

RWIND - control the generation of regional scale gridded winds.

MWIND - control the generation of mesoscale gridded winds.

These procedures are further detailed in a subsequent section.

1.2.4 Model Run Generation (SUBSYS3)

SUBSYS3 allows the user to select a model and input specifics for the run, assemble the required operational data files, and initiate and monitor the execution of the model task (Figure 1.6) .

The system task MENUS3 guides the user through the model run process, as well as allowing a transfer to be initiated to one of the other subsystems for retrieval and cataloguing tasks.

SELECT provides an interactive environment for selecting the model to be run and specifying model input data such as start and stop dates for the simulation, selection of data types to be used, specific output required and cataloguing information. By running the appropriate preprocessing routine for the model to be used, SELECT generates the file RUNLIST which contains a list of input files required by the model. The preprocessing routines also generate the file MODIN which contains the pertinent run information for the model.

The procedure OPERDAT permits the user to assemble the operational data files required through an interactive session. Missing files are flagged in LISREQ and must be retrieved or generated by the user before the model can be run.

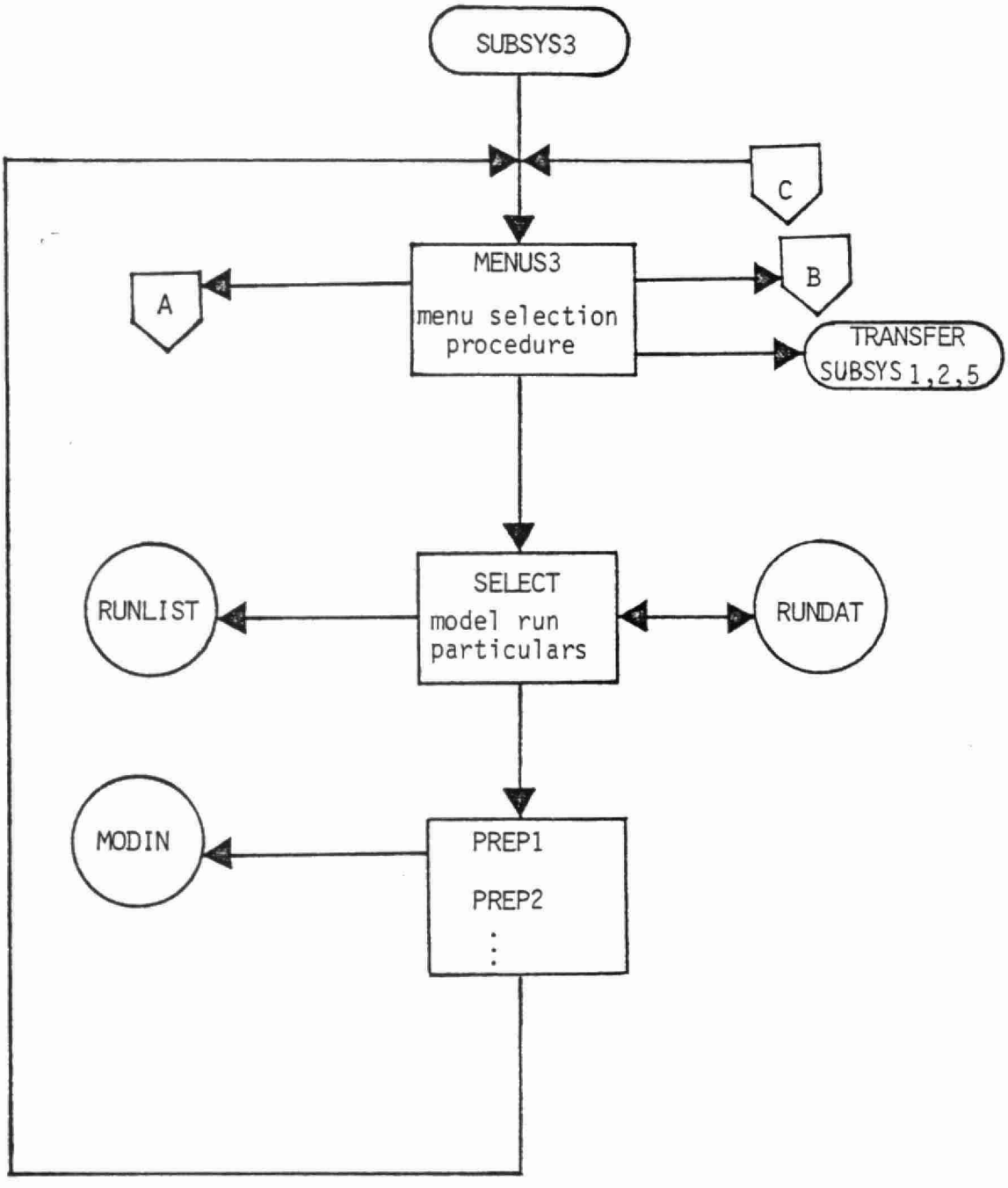
SUBSYS3
C
MENUS3
menu selection procedure
A
B
TRANSFER SUBSYS 1,2,5
SELECT
model run particulars
RUNLIST
RUNDAT
MODIN
PREP1
PREP2

Figure 1.6

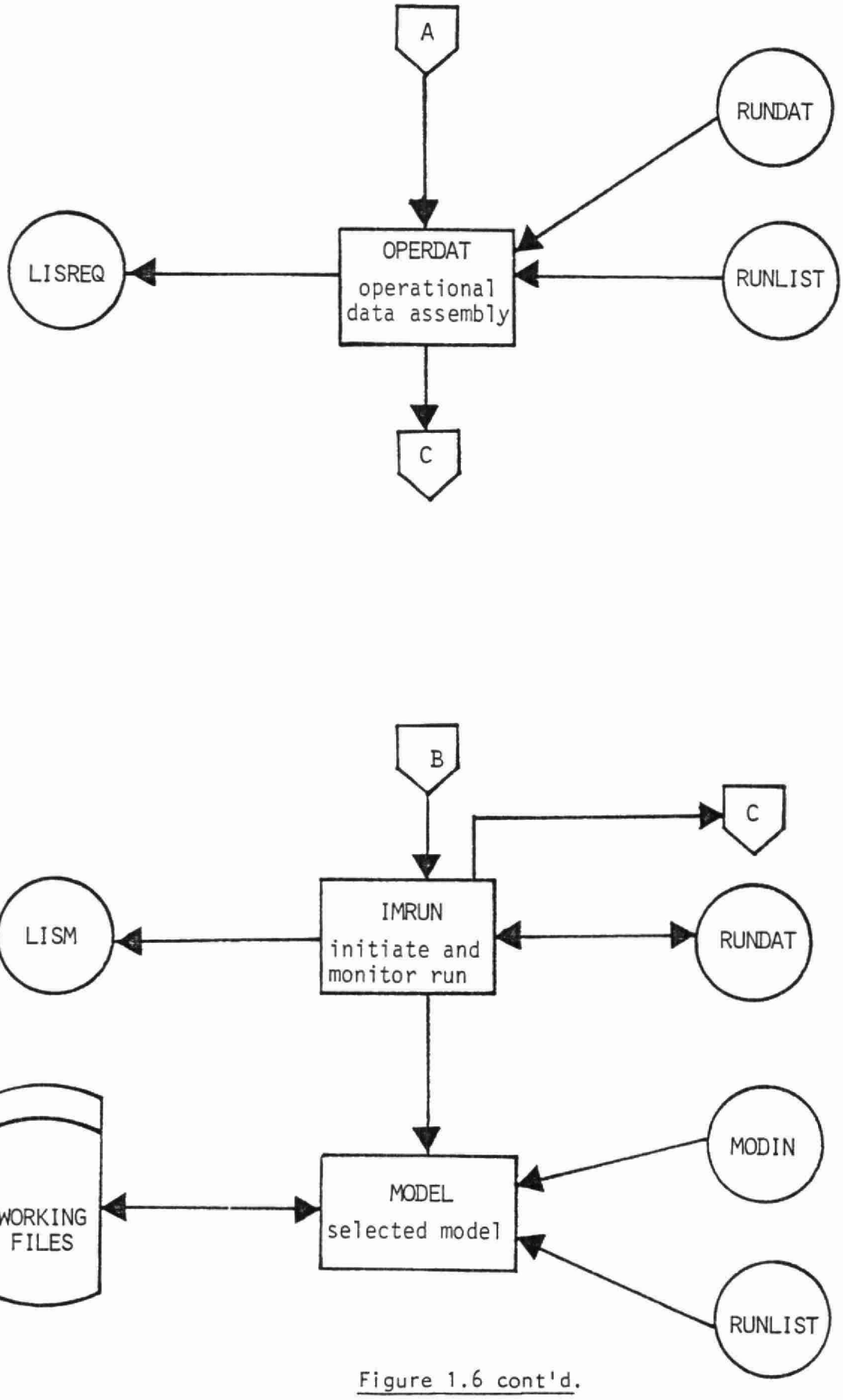

Figure 1.6 cont'd.

The procedure IMRUN sets up the model run and updates the RUNDAT file. The list file LISM is created as input to the cataloguing routine (CM) . The model is invoked, and uses the RUNLIST to retrieve the operational data files. The MODIN file is used to specify the model run, and the output files are written to disk and subsequently catalogued and archived (if necessary) .

1.2.5 Run Analysis and Display (SUBSYS4)

SUBSYS4 provides the facilities to carry out analysis of model resuits, perform statistical evaluation with measured data, and display selected parameters (Figure 1.7) .

MENUS4 allows the user to select the intended operation. Prior to analysis and display functions, the user can transfer to other subsystems to retrieve appropriate data files or generate files which are not available.

MODANAL performs analysis and synthesis of gridded model results to extract predicted concentrations and depositions applicable to the selected sampling locations and periods.

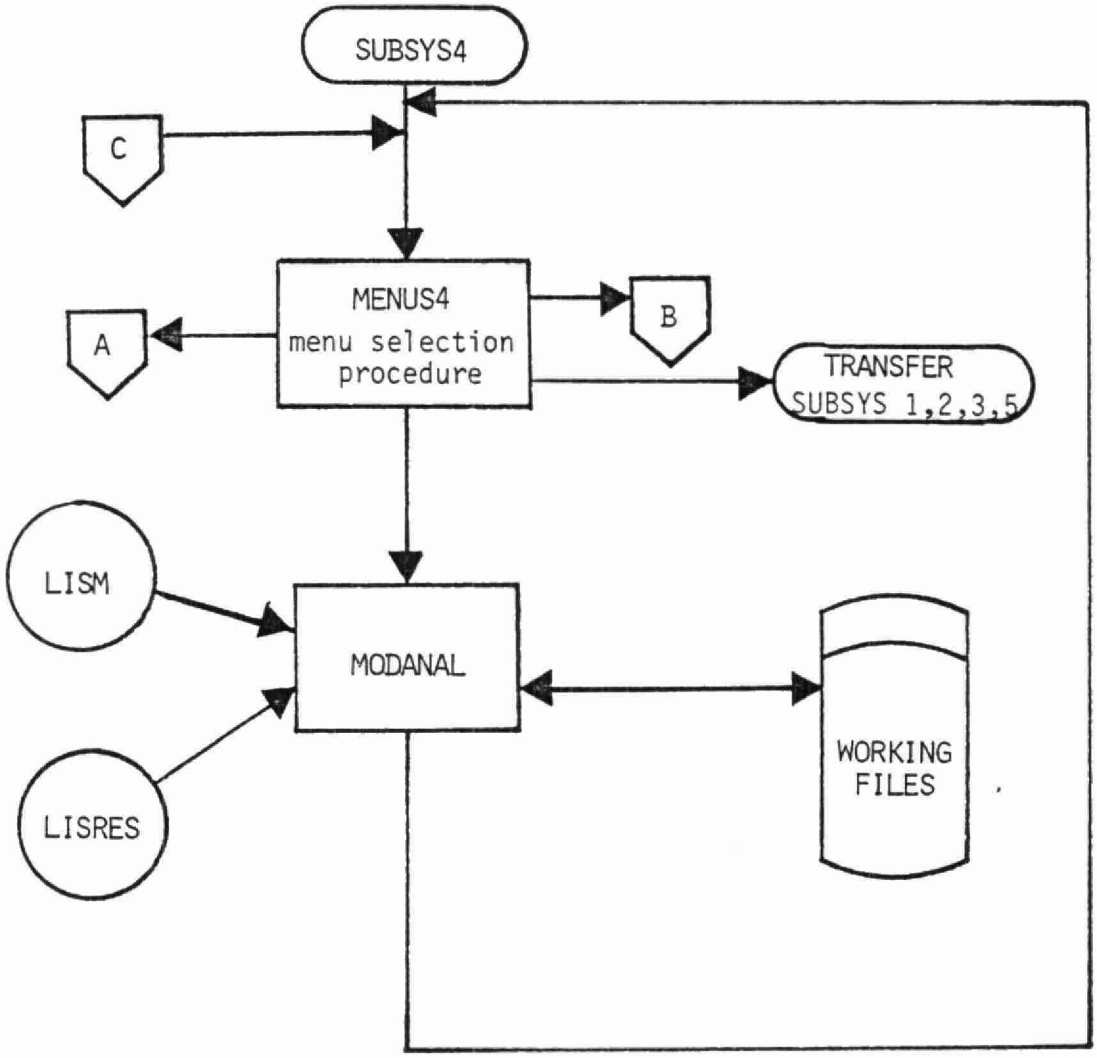
SUBSYS4
C
MENUS4
menu selection
procedure
A
B
TRANSFER
SUBSYS 1,2,3,5
LISM
MODANAL
WORKING
FILES
LISRES

Figure 1.7

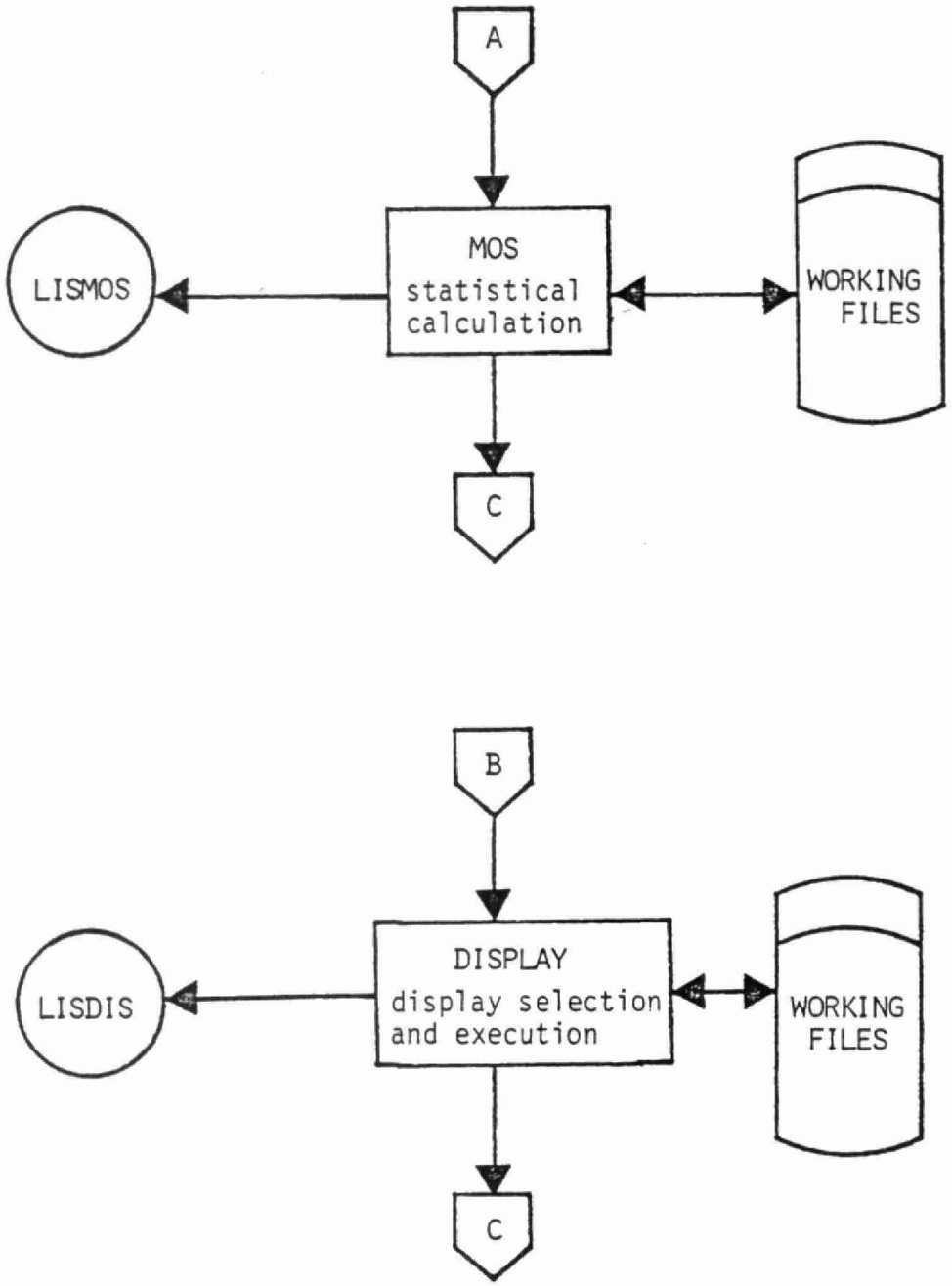

Figure 1.7 cont'd.

MOS consists of a number of statistical calculations which allow evaluation of model results against observations, or against other model run results.

DISPLAY is a series of display programs linked through the general interactive module DISPLAY . The input can be any of the operational and model results files. The output is in the form of plots, scattergrams, contour plots, tabulations and other formats as appropriate. Different display systems will be available, such as printer, Tektronix CRT, Versatech plot, Calcomp plot.

1.2.6 Model Generation and Linking (SUBSYS5)

SUBSYS5 provides the facilities for creating, cataloguing, linking and maintaining the modules which comprise the various models within the system. (Figure 1.8) .

MENUS5 allows the user to select the intended operation. A transfer to one of the other subsystems is a possible option.

CMOD is a cataloguing program for modules and tasks. The catalogue information includes identifiers for algorithm, read and write programs, linking information, creation and update information.

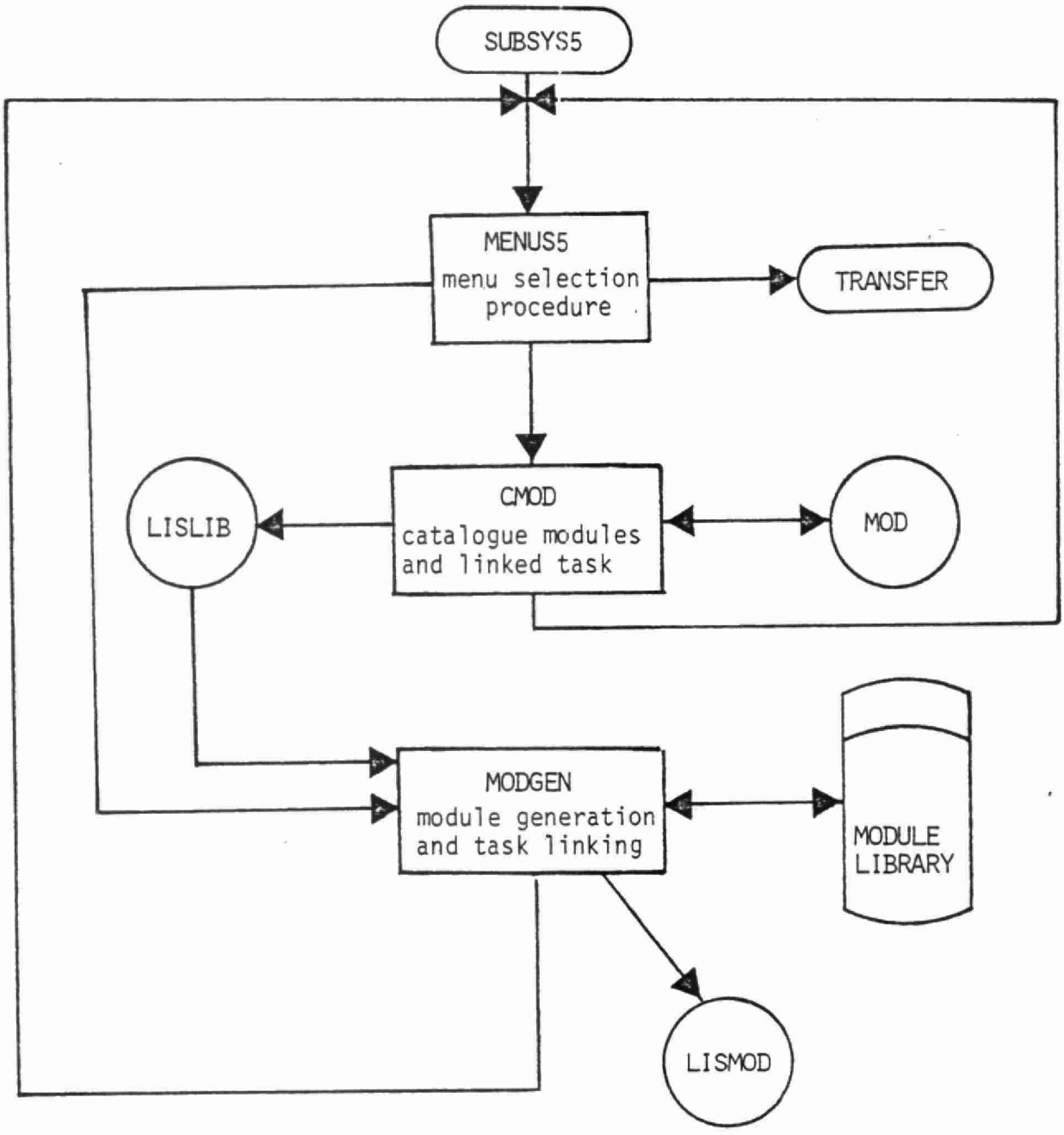
SUBSYS5
MENUS5
menu selection procedure
TRANSFER
CMOD
catalogue modules and linked task
LISLIB
MOD
MODGEN
module generation and task linking
MODULE LIBRARY
LISMOD

Figure 1.8

MODGEN allows specification of principal components to be linked for a particular model version. It retrieves the linking information form the file MOD, and retrieves the appropriate modules. A command list is created which allows assembly of the complete executable task.

1.3 System Installation Requirements

The computer requirements for the operation of the proposed system and models are dependent on the scope of the system and of the component models, as well as the anticipated mode of operation of the modeling system. In this section, these requirements are discussed to the extent that they can be determined at the present stage of design.

1.3.1 Anticipated Mode of Operation

The modeling system will be an interactively driven set of procedures with an overall controlling system (ideally written in a command control language) which maintains system and file integrity. The optimum environment for the system is a multi-user virtual memory operating system, as this would permit efficient operation of the several components of the system by one or several operators simultaneously. The segmentation of the system ensures that only a small part of the code is contained in core at a given time, the remainder of the system being resident on disk. The various models (dispersion, chemistry, wind field) are separate modules callable from the interactive system routines, and are disk resident.

User interaction will be via a CRT terminal, which could also serve as a graphics display terminal. A hard-copy display unit will be required for model display outputs.

The large amount of input data and the multiple processing of data will require a large capacity assignable disk drive and dual tape drive capability.

The system will comprise a large amount of code and will require the maintenance on-line of catalogue and control files, necessitating the provision of ample disk capacity on a fast disk.

1.3.2 Projected System Requirements

The projected requirements for computer resources to effectively operate the Data Management System include as a minimum:

- mid-range mini-computer (32 bit) with half a megabyte of physical core available to the user;
- two CRT terminals and a line printer
- virtual memory operating system allowing for a true time-sharing interactive environment
- 80 MB disk capacity
- dual tape drives (1600 bpi)

- Fortran IV language compiler
- Hard-copy display unit (Versatech, Calcomp) and associated driver software.

The Wind Field Model could also operate within this environment acceptably if a hardware floating point unit were available on the system.

The Dispersion and Chemistry Models impose a much greater demand on computer resources both in terms of core memory and CPU usage. The efficient running of these models will likely require a fast (vector) computer with large core memory availability, such as provided by the high-end CDC machines.

The ideal arrangement which would accommodate both modes of operation in an efficient manner can be set-up by installing the Data Management System on an in-house mini-computer configuration as outlined above, and installing the Wind Field Model and the Dispersion and Chemistry Models on a fast mainframe, linked to the mini by a high speed communications facility. Such a configuration would be highly interactive without incurring the large cost of CPU time on the mainframe. All runs on the mainframe would be in batch mode, with all JCL set-up by program on the mini-computer, with the results

transmitted to the mini for analysis and display functions, or placed on tape for transfer to the mini.

Since much of the work in model running is in the preparation of input data and analysis of results, this arrangement would give maximum control to the model operator, and minimize the costs of the batch runs.

1.4 Data Base Components

The Data Management System described in Section 1.2 consists of the cataloguing and archiving routines with associated library of data sets, and the data analysis routines. This section elaborates on the availability of the various data types, while Section 1.5 describes the data analysis and gridding procedures.

1.4.1 Emissions Data

The emissions data requirements for the Dispersion and Chemistry Models include the following parameters:

- SO_2
- NO/NO_2
- primary SO_4
- total particulate
- reactive hydrocarbons in 8 classes
- other hydrocarbons

For point sources, emissions parameters such as location, stack height, volume flow rate, temperature and temporal variations are essential data elements. For area sources, region of coverage and temporal variation are the required parameters.

Table 1.4 presents a compilation of relevant emissions inventories available at present. Additional detail is available in EPA (1976), Bosch (1982), Benkovitz (1982), Voldner et al (1980), Clark (1980), and Wong (1975) .

Much of the available data relates to SO_x and NO_x and no extensive coverage exists for primary sulphate. On the regional scale, only total hydrocarbon emissions data is available, necessitating a methodology for partitioning into the required subclasses.

For some source categories it is possible to obtain details on the diurnal, weekday/weekend, and seasonal variations in total emissions. However, deviations from these patterns on any given day can be significant, so that the use of such inventory data for a specific series of 4 to 5 days introduces a potentially large error. For area sources, little information on diurnal patterns is available on the regional scale.

Table 1.4

Emissions Inventory Data Sources

EMISSIONS DATA SET	COMPILER	SPONSOR	POLLUTANTS	REGION	SOURCE TYPE	TIME FRAME	COMMENTS
NEDS National Emissions Data System	U.S. EPA	EPA	Particulates, SO_x, NO_x, HC, CO	USA	Point & Area	1971 and ongoing	detailed information for point sources, and county basis for area sources
Emissions History Information System	OAQPS	OAQPS Office of Air Quality Planning and Standards	Particulates, SO_x, NO_x, HC, CO	Total USA	All	1940 50,60, 70-80	lower resolution, used for defining emissions trends
Northeast Corridor Regional Inventory	GCA	OAQPS	NO_x, VOC, CO	14 Eastern States plus DC	All	1979 data with 1980 projection	based on NEDS and updates
OAQPS Historical Trends	NADB	OAQPS	SO_x, NO_x	Eastern States	Agglomerated By State	1950-1980	tabulations mainly used for trend analysis
U.S. SO_x Emission Inventory	MITRE Corp	Environment Canada	SO_x	Eastern States	By State and 9 Categories	1980	contains erroneous data
AIRTEST - 80	Teknekron Research	EPA	SO_x	Eastern States	Power Plants	1980	based on outdated generation and fuel quality data
E. H. Pechan Inventories	E.H. Pechan & Associates	ORD/EPA	SO_x, and NO_x	USA	Utilities	1976-1980	emission trends for 238 largest utility emitters in U.S.
SURE	GCA	EPRI	SO_x	Eastern States	All	77-78 & updated to 1979 (SURE I)	1975 NEDS used for non-utility emissions. SURE II contains adjustments which may be erroneous
MAP3S	BNL	DOE	Particulates, SO_x, NO_x, HC, CO	USA plus some of Canadian Sources	All	1978	presently configured as a computerized data base management system

Table 1.4 Continued

Emissions Inventory Data Sources

EMISSIONS DATA SET	COMPILER	SPONSOR	POLLUTANTS	REGION	SOURCE TYPE	TIME FRAME	COMMENTS
SEAS Strategic Environmental Assessment System	MITRE Corp.	EPA/DOE	SO_x,NO_x	USA	Aggregated	project to any year from 1978	based on econometric projections of interrelated industries
MFBI Major Fuel Burning Installations	DOE	DOE	Fuel Use	USA coal, oil, gas consumers	Data for 2000-5000 sources collected	1979-80	large industrial fuel users
FEUDS Facility Energy Utilization Data System	ULTRASYSTEMS INC.	DOE	Same As NEDS	USA	Point & Area	Annual Based on NEDS	based on NEDS plus additional plant-specific data
ICF Data Base	ICF	DOE/EPA/ORD	SO_x,NO_x	USA	Combination Sources	1978-79	used for emission scenario evaluation
EDS Energy Data System	SASD/OAQPS	SASD/OAQPS	Particulates, SO_x,NOx	USA	Power Plants	1969-1979	terminated in 1979
GURF Generating Unit Referencing File	Oak Ridge National Laboratory	DOE	SO_x	USA	Oil & Coal Fired Power Plants	1978-1979	
RAPS Regional Air Pollution Study	SAI	OAQPS/ORD	Particulates, SO_x,NO_x,HC,CO trace metals	St. Louis AQCR	Detailed Point & Area Sources	1975-1977	5 year intensive study period
National Emissions Inventory System	EPS Canada	EPS	Particulates, SO_x,NO_x,HC,CO primary SO_4 (partial)	Canada	All	1978, 1980 updates periodically	gridded inventories based on this data have been produced on a 127 km Polar Stereographic grid
Ontario Emissions Inventory	OME	OME	Particulates, SO_x,NO_x,HC,CO	Ontario	Point & Area	Yearly Update	Presently a development program has begun to generate an Acid Rain Emission Inventory Data Management System

In order to characterize the error associated with the inventory data, it will be necessary to determine the individual errors in the various source categories, and apply a weighted sensitivity analysis as in Ditto et al (1976) .

1.4.2 Physical Data

Topographic data can be obtained in digitized format (NCIR (1981)) to a resolution of $2^{o} \times 1^{o}$. These were digitized from a 1:250,000 map, and is therefore limited to the original resolution of the maps. More detailed maps for the mesoscale can be obtained from NCIR or EMNR (Ottawa), and manually digitized for inclusion in the data base. Gridded topographic data is also available, such as produced by Lawrence Livermore Laboratory.

Geographic information for natural boundaries is also available in digitized form to 1 km resolution from NCAR (Henderson and Clare, 1980).

Land use data is available on several scales of resolution and can be manually processed into gridded data. Additionally, the Ontario Center for Remote Sensing has developed a computerized procedure for interpreting Landsat data and producing averaged land use data to desired resolution (Pala, 1982) .

Maps of potential vegetation cover are available through the American Geographical Society (Kuchler, 1970), as well as regional conservation authorities and forestry services.

Seasonal gridded maps can be derived from these. Along with snow cover and land use information, vegetation cover and roughness parameter data can be used directly to produce gridded maps of deposition velocity as carried out by Sheih et al (1979) .

1.4.3 Air Quality and Precipitation Data

Verification and initialization of the dispersion models requires air concentration data on the following parameters; SO_2 SO_4, NO/NO_2, TSP, Reactive hydrocarbons in eight classes, ammonia, ozone and trace metals. Also required is precipitation chemistry data of the major cations and anions, as well as pH and conductivity.

Much of the data on air concentration is collected in support of compliance testing of local pollutant levels, and is of limited utility for long-range transport studies due to local influences as well as lack of precision at the low concentrations at locations characteristic of the regional conditions. In the U.S., the AEROS system (EPA, 1976) provides a computerized compilation of most of this data. In Canada, the EPS maintains the National Air Pollution

Surveillance network (NAPS, 1981) and the Ontario Ministry of the Environment maintains a dense network within Southern and Central Ontario (OME, 1981) .

This data is generally restricted to the criteria pollutants: SO_2, NO/NO_2, TSP, HC, O_3, CO . For validation of the dispersion models, it will be necessary to utilize the data from specialized experiments such as the SURE (Mueller et al, 1980), ERAQS (Mueller et al, 1981) and OSCAR (Hales et al, 1981) experiments.

Some networks, such as the APN in Eastern Canada, designed for precipitation chemistry also include air concentration measurements suitable for regional characterization. Additionally, local programs of short and long-term are run by provincial and state agencies.

For precipitation monitoring, a large number of programs have been launched since the late seventies. Wisniewski and Kinsman (1982) provide the results of a comprehensive survey of acid rain monitoring activities in the U.S. and Canada, both of national and local scale. Table 1.5 reproduces this compilation. The listing does not, however, identify networks which also measure air concentration parameters, such as APN, MAP3S/OSCAR, EPRI SURE, or the PEPE specialized experiment.

Table 1.5 - Acid Rain Monitoring Studies

Reproduced from Wisniewski and Kinsman (1982)

United States acid rain monitoring studies—National, regional, state, local, and recently completed.

Study/Network	Funding organization	Parameters monitored	Extent and location	Period of operation	Sampling and analysis	Contact
NATIONAL:						
National Atmospheric Deposition Program (NADP)	A consortium of government (USDA, NOAA, USGS, EPA, DOE, U.S. Forest Service, National Park Service, Bureau of Land Management, State Agricultural Experiment Stations), educational and private sector entities.	pH, conductivity, SO_4, NO_3, NH_4, Cl, PO_4, Na, K, Ca, Mg	As of 1 January 1982, the NADP consisted of 92 operating stations, with five more expected in early 1982. At its inception, the NADP was concentrated in the east but now a more balanced distribution exists from coast to coast, including sites located in Alaska, Hawaii and American Somoa.	The network was established in May 1978.	Each site utilizes an Aerochem Metrics 201 wet/dry deposition collector. Wet deposition samples are collected on a weekly basis and dry deposition is collected bimonthly. All samples are analyzed at the Illinois State Water Survey.	J. H. Gibson Natural Resources Laboratory Colorado State University Ft. Collins, Colo. 20910
NCA/BCR Precipitation Quality Network	The network is funded by the National Coal Association (NCA) and managed by Bitiminus Coal Research, Inc. (BCR).	pH, conductivity, acidity, SO_4, NO_3, NH_4, Cl, Ca, Na, K, Mg (in order of priority in event of sample with small volume)	The NCA network will exist nationwide, with most sites east of the Mississippi. The network will be especially concentrated in the coal-producing regions of Illinois, Ohio, Pennsylvania, and West Virginia. Forty sites were in operation as of January 1982. Approximately 10 more sites will begin monitoring in 1982.	Initial sites began collection in early 1981.	Aerochem Metrics 201 wet/dry samplers will be used to collect weekly wet and biweekly dry samples. Analyses will be performed at laboratories located at each site. If no laboratory is available, analyses will be performed at Bituminus Coal Research, Inc.	James F. Boyer Manager, Environmental Research Bituminus Coal Research, Inc. 350 Hochberg Rd. Monroeville, Pa. 15146
National Urban Runoff Program (NURP)	Environmental Protection Agency (EPA), U.S. Geological Survey (USGS)	pH, conductivity, SO_4, NO_3, NH_4, Cl, P, PO_4, Na, K, Ca, Mg, Cd, Cu, Pb, Zn. Also, some multi-element trace metal scans, carbonate, bicarbonate, TOC and DIC.	The network consists of up to nine precipitation collectors in each of 28 cities nationwide.	The earliest sites have been in operation since summer 1978. Three-year data collections are in progress at most sites.	The network uses Aerochem Metrics 201 wet/dry precipitation collectors principally, along with two other very similar models. Wet deposition is collected on an event basis and dry deposition collection is monthly or bimonthly. Analyses are performed at the EPA laboratory in Kansas City, at the USGS laboratories in Denver and Atlanta, and at various universities and private firms.	Dennis N. Athayde WH554, EPA 401 M St., S.W. Washington, D.C. 20460 Ernest D. Cobb USGS-WRD, Mail Stop 415 Reston, Va. 22092
Utility Acid Precipitation Study Program (UAPSP)	The network is funded by 34 electric utilities in the eastern U.S. Technical management is provided by EPRI.	pH, conductivity, SO_4, NO_3, NH_4, Cl, P, Na, K, Ca, Mg	The network consists of 19 sites, extending from eastern South Dakota south to eastern Texas and east to Maine. The network includes five stations from the recently completed EPRI Eastern Regional Chemistry Network.	The six sites from the EPRI Eastern Regional Chemistry Network have been in operation since September 1978. The other 13 sites include two sites initiated in April 1981 and 11 sites initiated in October 1981.	Aerochem Metrics samples are used to collect wet-only precipitation daily. Analyses are performed by Rockwell International. Acidity is measured at the site.	Chuck Hakkarinen Energy Analysis and Environment Division Electric Power Research Institute P.O. Box 10412 3412 Hillview Ave. Palo Alto, Calif. 94303

Table 1.5 (continued)

EPA/NOAA/WMO Precipitation Chemistry Network	Environmental Protection Agency (EPA), National Oceanic and Atmospheric Administration (NOAA), World Meteorological Organization (WMO)	pH, conductivity, SO_4, NO_3, NH_4, Cl, PO_4, Na, Ca, Mg	The network consists of 12 stations. Ten sites are located within the continental U.S., with one site each on Mauna Loa, Hawaii, and American Somoa. All sites in this network are also members of the NADP network since 1979.	The network began operation during 1972.	The network switched to Aerochem Metrics 201 wet/dry deposition collectors in mid-1979. Sampling is performed weekly for wet deposition and bimonthly for dry deposition. All samples are analyzed at the Illinois State Water Survey.	John M. Miller NOAA-Air Resources Laboratories 8060 13th St. Silver Spring, Md. 20910
REGIONAL:						
EPA Great Lakes Atmospheric Deposition Network	Environmental Protection Agency (EPA)	pH, conductivity, alkalinity, acidity, SO_4, NO_3, NO_2, NH_3, total N, Cl, total P, Na, K, Ca, Mg, Si, TOC, and 23 metals. Thirteen toxic organics will be analyzed in the bulk collections at all sites and 12 sites will be selected for annual complete toxic organic scans.	The network is to encompass the area along the 8045 km U.S. shoreline of the Great Lakes, from Minnesota to the St. Lawrence River. Approximately 30 monitoring sites were active as of mid-August 1981. The network is expected to be fully operational with 41 sites.	This program replaces and includes several sites from the Atmospheric Pollutants Loading Study of EPA Region V, which was initiated in 1977.	Two types of collectors are currently used: an Aerochem Metrics 201 wet/dry sampler and a regular bulk collector. Later in the project a special bulk collection will be used, which separately collects nutrients, metals, and organics. Wet and dry deposition samples are collected weekly and bulk samples monthly. Analyses are performed at the EPA Region V Central Regional Lab in Chicago.	David Lueck U.S. EPA-GLNPO-SRS 536 S. Clark St. Chicago, Ill. 60605
University of Nevada Study	Bureau of Reclamation, Department of Interior; State of Nevada	pH, Na, K, Ca, Mg, Ag, Ce, Fe, I, In, Mn, Rb	The network has included collection of precipitation samples at various sites in the Sierra-Nevada Mountains, northeastern Colorado and Antarctica since its inception. Currently, samples are collected at approximately 30 sites in the Truckee-Tahoe, Carson-Walker, and Spring Mountain catchment basins in Nevada.	Initial sampling took place in 1966.	Since the majority of samples are in the form of snow, mechanical devices used for coring and profile analysis are used in sample collection. Analyses are performed at the Desert Research Institute Laboratory in Reno.	J. A. Warburton Desert Research Institute University of Nevada System Reno, Nev. 89506
Tennessee Valley Authority (TVA) Network	Tennessee Valley Authority (TVA), Electric Power Research Institute (EPRI)	pH, conductivity, weak acidity, strong acidity, SO_4, NO_3, NH_4, Cl, F, PO_4, Na, K, Mg, Ca	The TVA network currently consists of 11 monitoring sites; including trend stations, watershed collection sites and sites located in the vicinity of coal-fired power plants.	Some monitoring has been conducted since 1971 in connection with various studies. Calendar year 1979 marked the first full year of operation for all 11 stations.	Collection sites employ TVA wet/dry precipitation collectors similar to the Aerochem Metrics 201 collectors. The majority of sampling is biweekly wet and bimonthly dry. Samples are shipped to the TVA laboratory at Chattanooga, Tenn., for analyses.	W. J. Parkhurst Tennessee Valley Authority Air Resources Program River Oaks Bldg. Muscle Shoals, Ala. 35660
Multi-State Atmospheric Power Production Pollution Study/Research in Acidity from Industrial Emissions (MAP3S/RAINE)	Environmental Protection Agency (EPA), Department of Energy (DOE)	pH, conductivity, SO_4, SO_3, NO_3, NH_4, Cl, PO_4, Na, K, Ca, Mg	The network consists of nine stations, mostly in the northeast.	The initial four stations began operating in 1976 and an additional four began in 1978. Oak Ridge National Laboratory was added as the ninth site in early 1981.	Modified wet-only Battelle precipitation collectors are being replaced by HASL automatic wet-only collectors. Samples are collected on a modified-event basis defined by the operator and are shipped to Pacific NW Laboratories for analyses.	M. Terry Dana Battelle, Pacific NW Laboratories P.O. Box 999 Richland, Wash. 99352

(continued on next page)

Table 1.5 (continued)

Study/Network	Funding organization	Parameters monitored	Extent and location	Period of operation	Sampling and analysis	Contact
Great Smoky Mountains National Park Precipitation Network	U.S. Forest Service	pH, conductivity, SO_4, NO_3, turbidity	The network consists of four sites at lower elevation (610 to 730 m): two in Tennessee and two in North Carolina. A fifth site is located at Clingman's Dome, North Carolina (1830 m).	Monitoring began in early 1979.	The Elkmont site is part of the NADP network and utilizes an Aerochem Metrics 201 wet/dry collector. All sites also collect wet precipitation with TVA collectors. Dry deposition is sampled bimonthly at the Elkmont site. Wet deposition is sampled weekly at all sites. Analyses are performed at the Uplands Field Research Laboratory.	Lab Director Uplands Field Research Laboratory Twin Creeks Area Route 2 Gatlinburg, Tenn. 37738
STATE:						
Clemson University Experiment	Clemson University	Sulfur in air and precipitation at 15 sites; pH, conductivity, SO_4, NO_3, Cl, PO_4, Na, K, Ca, and Mg at the NADP site.	The sulfur network consists of 15 sites throughout South Carolina, three of which are the same as operated during a 1953 to 1955 monitoring effort. Clemson also operates one NADP station.	Clemson has monitored sulfur from 1953 to 1955, and from 1973 to present. The NADP site was initiated in 1979.	Each site in the sulfur network collects precipitation in three liter plastic bulk buckets and sulfur in air using PbO_2 candles. Sampling occurs every 30 days to replicate 1953-55 sampling conditions. The NADP site collects weekly wet samples and bimonthly dry samples with an Aerochem Metrics 201 wet/dry precipitation collector. NADP analyses are performed at the Illinois State Water Survey.	U.S. Jones Department of Agronomy & Soils 277 P & AS Building Clemson University Clemson, S.C. 29631
Florida Acid Deposition Study	Florida Electric Power Coordinating Group	pH, conductivity, SO_4, NO_3, NO_2, NH_4, Cl, PO_4, Na, K, Ca, Mg	The network includes 14 sites throughout Florida.	Collection started at all sites in July 1981 and will continue for three years.	The study utilizes Aerochem Metrics 301 wet/dry collectors, with all sites having weekly collection and two sites having colocated daily collection. Analyses will be performed by Environmental Science and Engineering, Inc.	Bill Palmer Florida Electric Power Coordinating Group 402 Reo St., Suite 214 Tampa, Fla. 33609
USGS New York State Precipitation Monitoring Network	U.S. Geological Survey (USGS)	pH, conductivity, SO_4, NO_3, NO_2, NH_3, organic N, Cl, total P, Na, K, Ca, Mg, Pb, bicarbonate when the pH is greater than 4.5	The network began with nine stations, of which five are still in existence. The network currently includes 12 stations.	The network was established in October 1964.	The network collects bulk precipitation monthly but is in the process of converting six stations to Aerochem Metrics 301 wet/dry samplers, which will sample on the event basis whenever an event is greater than [illegible] cm.	Roy Schroeder USGS P.O. Box 1350 Albany, N.Y. 12201

Table 1.5 (continued)

Minnesota/Wisconsin Power Supply Group Precipitation Monitoring Program	Minnesota/Wisconsin Power Supply Group	The following parameters are measured for wet precipitation: pH, SO_4, NO_3, NO_2, NH_4, Br, Cl, F, I, PO_4, Na, K, Ca, Mg, Al, B, Cu, Fe, Mn, Ni, Pb, and Zn. Dry deposition samples are analyzed for SO_4, NO_3, NO_2, Br, Cl, F, I, PO_4, K, Ca, Al, As, Ba, Fe, Hg, Mn, Pb, S, Si, V, and Zn.	This summer-sampling network consisted of six sites distributed throughout Minnesota and one site in southwest Wisconsin during 1981.	Various acid rain-related monitoring activities have been conducted by the University of Minnesota since 1973. The first year of funding by the Minnesota/Wisconsin Power Suppliers Group was in 1981.	Each site is equipped with a wet/dry precipitation collector designed by the University of Minnesota. Wet samples are collected sequentially on a sub-event (0.25 cm) basis from mid-April to the end of October. Samples are picked up within 48 h of collection and analyses are performed at the University of Minnesota. Dry deposition is collected for 24 h every sixth day, using virtual impaction dichotomous air samplers.	S. V. Krupa Department of Plant Pathology 1515 Gortner Ave. University of Minnesota St. Paul, Minn. 55108
Texas Air Control Board Precipitation Chemistry Network	Texas Air Control Board	pH, SO_4, NO_3, NH_4	The network began with three sites across Texas, with a fourth site added later.	The initial three sites began sampling in mid-1979 and the fourth site was added six months later. Two NADP sites will be added in early 1982.	Sampling is done with a funnel collector on the event basis, with a pH electrode used at the site to determine sample pH.	T. H. Porter Texas Air Control Board 6330 Highway 290 East Austin, Tex. 78723
Wisconsin Acid Deposition Monitoring Project	Wisconsin Utilities Association	pH, conductivity, total acidity, strong acidity, SO_4, NO_3, NH_4, Cl, Na, K, Ca, Mg, Al, PO_4 and alkalinity (in order of priority in the case of small sample volume).	The network will consist of three sites: one each in northwest, central, and southeast Wisconsin.	The network is scheduled to begin operation in late March 1982 and to continue for 24 months.	Wet deposition will be collected daily using an Aerochem Metrics 301 sampler. Dryfall will be collected biweekly at the northwest site. pH and conductivity will be measured at the site and the remainder of the sample will be shipped to Pacific NW laboratories for analyses.	John Flickinger Wisconsin Power and Light Company 222 West Washington Ave. P.O. Box 192 Madison, Wis. 53701
Precipitation Chemistry in North Dakota Study	Water Resources Division, U.S. Geological Survey (USGS); North Dakota State Health Department	pH, conductivity, alkalinity, SO_4, NO_3, NH_4, Cl, F, PO_4, Na, K, Ca, Mg, Al, Ag, As, Cd, Cr, Cu, Fe, Hg, Mn, Mo, Ni, Pb, Se, V, Zn	Currently the North Dakota State Health Department operates two sites (Dunn Center and Woodworth). The USGS operated three additional sites (Wibaux, Beulah, and Gascoyne) until October 1981.	The North Dakota State Health Department sites, Dunn and Woodworth, were initiated in October 1980 and June 1981, respectively, and are funded through the end of 1986. The USGS sites began collection in May 1981. Several or all of the USGS sites may resume operation in 1982.	The North Dakota State Health Department sites use Aerochem Metrics collectors, sampling wet deposition on the event basis and dry deposition monthly. Analyses are performed by the North Dakota State Health Department. The USGS sites used colocated Aerochem Metrics and Leonard Mold and Die collectors, sampling wet deposition on the event basis and dry deposition monthly. Analyses were performed by the USGS laboratory in Denver.	Robert L. Houghton USGS, WRD 821 E. Interstate Ave. Bismarck, N.D. 58501 Robert Angelo North Dakota State Health Department Division of Environmental Research 1200 Missouri Ave. Bismarck, N.D. 58505

(continued on next page)

Table 1.5 (continued)

Study/Network	Funding organization	Parameters monitored	Extent and location	Period of operation	Sampling and analysis	Contact
LOCAL:						
Wet Deposition in Southern California Study	Southern California Edison Company	pH, conductivity, alkalinity, acidity, SO_4, NO_3, NO_2, NH_4, Cl, Na, K, Ca, Mg, Al, Fe, Ni, Pb, V	The network consists of 13 stations within a 80 km radius of Los Angeles and two stations in the east central California desert.	The Los Angeles area stations began collection during the 1979–80 winter rainy season. The two desert sites began collection in 1981 and will continue to collect all wet deposition through at least 1983.	Wet-only precipitation is collected on the event basis using a rain-triggered funnel arrangement, which separates the sample into an initial 0.1 inch increment and a "rest of event" sample. Measurements are performed by Global Geochemistry Corporation in Canoga Park, Calif. pH, acidity, conductivity, and NH_4 are measured within 12 h after collection.	E. C. Ellis Southern California Edison Co. Research and Development P.O. Box 800 Rosemead, Calif. 91770
McDonald's Branch Watershed Network	University of Pennsylvania, Yale University	pH, conductivity, NO_3, NH_4, total P, Na, K, Ca, Mg, Al, Cd, Cr, Cu, Fe, Mo, Mn, Ni, Pb, Zn	Ten precipitation collectors are located within a 6 km^2 area in the McDonald's Branch Watershed, which is situated in the Lebanon State Forest of the south New Jersey pine barrens.	Initial sampling began in May 1978 and the status of the network will be reviewed after the initial three-year sampling period.	Funnel-type bulk collectors with evaporation traps are located at nine of 10 stations. A project-designed wet-only precipitation collector is located at the tenth site. Sampling has varied from event to biweekly to monthly (currently). Analyses are performed at the University of Pennsylvania and Yale University.	Arthur H. Johnson Department of Geology University of Pennsylvania 240 South 33rd St. Philadelphia, Pa. 19104
Tesuque Watershed Precipitation Network	University of New Mexico	pH, conductivity, NO_3, NH_4, organic N, Cl, Na, K, Ca, Mg, Cu, Fe, Pb	The network consists of nine monitors in the Tesuque Watershed of the Santa Fe National Forest.	The network is part of a study conducted by the University of New Mexico since 1971.	Samples are collected using funnel-and-bottle bulk collection devices for rain. Snow is collected in open, exposed containers. Summer sampling is weekly or more frequently. Winter samples are collected once containers are full of snow. Samples are analyzed at the University of New Mexico.	James R. Gosz Department of Biology Room 173 University of New Mexico Albuquerque, N.M. 87131
Monongahela National Forest Study	U.S. Forest Service	pH, conductivity, total alkalinity, total acidity, SO_4, NO_3, NO_2, Cl, PO_4, Na, K, Mg, Al, Cu, Mn, Pb, Zn	Initially the network included 24 sites statewide but currently only eight sites exist.	The first site began monitoring in 1972. Since late 1981, only pH and conductivity analyses have been performed.	Wet and bulk deposition samples are collected on a variety of time schedules (event, weekly, biweekly and monthly) with Bellford rain gages. Analyses are conducted at the Monongahela National Forest hydrology laboratory.	Forest Hydrologist Monongahela National Forest U.S. Forest Service P.O. Box 1548 Elkins, W. Va. 26241

Table 1.5 (continued)

NASA/Kennedy Space Center Network	National Aeronautics & Space Administration (NASA)	pH, conductivity, H, excess SO_4, marine SO_4, NO_3, NH_4, Cl, F, Na, K, Ca, Mg	The network consists of seven sites within a 400 km^2 area in central Florida. At one time, 14 sites covering 700 km^2 were in operation.	The network was initiated in July 1977.	Aerochem Metrics model 201 precipitation collectors are used to sample wet precipitation weekly at six sites and daily at one site. Samples are analyzed at the J. F. Kennedy Space Center.	W. Knott MD-RSB-2 J. F. Kennedy Space Center Cape Canaveral, Fla. 32899
Washington, D.C. Precipitation Network	National Oceanic and Atmospheric Administration (NOAA)	pH, conductivity, and occasionally a full chemical analysis for major ions	The study presently includes six sites in the Washington, D.C., area.	The network began operation in April 1974.	Bulk samples are collected daily, with pH and conductivity measured within 48 h at the NOAA Air Resources Laboratory in Silver Spring. Occasionally, a full chemical analysis for major ions is performed at the University of Virginia.	John M. Miller NOAA-Air Resources Laboratory 8060 13th St. Silver Spring, Md. 20910
Maryland Geological Survey Acid Precipitation Project	U.S. Geological Survey (USGS), Environmental Protection Agency (EPA)	pH, conductivity, acidity, SO_4, NO_3, NO_2, NH_4, Br, Cl, F, P, PO_4, Na, K, Ca, Mg, Be, C, Cd, Cr, Cu, Fe, Ni, Pb, Si, Zn, anthropogenic organic compounds, filtratable solids	Six samplers are located on the Maryland portion of the Chesapeake Bay: three each on the western and eastern sides.	Sampling began in March 1981.	Wet and dry samples are collected in automatic collectors. Wet events of one inch or greater over a 24 h period are collected. Dryfall samples are allowed to accumulate for at least three months. Analyses are performed by the Maryland Geological Survey, except anthropogenic organic compounds (Virginia Institute of Marine Science) and trace metals in particulates (National Bureau of Standards).	Robert D. Conkwright Maryland Geological Survey 2100 Guilford Ave. Baltimore, Md. 21218
Tahoe Monitoring Program	University of California at Davis, California Air Resources Board, California State Water Resources Control Board	pH, conductivity, alkalinity, SO_4, NO_3, NH_3, DON, Cl, PO_4, Na, K, Ca, Mg	Five sites are located in the Tahoe Basin, approximately 260 km northeast of the San Francisco Bay.	Monitoring has existed since November 1978, initially as a member of the UC/CARB network, which ended in May 1979. At least three more years of funding are expected.	The network now operates three wet/dry stations and two bulk deposition stations. The wet/dry sites use Aerochem Metrics 201 wet/dry collectors, sampling on the event basis. Tipping bucket bulk deposition collectors are used at all five sites. Dry samples are collected concurrently with wet samples, or at least weekly during dry periods. Analyses are performed at the University of California laboratories at Tahoe and Davis.	Robert C. Leonard Director, Tahoe Monitoring Program P.O. Box 1125 Tahoe City, Calif. 95730
Integrated Lake Watershed Acidification Study (ILWAS)	Electric Power Research Institute (EPRI)	pH, conductivity, SO_4, NO_3, NH_4, Cl, Na, K, Ca and Mg. Al, DOC, total P, and total acidity analyses were performed in the past.	ILWAS currently consists of four watershed sites on the western slope of the Adirondack Mountains in New York state near Old Forge. The network operates up to seven samplers.	Sampling began in March 1978 and should continue through the end of 1981.	All sites employ Aerochem Metrics 201 wet/dry samplers. Wet deposition is collected on an event basis and dry deposition is collected weekly. Bulk samplers also are located at each site, with collection on the event basis. Analyses are conducted at the Rensselaer Polytechnic Institute.	A. H. Johannes Department of Environmental Engineering Rensselaer Polytechnic Institute Troy, N.Y. 12181

(continued on next page)

Table 1.5 (continued)

Study/Network	Funding organization	Parameters monitored	Extent and location	Period of operation	Sampling and analysis	Contact
EML Deposition Chemistry Study	Department of Energy (DOE), Environmental Measurements Laboratory (EML)	pH, conductivity, SO_4, NO_3, NH_4, Cl, PO_4, Na, K, Ca, Mg, bicarbonate. Trace metals (Al, As, Cd, Cr, Fe, Mn, Ni, Pb, V, Zn) are measured in samples from each site every three months.	The network included seven stations nationally from its inception until June 1981. Sampling outside the New York-New Jersey region ended in June 1981, but additional sampling sites are being set up within that smaller region. Currently four sites exist, two each in New York city and New Jersey.	The network was established in July 1976.	The network collects bulk, wet and dry samples monthly; event samples also are collected. HASL and Aerochem Metrics collectors are used to obtain the wet and dry samples. Analyses are performed by Rockwell International, Inc.	Herb Feely DOE-EML 376 Hudson St. New York, N.Y. 10014
Effects of Energy Production Emissions on Colorado Lakes	U.S. Geological Survey (USGS)	pH, acidity, SO_4, NO_3, NO_2, NH_4, organic N, Br, Cl, F, PO_4, Na, K, Ca, Mg	The network consists of four sites in northwestern Colorado.	Sampling began at one site in December 1980.	Wet and dry deposition is sampled with variable frequency using Leonard Mold and Die collectors. Samples are analyzed at the USGS lab in Denver, Colorado.	John T. Turk USGS Building 53, Mail Stop 415 Denver Federal Center Lakewood, Colo. 80225
Atmospheric Inputs to the Chesapeake (ATIC) Study	Environmental Protection Agency (EPA)	pH, conductivity, SO_4, NO_3, NO_2, NH_3, Cl, F, PO_4, Na, K, Ca, Mg, Be, Cd, Cr, Cu, Fe, Mn, Ni, Pb, Si, Zn, TOC, TIC, hydrocarbons	The network consists of four stations on the lower Chesapeake Bay in Virginia.	Sampling was initiated in December 1980. Present funding ends in March 1982.	Aerochem Metrics 301 wet/dry collectors are used to sample wet events, which are collected as soon as possible after the event. Analyses are conducted at the Department of Oceanography, Old Dominion University.	Terry L. Wade or George T. Wong Old Dominion University Department of Oceanography Norfolk, Va. 23508
Chemical Quality of Atmospheric Deposition in Alabama Study	U.S. Geological Survey (USGS)	pH, conductivity, alkalinity, SO_4, NO_3, NH_4, Na, K, Ca, Mg, Al, Cd, Cu, Fe, Mn, Pb, Zn	This network will consist of three sites in central Alabama.	Initial sampling will begin in January 1982.	Wet samples are collected both after major rainfall events and weekly. The first three parameters are measured in the field. All other analyses are made at the Geological Survey of Alabama laboratory.	Ira A. Giles USGS 1317 McFarland Boulevard, East Tuscaloosa, Ala. 35405
West Point Area Study	Environmental Protection Agency (EPA), Army Research Office.	pH, SO_4, NO_3, NH_4, Cl, PO_4, Na, K, Ca, Mg	Two sites are located 10 km apart on the U.S. Military Academy Reservation in West Point, New York.	Collection has occurred intermittently since 1976 at one site. A second site, to be colocated with a NADP site, will be activated in spring 1982.	Collection is on the event basis. Collection is by intensity-weighted wet-only samplers that break a storm into 0.01 inch "increments." pH is measured in the field and other analyses are conducted in the Science Research [illegible] Laboratory.	Major John K. Robertson Science Research Laboratory U.S. Military Academy West Point, N.Y. 10996

Table 1.5 (continued)

RECENTLY COMPLETED:

Northeastern Region Snow Chemistry Reconnaissance Study	Water Resource Division (WRD), U.S. Geological Survey (USGS)	pH, conductivity, SO_4, NO_3, NO_2, NH_4, F, K, Ca, Mg, As, Ba, Be, Cd, Co, Cu, Fe, Hg, Li, Mn, Mo, Ni, Pb, Se, Si, V, Zn, TIC. The suspended material from 20 sites will be analyzed for semiquantitative determinations of 80 elements and 10 major inorganic constituents.	The network consisted of 180 sites extending from Maine to Minnesota and south to eastern West Virginia and western Maryland.	The network operated from approximately December 1980 through March 1981.	Collectors consisted of 18 inch diameter, 6 foot high cardboard tubes (sonotubes) with polyethylene bags. Three-month bulk collections were conducted. All analyses were done by the National Water Quality Laboratory in Denver, Colo.	Norman E. Peters WRD, USGS P.O. Box 744 Albany, N.Y. 12201
Oxidation Scavenging Characteristics of April Rain (OSCAR) High-Density Precipitation Chemistry Experiment	This project was undertaken as part of the MAP3S/RAINE study, which is supported by the Environmental Protection Agency (EPA) and the Department of Energy (DOE).	pH, conductivity, SO_4, SO_2, NO_3, NO_2, NH_4, Cl, PO_4, Na, K, Ca, Mg, Al, Pb	The high-density network consisted of 47 sites within a 100 km^2 area surrounding Ft. Wayne, Ind.	The project operated for four precipitation events during April 1981.	Each site was equipped with a nine-stage sequential precipitation collector. The first eight stages each collected 0.7 mm of precipitation and the final stage collected the remaining precipitation of the event, up to 11 mm. All analyses (except field pH) were conducted at Pacific NW Laboratories in Richland, Wash.	Richard C. Easter Battelle, Pacific NW Laboratories P.O. Box 999 Richland, Wash. 99352
Oxidation Scavenging Characteristics of April Rain (OSCAR) Intermediate-Density Network	This project was undertaken as part of the MAP3S/RAINE study, which is supported by the Environmental Protection Agency (EPA) and the Department of Energy (DOE).	pH, conductivity, SO_4, NO_3, NO_2, NH_4, Cl, PO_4, Na, K, Ca, Mg, Al	The intermediate-density network consisted of each of the nine MAP3S sites adding from one to five satellite sites, plus 11 stations not connected with the MAP3S program, for a total of 38 sites throughout the northeast. This density provided approximately 100–150 km spacing between stations.	The project operated during four precipitation events in April 1981.	The intermediate-density network sampled precipitation sequentially using a funnel and jar collection system. All analyses (except field pH) were conducted at Pacific NW Laboratories in Richland, Wash.	Gilbert S. Raynor Department of Energy & Environment Brookhaven National Laboratory Upton, N.Y. 11973
Acid Precipitation in Hartford, Conn. Area Study	TRC Environmental Consultants, Inc.	pH	This network consisted of 12 stations within a 48 km radius of Hartford, Conn.	Initial sampling began in August 1980. However, quality assurance analyses indicated problems with pH determination and operation was suspended in September 1981. The network is currently under review.	Samples were collected in a plastic wedge-type rain gage on the event basis. Occasionally sequential sampling was undertaken. pH measurements were determined by the use of narrow range pH paper.	Michael Anderson TRC Environmental Consultants, Inc. 800 Connecticut Ave. E. Hartford, Conn. 06108
EPRI Eastern Regional Chemistry Network	Electric Power Research Institute (EPRI)	pH, acidity, SO_4, NO_3, NH_4, Cl, PO_4, Na, K, Ca, Mg, DOC, Al, total acidity, and strong acidity	The network originally consisted of nine sites spread throughout the northeastern United States.	Sampling was initiated in August 1978 and completed in June 1980.	Each site was equipped with two Aerochem Metrics 201 wet/dry collectors. Wet-only samples were collected daily and combined over a week. Samples were analyzed by Rockwell International, Inc.	Ralph Perhac Energy Analysis & Environment Division Electric Power Research Institute 3412 Hillview Ave. Palo Alto, Calif. 94304

(continued on next page)

Table 1.5 (continued)

Orange County Network	Environmental Management Agency, County of Orange, California	pH, conductivity, SO_4, NO_3 plus NO_2, NH_4, TKN, PO_4, Pb, Zn, TDS.	This network consisted of 11 sites from 1974 to 1978 in Orange County, approximately 60 km southwest of Los Angeles. The network was reduced to two sites in 1979.	This network was established with two sites in 1973.	The network uses a self-designed wet-only precipitation collector and sampling is on the event basis. Analyses are performed by a contractor laboratory under a quality control program administered by the Environmental Research Laboratory of Orange County.	Chief of Environmental Management Agency Environmental Management Agency Environmental Resources Section P.O. Box 4048 Santa Anna, Calif. 92702
University of Colorado Study	U.S. Forest Service (through the Eisenhower Consortium), University of Colorado	pH, conductivity, H, SO_4, NO_3, NO_2, NH_3, organic N, Cl, P, Na, K, Ca, Mg, DOC, and DON. Also, C, H, N, and P in dry particulate matter.	One site with two stations one kilometer apart is operated in the Como Creek Watershed, Boulder County, Colorado.	Sampling began in the spring of 1975.	Bulk deposition is collected weekly and analyses are generally performed within six hours of collection at the University of Colorado laboratory. A dry-only fraction was collected and analyzed for five and one-half years.	Michael C. Grant Department of Environmental, Population & Organismic Biology University of Colorado Boulder, Colo. 80309
Shenandoah Watershed Acidification Study	Air Quality Office, National Park Service	pH, conductivity, SO_4, NO_3, NH_4, Cl, Na, K, Ca, Mg, Si	The study includes two watersheds centered 32 km northwest of Charlottesville, Va.	The network began operation during November 1979.	The study utilizes Hubbard Brook-type funnel collectors. Analyses are performed at the Department of Environmental Sciences, University of Virginia.	James N. Galloway Dept. of Environmental Sciences University of Virginia Charlottesville, Va. 22903
Hubbard Brook Ecosystem Study	National Science Foundation	pH, conductivity, SO_4, NO_3, NH_4, Cl, P, Na, K, Ca, Mg and SiO_3. Occasionally Al, DOC, and DON are tested for. Trace metal sampling existed from 1975 to December 1979 and has recently been resumed.	Two to four sites are located within the 3035 hectare watershed near West Thornton, N.H. The number of sites depends on the number of projects in operation.	Precipitation samples have been collected since 1963.	Weekly bulk precipitation is collected in Hubbard Brook-type funnel collectors. One NADP site is located within the Hubbard Brook Experimental Forest, with collection performed using an Aerochem Metrics 201 wet/dry collector. At this site, the study also maintains a similar wet/dry sampler. pH and conductivity are measured at the site. Samples are shipped to Cornell University for chemical analysis.	G. E. Likens Section of Ecology & Systematics Langmuir Lab Cornell University Ithaca, N.Y. 14850
University of Arkansas Site	Office of Water Resources Research, U.S. Department of the Interior	pH, conductivity, SO_4, NO_3, NH_4, PO_4, Cl, K, Na, Ca, Mg, Fe, Mn, Zn	The single station is located at Fayetteville, Ark.	Current collection and analysis procedures have been in use since April 1980. Other monitoring efforts have existed for several years. The site is also a member of the NADP network since May 1980.	The site is equipped with an Aerochem Metrics 201 wet/dry sampler. A second wet/dry collector collects wet deposition episodically and dry deposition bimonthly. Trace metal analyses are performed at the University of Arkansas laboratory, with other analyses performed at the Illinois State Water Survey.	George H. Wagner Geology Department University of Arkansas Fayetteville, Ark. 72701

(continued on next page)

Table 1.5 (continued)

Study/Network	Funding organization	Parameters monitored	Extent and location	Period of operation	Sampling and analysis	Contact
Oak Ridge National Laboratory (ORNL) Site	Department of Energy (DOE), Electric Power Research Institute (EPRI)	pH, conductivity, SO_4, NO_3, NH_4, Cl, PO_4, Na, K, Ca, Mg, Cd, Mn, Pb, Zn, strong and weak acidity	Currently one centralized monitoring site is used for the collection of data for both the NADP and MAP3S networks. Previously, up to five permanent stations existed in the Walker Branch Watershed. Temporary sites occasionally operate to satisfy various research projects.	The ORNL monitoring effort has existed since 1967 for hydrological monitoring and since 1976 for precipitation chemistry monitoring.	The permanent site utilizes an Aerochem Metrics 201 wet/dry deposition collector. Wet deposition samples are collected weekly and dry deposition biweekly, as part of the NADP network. Wet-only samples are collected on the event basis for the MAP3S network. Analyses are performed at the Illinois State Water Survey, at Pacific NW Laboratories, and at Oak Ridge National Laboratory.	S. E. Lindberg Oak Ridge National Laboratory Environmental Sciences Division Oak Ridge, Tenn. 37830
University of California at Berkeley Study	California Air Resources Board, Agricultural Experiment Station of the University of California at Berkeley	pH, conductivity, SO_4, NO_3, NH_4, Cl, Na, K, Ca, Mg, Fe, Mn, Zn, Cl, Fe	This site is located at Berkeley, Calif., approximately 20 km east of the San Francisco Bay.	Initial monitoring at Berkeley began in December 1974. This site was also a member of the California Air Resources Board (CARB) network, established in November 1978 and completed in May 1979. This site has existed as an independent site the past two rainy seasons.	Samples are collected on an event basis with an Aerochem Metrics 201 wet/dry collector. Analyses are performed at the University of California at Berkeley laboratory.	John G. McColl Department of Plant & Soil Biology University of California Berkeley, Calif. 94720
Within-Event Sequential Precipitation Chemistry Study	Department of Energy (DOE), Environmental Protection Agency (EPA)	pH, conductivity, SO_4, NO_3, NO_2, NH_4, Cl, Na	One site is located at Brookhaven National Laboratory in Upton, N.Y.	Monitoring began in June 1976. An additional station is planned.	Automatic sequential precipitation samplers developed by Brookhaven National Laboratory are used to collect hourly samples during precipitation events. Analyses are performed by the Analytical Chemistry Laboratory of Brookhaven National Laboratory.	Gilbert S. Raynor Atmospheric Sciences Division Department of Energy and Environment Brookhaven National Laboratory Upton, N.Y. 11973
Global Precipitation Chemistry Project (GPCP)	National Oceanic and Atmospheric Administration (NOAA), Environmental Protection Agency (EPA), Department of Energy (DOE)	pH, SO_4, NO_3, NH_4, Cl, Na, K, Ca, Mg and SiO_4. Also, PO_4, acidity and weak organic acids in selected samples.	Currently one North American station, located in central Alaska, is in operation. In addition, the network includes four other sites (southern Indian Ocean, Bermuda, northern Australia and southern Venezuela), with a sixth site in Argéntina presently readying for collection. Future plans call for expansion to 11 stations.	The network began operations in April 1979.	Four different types of collectors are used in the GPCP, depending on site conditions: Aerochem Metrics 201 wet/dry, HASL wet/dry, Hubbard Brook bulk and a GPCP-type collector designed especially for this project. Samples are collected on the event basis and special measures are used to minimize dry deposition in bulk collections. Field pH is measured at each station. Laboratory pH and all other analyses are performed at the University of Virginia.	James N. Galloway or William C. Keene Department of Environmental Sciences University of Virginia Charlottesville, Va. 22903

Table 1.5 (continued)

Study/Network	Funding organization	Parameters monitored	Extent and location	Period of operation	Sampling and analysis	Contact
California Air Resources Board, (CARB) Network*	California Air Resources Board	The 1978–79 effort consisted of the monitoring of pH, conductivity, SO_4, Cl, Na, K, Ca, Mg, Cu, Fe, Ni, Zn, and occasionally NH_4 and NO_3. The 1981–82 effort consisted of pH and conductivity analyses.	The UC/CARB network consisted of up to eight sites mainly in the central California area for the 1978–79 effort. Six sites, five in the vicinity of Los Angeles and one near San Diego, existed for the 1981–82 rainy season.	The network has operated during the 1978–79 and 1981–82 rainy seasons. Future expansion is likely.	Each site employed Aerochem Metrics 201 wet/dry precipitation collectors. For the 1978–79 effort, samples were collected on an event basis and shipped to the University of California laboratories at Berkeley or Tahoe for analyses. For the 1981–82 effort, samples were collected weekly and were analyzed by CARB.	Doug Lawson Air Resources Board 1102 Q St. P.O. Box 2815 Sacramento, Calif. 95812
Florida Atmospheric Deposition Study	Environmental Protection Agency (EPA)	pH, conductivity, SO_4, NO_3, NO_2, TKN, NH_4, Cl, PO_4, total P, F, Na, K, Ca, and Mg. Cd, Cu, Pb, SiO_2, and Zn were measured quarterly.	A network of up to 24 sites was operated throughout Florida from 1977 to 1979. A reduced network of seven wet/dry collectors existed during 1980.	Monitoring existed from mid-1976 to mid-1981.	Aerochem Metrics 201 wet/dry collectors were utilized, with event wet deposition collection at Gainesville and biweekly or weekly wet deposition collection at other sites. Dry deposition was collected biweekly at all sites. Analyses were performed at the University of Florida laboratory.	Charles D. Hendry Environmental Science and Engineering, Inc. P.O. Box ESE Gainesville, Fla. 32602
Minnesota-North Dakota Precipitation Monitoring Network	Department of Energy (DOE), University of Minnesota Computer Center	pH, conductivity, alkalinity, SO_4, NO_3, NH_4, Cl, total P, Na, K, Ca, Mg, Al, Cd, Cr, Cu, Fe, Mn, Ni, Pb, Zn	Three sites existed along a transect from southeastern North Dakota to northeastern Minnesota.	Sampling took place from April 1978 to June 1979.	Aerochem Metrics 201 wet/dry precipitation collectors were used to sample wet precipitation on the event basis and dry fallout samples biweekly or monthly. Analyses were performed at the University of Minnesota.	E. Gorham Department of Ecological and Behavioral Biology 108 Zoology Bldg. 318 Church St., SE University of Minnesota Minneapolis, Minn. 55455
Pennsylvania Cooperative Fisheries Research Unit Study	U. S. Fish and Wildlife Service, Pennsylvania Fish Commission	pH, alkalinity, acidity, SO_4, NO_3, PO_4	The monitoring effort began with three sites in north central Pennsylvania (approximately 41°N and 78°W).	The first precipitation collectors were installed in October 1976. The network ceased operations in August 1980.	The network used Taylor two liter bulk rain collectors, with samples collected about every 10 days.	Dean Arnold 208 Erwin W. Mueller Lab The Pennsylvania State University University Park, Pa. 16802
Elk Mountain, Wyoming Site	Office of Water Research and Technology, Department of Interior; National Science Foundation	pH, SO_4, NO_3, NO_2, Cl, F, PO_4, Na, K, Ca, Mg, plus multi-element scans.	One site was located at Elk Mountain (elevation 3,533 m), approximately 160 km northwest of Laramie.	Snow samples were collected at Elk Mountain independently by the two researchers during winter 1980.	Snow pack and snowfall samples were collected on the event basis by scoops and coring equipment and were analyzed at the University of Rhode Island or the University of Wyoming.	Carol Baird 8820 Cottonwood Lenexa, Kans. 66215 Richard J. McCaffrey 60 Crestwood Dr. Narragansett, R.I. 02882

* This network was reactivated during the 1981–82 rainy season with six sites, five near Los Angeles and one near San Diego. pH and conductivity analyses were performed by the California Air Resources Board on samples collected weekly. Future expansion is likely. (Network information updated and footnote added in proof. As revised, this network entry should now be listed preceding the Tahoe Monitoring Program on p. 605.)

Table 1.5 (continued)

Study/Network	Funding organization	Parameters monitored	Extent and location	Period of operation	Sampling and analysis	Contact
NATIONAL:						
Canadian Network for Sampling Precipitation (CANSAP)	Atmospheric Environment Service, Environment Canada	pH, conductivity, alkalinity, acidity, SO_4, NO_3, NH_4, Cl, Na, K, Ca, Mg	The network consists of 59 stations distributed across Canada, including Canada's nine WMO stations.	The network was established in 1977.	Sampling stations employ automatic, wet-only Sangamo Type A precipitation collectors. Samples are collected on a daily basis, combined for one month periods and stored in the dark at 2°C until the sample is analyzed at the Inland Waters Directorate (IWD) Water Quality Lab at the Canadian Centre for Inland Waters in Burlington.	Malcolm Still Atmospheric Environment Service 4905 Dufferin St. Downsview, Ontario Canada M3H 5T4
REGIONAL:						
Canadian Centre for Inland Waters (CCIW) Precipitation Network	Canadian Centre for Inland Waters	pH, conductivity, alkalinity, SO_4, NO_3, NH_4, Cl, P, Na, K, Ca, Mg, Cu, Fe, Pb, Ni, Zn, SiO_3	The network consists of 15 sites around the Canadian shores of the Great Lakes.	The initial eight stations began monitoring in 1969.	Sangamo wet/dry collectors are used to collect monthly samples. Analyses are performed at the CCIW labs.	C. H. Chan Canadian Centre for Inland Waters Water Quality Branch 867 Lakeshore Rd. Burlington, Ontario Canada L7R 4A6
Canadian Air & Precipitation Monitoring Network (APN)	Atmospheric Environment Service, Environment Canada	pH, conductivity, acidity, H, SO_4, NO_3, NH_4, Cl, P, K, Ca, Mg	The network includes six sites, each located east of the Ontario-Manitoba border.	The network began with three sites during November 1978.	Samples are collected daily using a wet-only precipitation sampler. Every two weeks, samples are shipped to the Canadian Centre for Inland Waters laboratory in Burlington, Ontario, for analyses.	L. A. Barrie Atmospheric Environment Service 4905 Dufferin St. Downsview, Ontario Canada M3H 5T4
Environmental Protection Service (EPS) Atlantic Precipitation Monitoring Program	Environmental Protection Service, Environment Canada	pH, SO_4, NO_3, NH_3, Cl, Na, Ca, Mg	The network currently consists of six sites—three in Nova Scotia, two in Newfoundland and one on Prince Edward Island.	The first site was established in December 1978.	Samples are collected with a Sangamo Type A precipitation collector. The three Nova Scotia sites collect precipitation on the event basis, whereas the other three sites collect weekly. Analyses are performed at the Bedford Institute of Oceanography in Dartmouth, Nova Scotia, and at the Newfoundland Forest Research Centre in St. John's, Newfoundland.	J. R. Machell Environmental Protection Service Environment Canada Queens Square 45 Alderny Dr. Dartmouth, Nova Scotia Canada B2Y 2N6

(continued on next page)

Table 1.5 (continued)

Study/Network	Funding organization	Parameters monitored	Extent and location	Period of operation	Sampling and analysis	Contact
PROVINCIAL:						
Quebec Network for the Collection of Precipitation	Quebec Ministry of the Environment	pH, conductivity, alkalinity, acidity, SO_4, NO_3, NH_4, Cl, F, Na, K, Ca, Mg	The network consisted of 40 sites as of 1 April 1982 and five sites will be added by summer 1982.	The first site began operation during August 1980.	Samples are collected using samplers similar to the Sangamo wet/dry collectors. Samples are collected weekly with analyses performed at the Ministry of Environment laboratories in Saint Foy.	Levis Talbot Ministère de l'Environnement Qualité des eaux 2360, chemin Ste. Foy Ste-Foy, Quebec Canada G1V 4H2
Acidic Precipitation in Ontario Study (monthly network)	Air Resources Branch, Ontario Ministry of Environment	pH, conductivity, acidity, SO_4, NO_3, NH_4, TKN, P, Na, K, Ca, Mg, Al, Cd, Cu, Fe, Mn, Ni, Rb, Zn	This network consists of 34 sites throughout Ontario, with future expansion expected.	The network has operated since September 1980 and at least five years of data acquisition are expected.	All sites are equipped with Sangamo Type A wet/dry collectors. Samples are collected on a monthly basis and are analyzed at the Ontario Ministry of the Environment Laboratory Service Branch in Toronto.	Walter H. Chan Air Resources Branch Ontario Ministry of the Environment 880 Bay St. Toronto, Ontario Canada M5S 1Z8
Acidic Precipitation in Ontario Study (event network)	Air Resources Branch, Ontario Ministry of Environment	pH, conductivity, acidity, SO_4, NO_3, NH_4, Na, K, Ca, Mg, gaseous and particulate N and S	Sixteen sites make up this network: four each in the Kingston, London, Dorset, and Atikokan areas.	This network has operated since January 1981.	Sites are equipped with Aerochem Metrics 201 wet/dry samplers. Samples are collected on a 24 h modified event basis and are analyzed at the Ministry's Laboratory Service Branch in Toronto.	Walter H. Chan Air Resources Branch Ontario Ministry of the Environment 880 Bay St. Toronto, Ontario Canada M5S 1Z8
Ontario Hydro Atmospheric Deposition Monitoring Network	Chemical Research Department, Ontario Hydro Research Division	pH, SO_4, NO_3, NH_4, Cl, Na, K, Ca, Mg	The network currently includes six stations located throughout Ontario.	This network was established in 1975.	Sites are equipped with wet-only Sangamo collectors. Precipitation is sampled on an event basis and analyzed at the Ontario Hydro Laboratory.	O. T. Melo Chemical Research Department Ontario Hydro Research Division 800 Kipling Ave. Toronto, Ontario Canada M8Z 5S4
Precipitation Quality Monitoring Program	Department of the Environment, Province of Alberta	pH, conductivity, SO_4, NO_3, NH_4, Cl, total P, Na, K, Ca, Mg	The network consisted of six sites throughout the province as of mid-1981 and will be expanded to 10 sites in 1982.	Sampling was initiated in April 1978.	Bulk samples are collected monthly using Sangamo Type A precipitation collectors. Analyses are performed by the Alberta Environment Centre at Vegreville, Alberta.	J. E. Torneby or R. P. Angle Air Quality Control Branch Alberta Environment 9820–106 St. Edmonton, Alberta Canada T5K 2J6
Nova Scotia Department of the Environment Precipitation Network	Nova Scotia Department of the Environment	pH, conductivity, alkalinity, acidity, SO_4, NO_3, NO_2, NH_3, total N, Cl, total and dissolved P, Na, K, Ca, Mg, Al, As, Cd, Co, Cr, Cu, Fe, Mn, Ni, Pb, Se, Zn, TOC	Currently this network includes five sites throughout Nova Scotia. A maximum of nine sites operated between September 1977 and December 1979.	The network began operation in September 1977, and should continue at least until 1984.	Each site is equipped with a Sangamo wet/dry collector. Weekly samples are collected and analyzed at the Environmental Chemistry Laboratory of the Department of Health in Halifax.	J. Underwood Nova Scotia Department of the Environment P.O. Box 2107 Halifax, Nova Scotia Canada B3J 3B7

Table 1.5 (continued)

Environment New Brunswick Precipitation Monitoring Network	Environment New Brunswick, Province of New Brunswick	pH, conductivity, alkalinity, SO_4, NO_3, NH_4, Cl, Na, K, Ca, Mg	The network currently consists of three sites, with two additional stations to be added by 30 May 1982. At this time one of the original three sites will cease operations.	The initial stations were established in November 1980. The network will be reviewed at the end of 1986.	Wet precipitation samples are collected daily with Sangamo Type A collectors and combined to form a monthly composite sample. Analyses are performed by Laboratory Services, Environment New Brunswick at Fredericton, New Brunswick.	Jane Spavold Environmental Service Branch Environment New Brunswick P.O. Box 6000 Fredericton, New Brunswick Canada E3B 5H1
LOCAL:						
Long Range Transport—Snow Total Deposition Study	Noranda Mines Limited	pH, SO_4, SO_2, NO_3, Cl, Na, K, Ca, Mg, selected heavy metals	Samples are collected at 28 sites, all in northwest Quebec.	Initial sampling began in 1977.	Snow core samples are collected once a year. Analyses are performed by Noranda Mines Limited.	F. Frantisak Director of Environmental Services Noranda Mines Limited P.O. Box 45 Toronto, Ontario Canada M5L 1B6
Event Rain Sampling and Chemical Analyses in the Oil Sands Area of Northern Alberta Study	Research Management Division, Alberta Environment	pH, conductivity, SO_4, NO_3, Cl, F, Na, K, Ca, Mg, Al, Cd, Cu, Fe, Mn, Ni, Pb, V, Zn	The network consists of 13 sites in northeastern Alberta, near Ft. McMurray.	The network began in May 1981. Expansion to the rest of the province is proposed for 1982.	Samples are collected on the event basis, using plastic bags fitted in a large barrel. Analyses are performed at the Alberta Environment provincial laboratory at Vegreville, Alberta.	Air System Manager Research Management Division Alberta Environment 9820–106 St. Edmonton, Alberta Canada T5K 2J6
Acid Precipitation in Ontario Study, Limnology Unit Network	Ontario Ministry of the Environment	pH, conductivity, alkalinity, SO_4, NO_3, NH_4, TKN, Cl, total P, Na, K, Ca, Mg, Al, Cu, Fe, Mn, Ni, Pb, Si, Zn, DOC, DIC	The network has included up to 19 stations located around lakes in Ontario. Currently five sites exist within a 50 km radius of Dorset, approximately 225 km north of Toronto.	The network was established in June 1976. The five current stations probably will be kept in operation for at least five more years.	Bulk collectors are present at all five sites. One site has two Earth Science wet deposition collectors and two bulk collectors. Samples are collected when there is a large enough volume for analysis (on the average of seven to 10 days). Perishable parameters are analyzed within 24 h of collection on site, while the remaining parameters are analyzed at the Ontario Ministry of the Environment laboratories in Toronto.	P. J. Dillon Limnology and Taxonomy Section Ontario Ministry of the Environment Box 213 Rexdale, Ontario Canada M9W 5L1
Northwest British Columbia Precipitation Monitoring Network	Atmospheric Environment Service, Ministry of Environment	pH, strong and total acidity, SO_4, NO_3, Cl, F, PO_4, Na, K, Ca, Mg, Al	The network consists of five sites in northwest British Columbia.	The network was initiated in September 1980.	Samples are collected after every event with a modified Hubbard Brook type collector. Analyses are performed by the British Columbia Ministry of Environment.	M. S. Kotturi Air Studies Branch Ministry of Environment Parliament Buildings Victoria, British Columbia Canada V8N 1X4
British Columbia Coastal Site Precipitation Monitoring Network	Atmospheric Environmental Service, Ministry of Environment	pH, strong and total acidity, SO_4, NO_3, Cl, F, PO_4, Na, K, Ca, Mg, Al	The network consists of three coastal sites in British Columbia.	The network was initiated in September 1980.	Samples are collected after every event with a modified Hubbard Brook type collector. Analyses are performed by the British Columbia Ministry of Environment.	M. S. Kotturi Air Studies Branch Ministry of Environment Parliament Buildings Victoria, British Columbia Canada V8N 1X4

(continued on next page)

Table 1.5 (continued)

Study/Network	Funding organization	Parameters monitored	Extent and location	Period of operation	Sampling and analysis	Contact
Newfoundland Provincial Precipitation Monitoring Network	Department of Environment, Government of Newfoundland and Labrador	pH, conductivity, acidity, SO_4, NO_3, NH_4, Cl, Na, K, Ca, Mg	The network consists of three sites in eastern Newfoundland.	The network started with two sites in September 1980 and is projected to continue for 8 to 10 years. The network is proposed to expand to six sites by 1983.	An automatic wet-only precipitation collector is used for weekly sampling. All chemical analyses are performed at the Canadian Forestry Service laboratory in St. John's, Newfoundland.	Les Hulett Department of Environment Government of Newfoundland and Laborador 100 Elizabeth Ave. St. John's, Newfoundland Canada A1C 1P7
Long Range Transport Study (LORA)	Noranda Mines Limited	pH, SO_4, SO_2, NO_3, Cl, Na, K, Ca, Mg and selected heavy metals in precipitation. SO_4, SO_2, NO_3, NO_2, and NH_3, in ambient air.	At its inception, the network consisted of seven sites in northwest Quebec. In 1979 the network was cut back to its current size of three sites.	Initial sampling began in 1977.	Wet-only samples are collected by event and also for eight day composite samples. Twenty-four hour ambient air samples also are collected.	F. Frantisak Director of Environmental Services Noranda Mines Limited P.O. Box 45 Toronto, Ontario Canada M5L 1B6
Manitoba Network for Precipitation Collection (MNPC)	Environmental Management Division, Province of Manitoba	pH, SO_4, NO_3, conductivity, acidity, Ca, NH_4, Mg, Na, Cl and K (in order of priority)	The network consists of two sites in northeast Manitoba.	The network was established in November 1980.	The network collects wet samples daily and dry samples monthly, utilizing a Sangamo Type A sampler. Wet samples are sent to a central laboratory weekly for analysis.	Dave Bezak Environmental Management Division Box 7, Building 2 139 Tuxedo Avenue Winnepeg, Manitoba Canada R3C OV8
RECENTLY COMPLETED:						
Ontario Ministry of the Environment Air Resources Branch (ARB) Precipitation Network	Ontario Ministry of the Environment	pH, acidity, SO_4, NO_3, NH_4, Cl, F, Na, K, Ca, Mg, Al, Cd, Cr, Cu, Fe, Ni, Pb, Si, Zn	Located in the Sudbury area, originally 10 sites operated, with expansion to 21 sites during mid-1979.	Sampling began in December 1977. The network was terminated in May 1980.	Wet deposition was collected with Sangamo Type A collectors. Bulk deposition also was collected at four stations.	Walter H. Chan Air Resources Branch Ontario Ministry of the Environment 880 Bay St. Toronto, Ontario Canada M5S 1Z8

TABLE 3. Mexican acid rain monitoring studies—National.

Study/Network	Funding organization	Parameters monitored	Extent and location	Period of operation	Sampling and analysis	Contact
Acid Rain in Mexico City Study	Department of Environmental Pollution, University of Mexico; Mexican Meteorological Service of the Ministry of Agriculture and Water Resources	pH, SO_4, NO_3, and NH_4, with conductivity to be added	As of May 1981 (the beginning of the rainy season), the network expanded to 25 sites nationally, including sites in southern Mexico and sites near the U.S.–Mexico border.	Sampling began during May 1980, with 12 precipitation collectors in Mexico City.	Samples are collected on an event basis in polyethylene bottles. Analyses are performed at the National University of Mexico in Mexico City on both event and weekly composite samples.	Humberto Bravo A. Depto. Contaminacion Ambiental Centro de Ciencias de la Atmosfera Ciudad Universitaria Mexico Mexico 20, D.F.

1.4.4 Meteorological Data

Meteorological data requirements include surface temperature, surface winds, upper level winds and temperatures (including dew point) at mandatory and special levels, precipitation, cloud amount and type, direct and net radiation. For the long-range transport model, the coverage must include all of Eastern and Central North America, so that available data sources are restricted to the National Meteorological Centers. Archived data of surface and upper air observations is available from National Climate Centre, Asheville and the Canadian Climate Center, Downsview. Analysis data is available for restricted periods on request from the CMC (Canadian Meteorological Center) as well as NCAR (Jenne, 1975) and NOAA (Ropelewski et al, 1980). These references provide catalogues of available data by type and period. The NCC publishes a catalogue of all available data and data summaries (Butson and Hatch, 1975) which can be used to order data sets. The Canadian Climate Center has a similar catalogue.

Except for standard surface observations, the density of observing points is of the order of 300 to 400 km . Therefore, for the mesoscale model, it will be necessary to use specialized data obtained over small regions or short periods to increase data density. Large-scale

experiments such as PEPE can be used to provide verification data of high resolution.

The procedure for generating the meteorological data base will be to assemble primarily the observational data with some supporting analysis data on the large scale. For selected periods to be used for validation, additional data will be located and assembled into the data archive.

1.5 Gridding Procedures

SUBSYS 2 provides a number of programs for the analysis of meteorological and physical parameters and the gridding of emissions data. Some of the procedures to be used for this analysis are described in this section.

1.5.1 Emissions

The primary emissions data files provide point source information and area source information on county or equivalent subdivision basis. For the LRT grid, most counties are sub-grid scale, and the standard practice is to allocate area sources to the grid by the location of the county centroid.

For the Mesoscale grid, the grid assignment must take account of sub-county detail. It is proposed to use available information on population census and land use to apportion total county emissions to the 10 km mesoscale grid (Benkovitz, 1982).

Both dispersion models will have ten vertical levels. It will therefore be necessary to apportion the emissions within each grid cell among these levels. This requires calculation of plume rise for point sources, using Briggs (1975), and distribution of plume mass by layer. For area sources, a standard distribution scheme will be used.

The information on time variability of emissions will be used to define multiple grids of emissions, one for each emission condition.

1.5.2 Physical Data

Gridded topography data will be produced for the LRT and Mesoscale grids using bi-cubic spline interpolation of existing digitized topographic data. Two files will be produced for the two grid resolutions, and smoothing algorithms applied to eliminate sub-grid scale detail.

For a particular model run, the appropriate subsection of the gridded data will be extracted to generate an operational data file.

Digitizing and gridding of land use maps would be carried out either on the OCRS (Ontario Center for Remote Sensing) computerized system (Landsat data) or manually for high resolution from detailed maps. The gridding is carried out by assigning to a grid square the dominant land use type within the grid square. Eight or more categories of land use will be used to provide adequate resolution. For the LRT case, a land use map for most of the area of interest to 0.5^{o} degree resolution already exists (Sheih et al, 1979).

Roughness length is characterized in terms of the land use classification using the scheme of Wieringa (1980) .

1.5.3 Meteorological Data

The Wind Field Model described in Section 3 carries out the gridding of winds, potential temperature, relative humidity, u_* and stability.

Separate programs are needed to produce gridded fields of precipitation and cloud cover as described below.

Precipitation

Precipitation amount (hourly) will be gridded using an inverse distance weighting scheme. Only stations within a prescribed radius of influence are averaged. In areas where observational data of hourly precipitation is sparse, observations of rain intensity from Class A stations will be used to supplement 24-hour totals (which are available on a denser network of stations) in order to apportion the total daily rainfall. The precipitation data for some networks is not corrected for undercatch and exposure variability. It is proposed that a standard procedure be adopted to make such corrections to the network date.

In addition to total hourly precipitation within each grid cell, a measure of the intermittency (spatially) of the rainfall will be defined by the proportion of stations within the radius of influence which are reporting precipitation.

For the mesoscale grid, the use of radar data will be evaluated. Radar information is now routinely digitized for transmission, and could be stored for selected periods in the future on request. The radar information provides a direct measure of intensity within its range of observation. By sorting and merging the information from a number of radar installations, a complete field of precipitation intensity can be produced. Time averaging of the data would be required to produce precipitation information corresponding to the model time resolution.

Cloud Cover

Information on cloud cover and type is used by the wind field model to determine insolation, and by the dispersion model to define diffusivity and estimate in-cloud wet scavenging processes.

The standard observations of cloud amount at observing stations can be handled in the same way as precipitation to produce gridded fields of average cloud cover. For selected periods, this information can be supplemented by satellite photos which would be manually interpreted to the grid.

Cloud type information at the observing stations within a specified radius of influence can be used to define the predominant type for the grid within several layers. This will provide a coded grid of cloud types which would be used in the wet scavenging module to define the relevant operative processes.

2. REVIEW OF STATE OF THE ART WIND FIELD MODELS

The following review of modeling techniques can be broken down into two categories: The first category of models contains those which are presently available and have been used for long-range transport and diffusion estimates: The second contains models which are presently available from related fields (such as Applied Meteorology) but which have not been implemented for LRT models.

Clearly the flow in the atmospheric boundary layer (ABL) is a critical component of the wind field model. Review of ABL models is deferred to Section 3 where they are more easily discussed within the context of present model development.

Tables 2.1, 2.2 and 2.3 give a brief summary and further details of some of the models and techniques reviewed in this section and in Section 3.

2.1 Available Wind Field Techniques Presently Used For LRT Models

As a general observation from a review of the literature, LRT modelers have devoted most attention and effort to atmospheric diffusion processes, and to chemical reaction mechanisms and

Table 2-1

Wind Field Models and Objective Analysis Methods

AUTHOR	YEAR	MESOSCALE OR LONG RANGE	NO. OF LAYERS	HORIZONTAL GRID	HORIZONTAL RESOLUTION	NO. OF DIMENSIONS	FUNCTIONAL CONSTRAINTS ON MASS-CONSIS.	COMMENTS
Tarbell et al.	1981	MS	6/7	30 x 35		3	$\vec{V} = \vec{V}_\phi + \vec{V}_\psi$	
Chang et al.	1980	MS			30/140 km	3	none	Using Bleck (1975) technique
Anthes et al.	1979	MS	6	70 x 70	60 km	3		See Keyser (1978) paper for details
Sasaki	1970b	LR						
Sasaki	1970a	MS	any	any		3	$\nabla \cdot \vec{V} = 0$	or any other constraints bounding the divergence
Sasaki	1958							
Dickerson	1978	MS	1	65 x 65		2	$\nabla \cdot \vec{V} = 0$	Variational method, weak constraint
Fankhauser	1974	MS	18	24 x 24	10 km	3	$\nabla \cdot \vec{V} = 0$	Kinematic method, weak constraint
Anthes	1976	MS	5	30 x 50	40 km	3	$\vec{V} = \vec{V}_\phi + \vec{V}_\psi$	non linear balance equation
O'Brien	1970	MS LR	any			3	$\nabla \cdot \vec{V} = 0$	Variational method, weak constraint
Stephens et al.	1978	MS		18 x 28	1 km	2	$\vec{V} = \vec{V}_\phi + \vec{V}_\psi$	Fourier Transform
Hoke et al.	1976	MS				2	P.E.	Dynamic initialization
Sherman	1978	MS	28	25 x 33	4.3 km	3	$\nabla \cdot \vec{V} = 0$	Variational method, weak constraint
Keyser	1978	MS	10	50 x 50	60 km	3	$\vec{V} = \vec{V}_\psi + \vec{V}_\phi$	non-linear balance equation
Tuerpe	1978	MS	8	30 x 40		3	$\nabla \cdot \vec{V} = 0$	Finite element variational method
Liu et al	1978	MS	5	40 x 50	2 km	3	$\nabla \cdot \vec{V} = 0$	Parameterization of vertical fluxes
Liu et al	1976	MS	1	40 x 25	3 km	3	$\nabla \cdot \vec{V} = 0$	Iterative method, observed winds are unchanged
Lamb	1981	MS	3			3	$\vec{V} = \vec{V}_\psi + \vec{V}_\phi$	"physical" boundary conditions

Table 2 - 2

Interpolation Techniques

AUTHOR	YEAR	NUMRER OF DIMENSIONS	COMMENTS
Bleck	1975	3	Optimum interpolation using geopotential and Montegomery potential
Cline	1974	1	Curve fitting using splines under tension
Hardy et al.	1978	2	Principal component analysis
Lee	1975	2	Surfate winds calculations using Rose's technique (see Rose, 1973) and isallobaric winds
Rose	1973	2	Inverse square interpolation
Shapiro	1973	2	High order interpolation from coarse to fine mesh grids
Walton et al	1978	2	Principle component analysis (see Hardy et al. 1978) plus least square determination of "typical" patterns

Table 2.3 - Wind Field Models

		INPUT DATA	NO. OF LAYERS	LAYER WINDS	VERTICAL VELOCITY	TOPOGRAPHY	MIXING HEIGHT
Fankhauser Mesoscale analysis of severe storms	1974	Rawinsondes - special releases to give 90 min frequency. - temperature - moisture, wind } profiles - surface up to 100 mb	18 1000-100 mb in steps of 50 mb	$u = u_{rot} + u_{div}$ - u_{rot} not changed by O'Brien's technique - adjust u_{div} only. $D^1 = \nabla^2\phi^1$ for discrepancies from $\nabla^2\phi = 0$ D^1 from O'Brien (1970) D^{11} $D^1 - D$ D calculated from u + v u^1 :adjusted $u = u + \frac{\partial p}{\partial x}$ $\nabla^2\phi^{11} = D^1 - D = D^{11}$ B.C: $\phi^{11} = 0$	-Obtained time-sections of measured variables at each sounding station -Interpolated to a regular grid using splines -grid 240 km x 240 km on 10 km intervals $D_k = \left[\frac{\partial u}{\partial x} + \frac{\partial v}{\partial y}\right] \Delta k = 50$ mb Intervals up to 100 mb $w'_p = w_p + \Delta p + D_k \Delta p$ Uses O'Brien's technique -w bottom layer from winds -w top layer from winds or $w^*_{top} = 0$	none	none explicitly
Lee Determination of surface winds in data sparse areas	1975	- surface temperatures - pressure tendency field - 900 mb temperatures - pressure dubbing using surface wind adjusted for stability and friction to give 900 mb wind: for winds of minimum 4 m/s. Assume equal to geostrophic and calculate $\frac{\partial p}{\partial x}$: use nearest pressure to calculate p. - smoothed p-field - interpolate all parameters to grid using $1/r^2$ weighting	10 x 10 grid Δ = 47.6 km 1(b.l.)	- calculate surface geostrophic wind - calculate isallobaric wind from $\frac{\partial p}{\partial t}$ and add to geo-components to give resultant wind above b.l. - modifies their wind for stability, roughness and latitude using Forecaster Reference Book Methods to give surface wind.	not considered	as a roughness parameter	none explicitly

		INPUT DATA	NO. OF LAYERS	LAYER WINDS	VERTICAL VELOCITY	TOPOGRAPHY	MIXING HEIGHT
Liu and Goodin comparison of their method with Dickerson and Endlich methods. - Holds observed winds fixed - final field is sensitive to initial guess. - Los Angeles Basin.	1976	Surface winds (22 obs) Los Angeles Interpolate to grid $1/r^2$ weight	40 x 25 x h Δ = 2 mi.	1) Calc D^n_{pq} 2) $\bar{u}^n_{pq} = \frac{-D^n_{pq}\,\Delta x}{f_{p+1,q} + f_{p-1,q}}$ f = 0 if obs at p,q = 1 otherwise 3) $u^{n+1}_{p+1q} = u^n_{p+1,q} + f_{p+1,q}\,\bar{u}^n_{pq}\,h_{p+1}$ etc. apply (1), (2), and (3) repeatedly to reduce D_{pq}.	$\frac{\partial h}{\partial t} = 0$ $D = \frac{\partial (uh)}{\partial x} + \frac{\partial (vh)}{\partial y}$	topography inc In calculation of h.	h presumed known $h = h_o + HQ + HD$ $-(h_t - h_{reg})$ HQ due to solar heating HD due to surface divergence h_{reg} = smoothed region surface h_t = topog. height $HQ = (HQ)_o \sin (\frac{\pi t}{Tn} + \phi_1) \sin (\pi S/L)$ $HD = (HD)_o \sin\left[\frac{2\pi t}{Tn} + \phi_2\right]$ (i.e. model of diurnal h cycle.)
Agnew Surface wind prediction for Beaufort Sea	1977	- surface pressure distribution - surface roughness - vertical temperature gradient	ABL	Compute Vg. compute $S = \frac{g}{f V_g}\left[\frac{\Delta\theta}{\theta}\right]$ Use Henry (1973) to get u_*, α_g, from $\frac{G \sin \alpha_g}{u_*} = \frac{1}{k} \ln\left[\frac{u_*}{z_o f}\right] + B_1(S)$ $\frac{G \cos \alpha_g}{u_*} = B_2(S)$ B_1 and B_2 given by Henry (1973)		none	

		INPUT DATA	NO. OF LAYERS	LAYER WINDS	VERTICAL VELOCITY	TOPOGRAPHY	MIXING HEIGHT
Draxler Trajectory model wind field. Not mass consistent	1977 1979	Surface winds 60 stations Rawinsondes 6 stations Surface station stability Pasquill Sondes are used only to determine adjustment factors for surface winds.	Single layer: the depth is determined to contain 90% of diff-using species	- average layer wind determined from sounding - interpolated using $1/r^2$ and $(1-0.5\lvert\sin\phi\rvert)$ (alignment weighting) - adjust surface winds by velocity factor and direction factor determined from sonde. - use 0000 GMT (1900 EST) for unstable stations - use 1200 GMT (0700 EST) for stable stations	not considered	none	none explicitly K(Z) used to determine diffusion depth for average layer
Stolzenbach et al Wind fields for oil slicks. Discussion paper.	1977	Surface pressure field	Surface Only	- calculate surface geo-strophic wind - apply Blackadar and Tennekes (1968) to give velocity defect and gives surface winds	not considered	Coastal Winds Lyons (1972) sea breeze parameter $= \frac{\Psi(\theta) G^2}{C_p \Delta T}$ $\Psi(\theta)$ depends on shore angle G = geo-wind	not considered

		INPUT DATA	NO. OF LAYERS	LAYER WINDS	VERTICAL VELOCITY	TOPOGRAPHY	MIXING HEIGHT
Dickerson MASCON. Single layer version of MATHEW. San Francisco Bay area experiment	1978	Surface winds averaged over 1 hour (for some), or instantaneous for others Rawinsonde to get mixing, height, H Interpolation of surface winds $v = \frac{\sum_{1}^{N} v_i e^{-0.1 r_i^2}}{\sum_{1}^{N} e^{-0.1 r_i^2}}$ N = 3 closest	one mixed layer of thickness $(H-h_t)$	$\frac{\partial h}{\partial t} + \nabla (hV) + w = \varepsilon$ minimize ε using Sasaki method $\frac{\partial h}{\partial t} + \nabla^2 \bar{\lambda} - \left(\frac{\alpha_1}{\alpha_2}\right)^2 \bar{\lambda} = \left[\nabla(hV)+w\right]_{obs}$ set $w_{obs} = 0$ initially $\bar{\lambda} = 0$ on boundary $uh = (uh)_o + \frac{\partial \bar{\lambda}}{\partial x}$ $w = (w_{obs} - \left(\frac{\alpha_1}{\alpha_2}\right)^2 \bar{\lambda}$ $\bar{\lambda} = \frac{1}{4}\left(\frac{1}{\alpha_1^2}\right)\lambda$ $\frac{\partial h}{\partial t}$ from ?	Computed from variational technique $w = 0$ initially	included in $h = H - h_t$	not clear how $\frac{\partial H}{\partial t}$ obtained or how spatial variation of H is achieved
Sherman MATHEW	1978	Tower wind measurements 16 stations Soundings 3 hours apart time interpolation at single site and assumed upper layer constant spatially $u = u_o \left(\frac{z}{z_o}\right)^p$ for profiling up to 100 m near neutral	51 x 51 x 15 layers $\Delta x = 500$ m $\Delta z = 25$ m	$\frac{\partial^2 \lambda}{\partial x^2} + \frac{\partial^2 \lambda}{\partial y^2} + \left[\frac{\alpha_1^2}{\alpha_2^2}\right]\frac{\partial^2 \lambda}{\partial z^2} =$ $-2\alpha_1^2\left[\frac{\partial u}{\partial x} + \frac{\partial v}{\partial y} + \frac{\partial w}{\partial z}\right]$ no $\frac{\partial h}{\partial t}$ measured.	Computed from variational technique $w = 0$ initially no $\frac{\partial h}{\partial t}$ term	Expressed in block form with 'no-flow' b.c.'s in a layer	not explicitly included

		INPUT DATA	NO. OF LAYERS	LAYER WINDS	VERTICAL VELOCITY	TOPOGRAPHY	MIXING HEIGHT
Stephens & Johnson Surface wind analysis Mesoscale decomposition of wind into divergent and rotational components	1978	Surface winds Interpolated using successive correction algorithm (no details)	2-D	$u = \frac{-\partial \Psi}{\partial y} + \frac{\partial X}{\partial x}$ $v = \frac{\partial \Psi}{\partial x} + \frac{\partial X}{\partial x}$ Ψ = stream function χ = velocity potential Helmholtz theorem	computed but not given explicitly	none	none
Keyser Initialization of numerical models. Uses non linear balance equation	1978	Rawinsondes calculates geostrophic wind at all levels Interpolation to grid points in each level using cubic splines	70 x 70 Δx = 60 km 10 levels up to 100 mb	$\nabla^2 \Psi = \zeta_{obs}$ $\zeta = \left(\frac{\partial v}{\partial x} - \frac{\partial u}{\partial y}\right)_{obs}$ correct to satisfy Stokes Balance equation $\nabla^2 \phi = \nabla \cdot \left(f \nabla \Psi\right) + 2J\left(\frac{\partial \Psi}{\partial x}, \frac{\partial \Psi}{\partial y}\right)$ RHS calculated from solution for Ψ	from Divergence	none	none

		INPUT DATA	NO. OF LAYERS	LAYER WINDS	VERTICAL VELOCITY	TOPOGRAPHY	MIXING HEIGHT
Heffter Trajectory model for 5-day LRT	1980	Rawindsondes Linear interpolation w.r.t. time uses $(1-0.5\lvert\sin\theta\rvert)$ alignment weighting + $1/r^2$ weighting 00, 06, 12, 18z obs.	One layer with 90% of diffusing species	Simple interpolation not mass consistent	None	Implicit in transport layer depth	Top of transport layer depth measured by sondes
Goodin, McRae and Seinfeld Mesoscale. Complex terrain. Los Angeles basin model.	1980	Surface winds Radiosonde profiles	Tested 5 layers. Terrain following. 50 150 300 550 1450 m	Surface winds interpolated using barrier + $1/r^2$ weight Anderson terrain adjustment used $\nabla^2\phi = D_t$ D_t is terrain induced pertubation. This is final surface layer wind-field with surface divergence. Upper Layers: Interpolated sonde data using $1/r$ weight after smoothing, reduced divergence to minimum using technique of Liu and Goodin (1976) putting back w_{k-1}	Surface layer w calculated from wind-field divergence Upper layers: smoothed u & v to reduce w in each layer assuming $w_{k-1} = 0$ $W = w - u\left[\frac{\partial h}{\partial x} + \rho\frac{\partial \Delta H}{\partial x}\right]$ $- v\left[\frac{\partial h}{\partial y} + \rho\frac{\partial \Delta H}{\partial y}\right]$ $- \rho\frac{\partial \Delta H}{\partial t}$ $\frac{\partial W}{\partial \rho} + \frac{\partial (u\Delta H)}{\partial x} + \frac{\partial (v\Delta H)}{\partial y} = 0.$	Used terrain following coordinates $\rho = \left[\frac{z-h_t}{H-h_t}\right]$ H = top of domain $0 \leq \rho \leq 1$ solved only for $\Delta H = H - h_t$ = constant	Not used as far as can be deduced. Is measured and interpolated

		INPUT DATA	NO. OF LAYERS	LAYER WINDS	VERTICAL VELOCITY	TOPOGRAPHY	MIXING HEIGHT
Wojcik Compares surface wind interpolation and winds derived from geopotential. Favours the latter.	1980	Geopotential height field from published weather maps interpolated usind bi-cubic splines.	one mixed layer	- calculates geostophic wind from geopotential - adjusts for surface drag, baroclinicity, stability, and diurnal variation using Hoxit (1973) to give average mixed layer wind.	None	None	Implicit and constant
Cats Analysis of surface wind observations. Netherlands	1980	Surface winds at 10 m averaged over 10 min.	Surface wind only	Uses optimum interpolation technique of Gandin (1963). Calculates surface divergence and vorticity from the data.	can be calculated from surface divergence	None	None
Carmichael and Peters Eulerian dispersion model. Eastern United States	1981	Radiosondes - (12-hourly) Surface winds temperature cloud cover (3-hourly) used for stability, deposition velocity and eddy diffusivity only.	12 layers Top at 3000 m	Interpolated soundings using $1/r^2$ weighting. Winds are not time interpolated but change in 12-hourly steps.	calculated from wind divergence	Terrain following coordinates $p=\left[\frac{z-h(x,y)}{H-h(x,y)}\right]$	From sounding: Varied diurnally using functions

		INPUT DATA	NO. OF LAYERS	LAYER WINDS	VERTICAL VELOCITY	TOPOGRAPHY	MIXING HEIGHT
van Dop and de Haan Eulerian model for dispersion	1981	Surface winds Optimum interpolation of Cats (1980). Surface pressure Calculates surface geostrophic wind 850 mb wind Interpolated to grid Cloud cover	17 x 17 x 12 Δx = 20 km Δz = 50 m	Surface Layer Interpolation of wind observations and averaged in layer using similarity. also uses tower data for lower wind profile. Upper Layers Linear vertical interpolation between surface geostrophic wind and 850 mb wind.	from wind divergence	None	Daytime Tennekes (1973) ABL night time Nieuwstadt (1981)
Bhumralkar et al EURMAP-2B Central and Western Europe Puff model	1981	Surface winds 850 mb winds	3 layers to 850 mb or 1450 m 50 km grid	Vertical interpolation between surface and 850 mb using logarithmic profile. Use Endlich (1967) to make each layer non-divergent.	no bulk transport between layers	Terrain following coordinates $\sigma = \frac{z-h(x,y)}{H(x,y)-h(x,y)}$ minimum thickness of 500 m.	constant at 850 mb but varies k(z) between layers according to stability profiles.

AUTHOR	DATE	PARAMATIZATION OR MODEL	DESCRIPTION
Holzworth	1964	Determination of mixing depth for unstable daytime conditions.	Mixing depth determined by extension of a dry adiabat from surface temperature to intersect radiosonde profiles.
Hanna	1969	PBL height under neutral or stable conditions	Recommendes Blackadar (1962) and Lettau (1962) $H = 0.2 \left(\frac{u_*}{f}\right)$ (neutral); $H = 0.75 \sqrt{g \left[\frac{}{T}\left(\frac{\Delta\theta}{\Delta z}\right)\right]^{\frac{1}{2}}}$
Arya	1981	PBL height under stable conditions	$H = 85.1 + 0.089 \left(\frac{u_*}{f}\right)$ for $\frac{u_*}{f} < 1600$ $= 0.142 \left(\frac{u_*}{f}\right)$ for $\frac{u_*}{f} \geq 1600$
Nieuwstadt	1981	PBL height under stable conditions steady state	$H = \frac{0.3 \left(\frac{u_*}{fL}\right)}{1+1.9\left(\frac{H}{L}\right)}$
Henderson-Sellers	1980	Simulation of urban mixing depth	Flat Terrain $h^2(x) = \frac{2}{C_p \rho \gamma a} \int_0^x Q_s \, dx$ a is rural potential temperature gradient (stable) Q_s surface heat flux. Terrain effect $T_o - \Gamma h^1(x) = \left[T_o - \Gamma h(x)\right]\left[(T_o + \Gamma z^1)/T_o\right]^{-\gamma/a}$ $h^1(x)$ = terrain corrected mixing depth $T_o(x)$ = T at z = 0 z^1 = (rural terrain height - city height) Γ = city mixed layer lapse rate. γ = rural lapse rate.

AUTHOR	DATE	PARAMATIZATION OR MODEL	DESCRIPTION
O'Brien	1970	constraint of objectively determined vertical velocity to preset top and bottom boundary values	$w_k^1 = w_k - \frac{S_k}{S_k}(w_k - w_T)$ where $w_k = w_{k-1} + \Delta ZD_k$ $S_k = \sum_1^k \sigma_i^2$ D_k is the horizontal divergence; σ_i^2 is the error variance
Agnew	1977 1978	computation of surface winds from the surface geostrophic wind	The surface geostrophic wind (G) is computed from the surface pressure distribution. Also required in the analysis are potential temperature at 850 mb and at the surface and surface roughness. Uses Henry (1973) $\frac{G \sin \alpha_o}{u_*} = \frac{1}{k} \ln \frac{u_*}{Z_o f} + B_1(s)$ $\frac{G \cos \alpha_o}{u_*} = B_2(s)$ $\frac{\Delta\theta}{\theta_*} = \frac{0.74}{k} \ln \frac{u_*}{Z_o f} + B_3(s)$ B_1, B_2 and B_3 given by Henry (1973). Compute u_* and α_o to give surface wind profile.
Nieuwstadt	1981	computation of surface winds from the surface geostrophic wind under neutral or stable conditions	$\frac{G \cos \alpha}{u_*} = \frac{1}{k}(\ln(R_o u_*/G) - B)$ $\frac{G \sin \alpha}{u_*} = -\frac{1}{k} A$ $A = -0.56 \left(\frac{\mu_o}{\mu}\right)$; $B = 1.1 - \ln\left(\frac{\mu}{\mu_o}\right) - 2.2\,\mu$ $\mu_o = \left(\frac{u_*}{fL}\right)$; $\mu = h/L$; $R_o = \left(G/fz_o\right)$ $\frac{h}{L} = \frac{0.3\left(\frac{u_*}{fL}\right)}{1 + 1.9\left(\frac{h}{L}\right)}$ need to estimate L or use Agnew (1977) to give θ_*

AUTHOR	DATE	PARAMATIZATION OR MODEL	DESCRIPTION
Thorpe & Guymer	1977	model of nocturnal jet	$\zeta_u = G + A_u \exp(-ift)$ $\zeta_L = \frac{ifG}{\left(\frac{ks}{h} + if\right)} + A_L \exp\left[-\left(if + \frac{ks}{h}\right)t\right]$ $\zeta = u + iv$ $k_s = C_D \bar{u}_s$ t = time since sunset Simplifies to (Lamb, 1981) $u = a \cos\theta_2 - b \sin\theta_2$ $v = a \sin\theta_2 + b \cos\theta_2$ $a = \lvert v_s \rvert \left[(\cos(\Delta\theta) + \sin(\Delta\theta) \sin(f(\Delta t)) \right]$ $b = \lvert v_s \rvert \sin(\Delta\theta) \cos(f\Delta t)$ θ_2 = geostrophic wind direction at sunset $\lvert v_s \rvert$ = layer average surface wind at sunset $\Delta\theta$ = layer average direction difference between surface layer and geostrophic wind at sunset Δt = time since sunset
Anderson	1971	topographic perturbation of mean wind field	$\overline{\nabla^2\phi'} = \frac{U}{H} \nabla h$ ϕ' = velocity potential of topographic perturbation U = unperturbed wind H = perturbed layer thickness h = topographic height (smoothed for regional effects)

kinetics. Wind field models have not, until recently, received the same close attention. Wind fields for LRT applications are generally derived in a very approximate manner from surface wind observations and/or radiosonde data. Simple linear, temporal interpolation of twice daily soundings and vertical extrapolation of surface observations are common. Other than for Lamb (1981), virtually no attempt has been made to incorporate synoptic scale analysis of vertical structure into the wind field.

Where a Eulerian diffusion model is used, adjustment of the wind field to render it mass consistent is done out of necessity to avoid spurious divergence which cannot be tolerated by the Eulerian computation, rather than in an effort to improve the wind field estimate. Vertical air motion is frequently regarded as an undesirable 'by-product' of divergence reduction and is eliminated by discarding the divergent component of the wind field. Vertical air motion, particularly near a frontal system cannot be ignored and can rival or surpass diffusion processes as a mechanism for vertical transport of pollutants.

Most LRT three-dimensional wind field models regard the atmospheric boundary layer as a separate entity with winds derived from surface

observations: Radiosonde data are used to define horizontal winds at the top of the boundary layer without regard to vertical motion. This approach is contrary to the classical development of hydrodynamics whereby an accurate description of the frictionless flow including vertical motion is essential before attempting to describe the boundary layer. This comment applies only to LRT models and not of course, to meteorological models for which a great deal of research and effort has been devoted to accurately define the frictionless atmosphere including vertical motion.

In areas where a very dense network of surface wind observations is available, there is justification for using wind observations to derive the mesoscale wind field in the boundary layer, particularly in complex terrain. Under these circumstances, the surface winds do contain information on mesoscale effects, the inclusion of which through parametization, is beyond present day capabilities. Nonetheless, the problems of noise in the data and resulting vertical motion at the top of the boundary layer are not alleviated.

A brief description in tabular form of the wind field techniques reviewed is given in Tables 2.1-2.3 . Lui and Goodin (1976) describe a mesoscale wind field analysis technique for the Los Angeles basin. A single layer averaged wind field for the flow between the topography and an elevated inversion is derived using twenty-two surface wind observing stations. The inversion height is parameterized in terms of wind divergence and solar insolation. Simple inverse-squared distance is used to interpolate data to the grid. Divergence over the domain is reduced to an insignificant level by adjusting interpolated wind components only, giving full weight to the observations.

Draxler (1977), (1979) proposed a LRT wind field model, (not mass consistent), for deriving a layer average transport wind to include only the diffusion depth for the species of interest. Sixty surface wind observing stations and six radiosonde stations were used. The surface data were extrapolated vertically using the radiosonde profiles.

Dickerson (1978), Sherman (1978), Racher et al (1980) use the variational technique first proposed by Sasaki (1958), (1970a), (1970b), to minimize the divergence over a specified domain. The latter two

models are multi-layered. Vertical motion at the top of the domain is set to zero. The extent to which mass consistence is achieved by damping out vertical motion within the domain, (by adjusting horizontal wind components), is controlled in the model. Racher et al comment that the initial guess horizontal wind field largely determines the final result. This implies that were it possible to apriori specify the distribution of vertical velocity the final horizontal wind field would be little changed unless vertical velocities were large.

Heffter (1980) for a 5-day LRT trajectory model, used linear temporal interpolation of six-hourly radiosondes to give hourly layer-averaged winds. An anisotropic, inverse-square distance interpolation of the data to the grid was used where the weighting depends on the alignment of grid point and observations: The wind field is not mass consistent.

Goodin, McRae and Seinfeld (1980) propose a multi-layered mesoscale model for the Los Angeles Basin. The wind field is derived from a dense network of surface wind observations and radiosonde data. Surface winds in the surface layer are interpolated to the grid using inverse-

squared distance weighting with provision for barriers to flow. The interpolation includes a terrain adjustment modeled after Anderson (1971). This constitutes the final surface wind field with divergence. The wind in upper layers is derived from sonde data using inverse distance weighting: The horizontal winds in the upper layers are smoothed to progressively reduce divergence. The wind field in the upper layers is then rendered mass consistent using the adjustment technique of Liu and Goodin (1976).

Carmichael and Peters (1981) developed a 12-layer model extending to 3 km . Wind fields are calculated in 12-hourly steps from radiosonde data using inverse-squared distance interpolation: There is no time interpolation. Vertical velocities are calculated from wind divergence.

Van Dop, de Haan and Cats (1981) based their model for a long-range Eulerian dispersion model on surface wind observations, surface pressure distribution and 850 mb winds interpolated to the grid. The model has 12 layers. Similarity theory was used to profile winds in the atmospheric boundary layer. Upper layer winds are derived by linear interpolation between the surface geostrophic wind and the 850 mb wind. Vertical motion is calculated from the wind field divergence.

Bhumralkar et al (1981) used vertical interpolation with logarithmic profiles between surface winds and 850 mb winds. The model has three layers: Divergence and therefore vertical motion was eliminated in each layer using an adjustment technique (Endlich (1967)).

Borghi (1981) recognized the importance of vertical motion as it affects long-range trajectories. Although a wind field model as such is not described, the calculation of trajectories which includes vertical motion is given. This is achieved by tracking air parcel trajectories isentropically rather than isobarically.

Lamb, (1981) describes a three-layer mass consistent wind field model for use in a Eulerian dispersion model. There is extensive parametization of inter-layer fluxes. Layer thicknesses are chosen to represent the subsidence inversion base, with the mixing layer divided into a lower and upper layer. Topography and parametization of the nocturnal jet and cumulus convection is included. The wind field model uses meteorological observation as input. A significant advantage of Lamb's model over other multi-layer models is that the vertical extent of the model layers is variable and dictated by the structure of the lower atmosphere rather than by computational convenience.

Liu, Yocke and McElroy, (1978) propose a three-dimensional, mass consistent wind field model but due to lack of observational constraints, the model is of limited use for present purposes. The model has several layers and the flow field is determined by parameterizing the horizontal divergence (or vertical fluxes) in each layer. Topography, heat island, wind profile and mountain/valley winds are considered. Observational data are not input to the model.

2.2 Meteorologically Based Wind Field Models and Analysis

In Section 2.1, review and discussion was limited to modeling techniques presently associated with LRT and mesoscale dispersion models. In this section a broader field of meteorological models is considered: In most cases the models have been developed for meteorological analysis. Many of the models are analysis schemes on a synoptic scale of radiosonde data for initializing prognostic models which use relatively sophisticated numerical solutions of the primitive equations of atmospheric motion. The stability and quality of the results from prognostic models are contingent on the accuracy of initialization.

Anthes, (1976) describes an initialization technique whereby geopotential heights are derived from observed wind data using

the balance equation. The stream function is derived from the vorticity of the observed winds. Further examples of the technique are given by Anthes and Keyser, (1979) and Keyser, (1978) .

Keyser (1978) and, Anthes and Keyser (1979) describe an initialization technique for numerical prediction models. Starting with radiosonde data, the geostrophic wind is obtained at ten levels up to 100 mb . The wind data are interpolated to a grid using cubic splines. Vorticity distribution is calculated from the wind components and a of stream function calculated by solving the Poisson equation with vorticity as the forcing function. The potential function is then obtained by solving the balance equation. Vertical velocity distribution is obtained from the horizontal divergence. All interpolation and analysis is done isobarically.

Hoke and Anthes, (1976) propose a dynamic-initialization technique for deriving wind fields from observations which are balanced with respect to the mass and momentum equations. Application of the method in two dimensions is described. Tarbell, Warner and Anthes, (1981) give a procedure for the initialization of the divergent wind component in a mesoscale, numerical weather prediction model. The iterative method is related to precipitation prediction.

While these methods do ensure successful initialization of numerical models they do not necessarily give the best representation of the observational data. Errors in the specification of boundary values and gradients of stream function or velocity potential can lead to inconsistencies with the observations at interior points.

A number of sophisticated prognostic numerical models for upper air movement are to be found in the literature. These dynamic models are generally based on solving the primitive equations of motion and energy which permits the computation of the evolution with time of a starting meteorological field. Hemispherical models are routinely used by weather prediction services around the world.

Continental scale models are available such as those described by Tarbell et al (1981) for precipitation prediction, Chang et al (1981) for investigating severe squall lines, Anthes and Warner (1978) for numerical weather prediction: This last model was compared with tetroon trajectories (Warner (1981)) with good results. The objectives in the development of prognostic models are rather different from those presently stated for the analysis of historical meteorological and air pollution data. For prognosis, one must of necessity use a full dynamic description of the atmosphere. These models which generally require large computer resources and time, have to be initialized through analysis of input data. Once initialized, the prognostic

models run forward in time and any errors in prediction will propagate. The objective of these models is to obtain a best estimate of the future meteorological fields without reliance on further data. The use of a prognostic model does not necessarily result in a better description of the wind fields, divergence and vorticity, than an analysis of observational data. Where prognostic models are perceived as being of value for the analysis of historical data, is in the temporal interpolation between 12-hourly observational intervals of 0000Z and 1200Z . Even when used in this manner, the model predictions have to be adjusted on the basis of surface observations.

2.3 Objective Analysis Schemes for Meteorological Data

Objective analysis schemes range from full three-dimensional analyses such as those used for initialization described in Section 2.2, to two-dimensional cross-sectional or surface analysis.

For the objective analysis of meteorological fields, the observational data invariably has to be interpolated to a regular grid. The manner in which this interpolation is carried out is extremely critical if excessive filtering of information is to be avoided.

The simplest interpolation is inverse distance weighting. Goodin, McRae and Seinfeld (1979) give a review and comparison of methods for interpolating sparse vector and scalar fields. They conclude that a second order polynomial fit with inverse-squared distance weighting gives superior results for the methods tested.

Sykes and Hatton (1976) describe a high order technique for interpolation in space and time using orthogonal polynomial fitting. The MEP Company has experience with this technique which is found to give good results for fitting and interpolation of pressure data.

Other interpolation techniques are found in the literature such as Lee (1975), Bleck (1975) and Walton et al (1978). A very useful interpolation technique which warrents special mention is that using cubic or bi-cubic splines. (Cline (1974), Ahlberg et al (1967) and de Boor (1962)). The method involves piece-wise fitting of data using a set of second order polynomials which match and have continuous derivatives at arbitrary node points. Spline interpolation has been extensively used for meteorological analysis.

Fankhauser (1974) carried out an analysis of a severe storm using radiosonde data up to 100 mb . Special ascents gave good temporal resolution. The wind components were interpolated isobarically to the grid and the resulting wind field was decomposed into a rotational non-divergent field and a irrotational divergent field. Vertical velocities calculated from the wind field divergence were adjusted to be consistent with boundary value constraints using O'Brien's (1970) variational technique.

Mancuso, Endlich and Ehernberger (1981) describe an objective isobaric/ isentropic technique for upper air analysis. Unlike most analysis schemes where interpolation of meteorological parameters is done isobarically, this technique recognizes that air movement tends to be along isentropic surfaces rather than isobaric surfaces. Once the isentropic surfaces are defined, all interpolation is done on these surfaces. Vertical air motion is far better resolved using this technique. Mancuso et al give an example of the analysis of a frontal system which is in good agreement with a subjective analysis of the same data. Divergence, stability and vorticity distributions are consistent with the frontal meteorology.

There are several techniques available for adjusting wind fields to match constraining relationships such as the continuity equation, or balance equation.

Tuerpe, Rodriguez, Gresho and Sani, (1978) compare the variational minimizing of divergence using finite element rather than finite difference techniques. The method is conceptually similar to those described by Sasaki, (1958), (1970a), (1970b): These papers describe the use of variational techniques for objective analysis of meteorological parameters. The techniques may be applied to reconcile observations with various functional constraints such as the quasi-geostrophic equation or balance equation.

Endlich (1967) gives a very attactive technique for iteratively altering the kinematic properties of wind fields. The method may be used to decompose the wind field into irrotational and non-divergent components, or the wind field may be altered to give a mass consistent wind field with a specified divergence and vorticity at each grid point. The method is simple to apply and does not require the specification of boundary conditions. The scheme described is two-dimensional but is easily extended to multi-layered models.

Stephens and Johnson, (1978) also describe a two-dimensional scheme, using Fourier transforms, to decompose wind field observations into divergent and rotational components.

O'Brien, (1970) describes a technique whereby the vertical velocity is objectively balanced through minimizing the variation integral of the divergence. A scheme for correcting the vertical velocity and constraining its boundary values is given. O'Briens method is frequently used to refine divergence estimates from upper air analysis (Fankhauser (1974), Keyser (1978)).

3. WIND FIELD MODELS

3.1 General Overview of Modeling Methodology and Objectives

3.1.1 Introduction

The specification of transport winds for the purpose of long-range transport is probably the most problematic aspect in short-term episodic modeling. This is due to the necessity of accounting for several ranges of phenomena as displayed in Figure 3.1, which shows the three scales which make up the bulk of available energy in the atmosphere.

The synoptic scale motions, which operate on the scale of several hundred kilometers and greater, are adequately monitored, for the most part, over the North American Continent. Standard analysis programs of the numerical weather prediction process provide data on the growth and movement of synoptic systems which can be used to determine the primary control on continental flow patterns. This analysis can also be used to obtain information on vertical motions due to the large-scale systems.

The mesoscale wind fluctuations reflect the effect of topographic and heat transfer differentials over scales of several tens of kilometers. Fluctuations on this scale are most difficult to

Figure 3.1

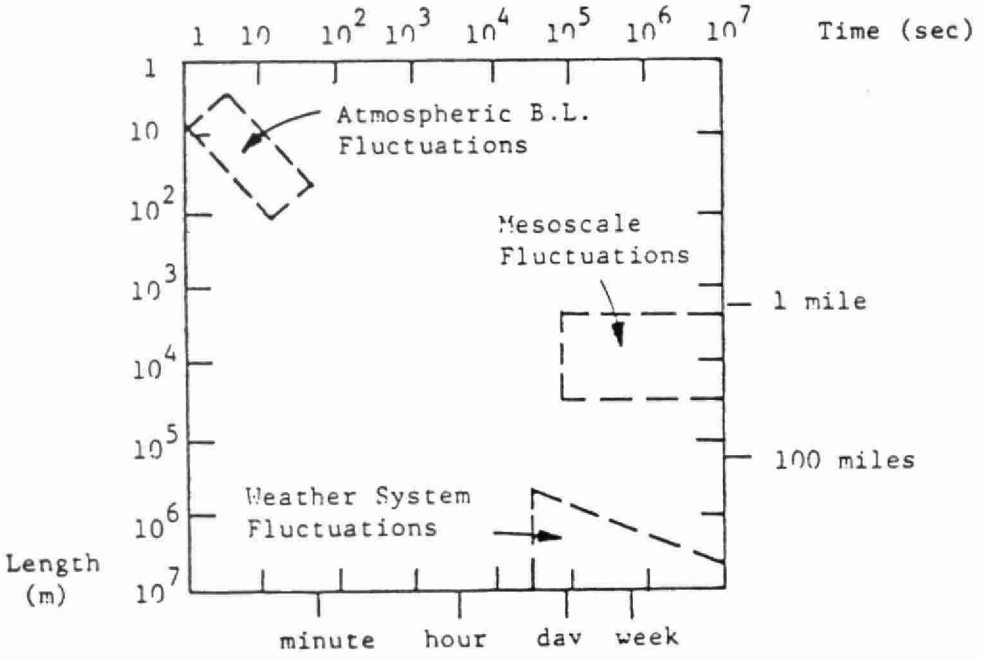

Scales of Wind Variation

treat adequately due to the large number of controlling variables. Nevertheless, mesoscale models have been developed and used for specific applications such as sea-breeze effects (McNider and Pielke, 1979), and urban situations (Pandolfo and Jacobs (1973), Bornstein and Runca (1977)).

The integration of the mesoscale description into the synoptic scale, to allow high resolution of the transport fields over long-range, poses a still more intractable problem, which is not adequately addressed by present-day long-range transport models.

The small-scale fluctuations in wind fields result from the turbulence imposed on flow in the planetary boundary layer by frictional effects of the roughness elements and the thermally generated small scale turbulence of the flow. The theory of the PBL structure and its characteristics is now fairly well understood. The effect of this scale of fluctuation on long-range transport of plumes is to induce growth of the plume in the horizontal and vertical dimensions, and is the major influence on dilution of the initial plume over the first few hours of travel. The vertical

growth of the plume also has the effect of imposing a changing transport wind regime, leading to shearing of the plume with height, and altering the trajectory of part of the plume material.

Since the wind field model which is to be designed is constrained by present day computer capability and availability of observational data, it will of necessity be a considerable simplification of a full description of the synoptic and mesoscale dynamics of the true wind field.

In order to proceed with the development of the wind field model it is necessary to set down the minimum requirements of the model which are consistent with those aspects which have high order effects on the transport and dispersion of airborne pollutants. A review of currently available methods for generating wind fields has been given in Section 2 . This section of the report details the modeling objectives and criteria which lead to the proposed model development which is described in Sections 3.2 to 3.4 .

3.1.2 Wind Field Model Requirements

The wind field model development is dictated by the degree of detail which will be included in the dispersion model: There is no point in over-definition of the transport winds if much of the detail is not resolved by the dispersion model. Dispersion of airborne material is to be modeled on two scales: The long-range scale extends to 4000 km with a spatial resolution of 1^{o} in latitude and longtitude while the mesoscale model has a resolution of 0.1^{o} and extends to 500 km . Fine vertical resolution is a feature of both scales with up to twelve levels extending, in both cases, to 5 km .

Since the dispersion model is of the Eulerian rather than Langrangian type, the wind field must be mass consistent: The dispersion model provides a numerical solution of the Eulerian mass conservation equation and unless the winds used in the advection terms are not themselves a solution of the continuity equation, meaningless results will be obtained due to spurious divergence in the mass field.

Vertical air motion is an extremely important feature of the wind field under some circumstances. Vertical transport of an airborne material can occur through diffusion and through bulk vertical motion of the transport winds. In most circumstances, the diffusion

processes are more rapid than vertical transport. In the vicinity of a frontal system, however, the reverse can be true and surface air can be lifted by the front at a greater rate than diffusion alone. The manner in which vertical motion is derived in the wind field model is extremely critical if a meaningful representation of vertical transport due to diffusion and vertical motion is to be retained by the Eulerian model. Under some circumstances, an incorrect specification of the vertical wind speed can 'swamp' the vertical diffusion terms of the model.

For past Eulerian models, the vertical motion problem has often been artificially eliminated by setting vertical wind components to zero. Clearly, such a model cannot give meaningful results near frontal systems. In the present model development a great deal of attention is given to the proper modeling of vertical air movement.

Another aspect of the wind field which has been recognized in recent years as extremely important is the nocturnal jet which may develop aloft under very stable conditions. The nocturnal jet flow is significantly super-geostrophic and since it occurs at a height within the day time mixed layer, it can transport pollutants over anomolous distances during the night hours. Well

validated models of the nocturnal jet are not available; However, it is too important a feature to neglect and a proposed nocturnal jet modeling scheme has been included in the wind field model.

Other aspects which assume importance on the mesoscale are the interaction between the surface winds and topography, and local circulation such as the urban heat island and land/sea or lake breezes.

3.1.3 Overall Model Description

3.1.3.1 Development of Wind Field Model Design Based on Originally Proposed Design Concept

Figure 3.2 shows schematically, the original wind field model design concept. The originally proposed wind field design was consistent with the stated requirements at that time, of the proposed diffusion model which did not include vertical motion and which had a modeling domain extending to 1,500 m . Both the wind field and diffusion model design concepts were submitted for Peer Review. The following changes to the diffusion model design, which affect the wind field model design, were recommended by the Peer Review Committee.

Original Wind Field Model Design

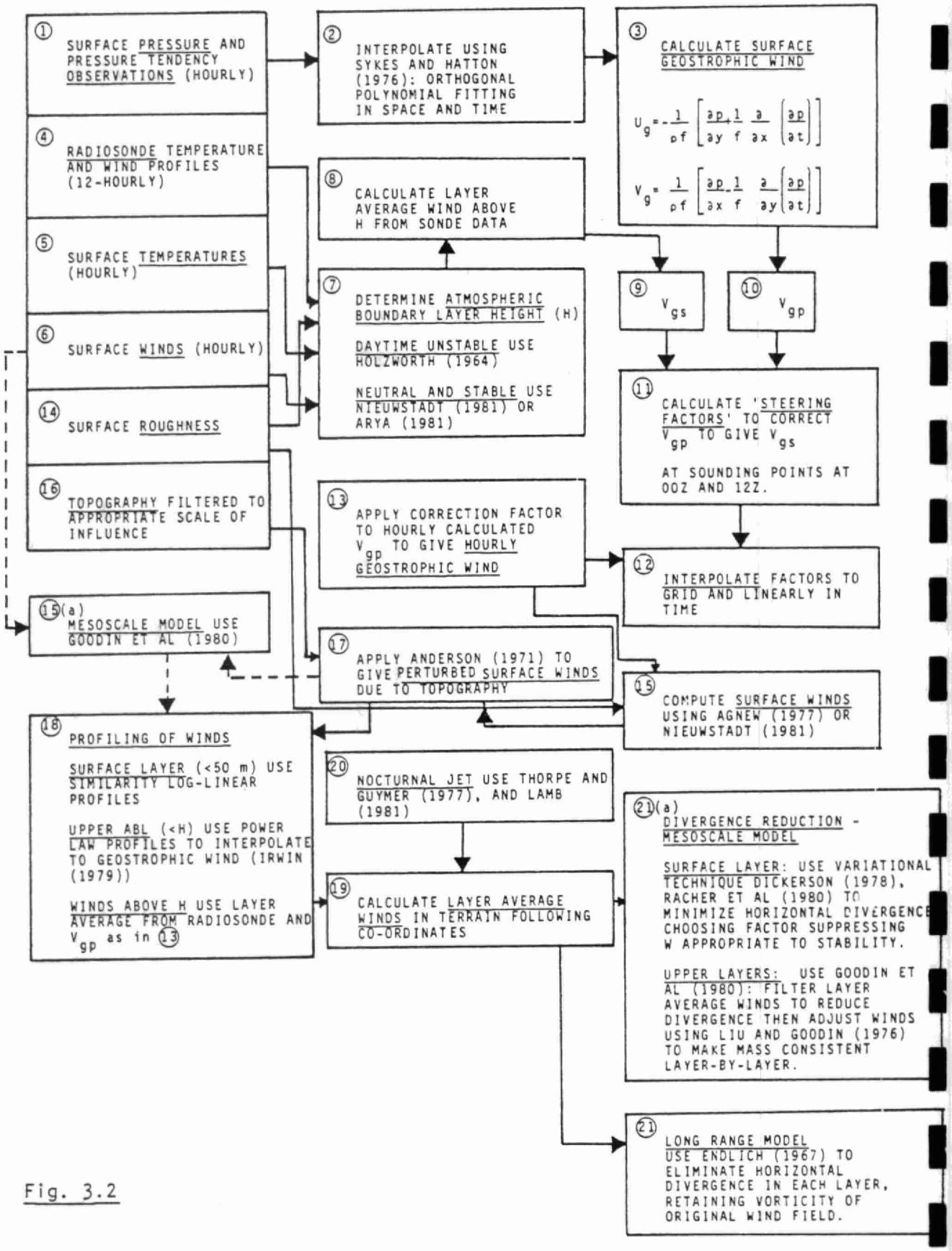

Fig. 3.2

i) Vertical motion should not be neglected in the diffusion model.

ii) The modeling domain for diffusion should extend to 5 km instead of the proposed 1.5 km .

These recommendations have necessitated modifications to the design proposal as follows:

i) Step (18) (See Figure 3.2): Since the revised diffusion modeling domain extends to 5 km (approximately 550 mb) and includes vertical motion, it is not feasible to calculate layer average winds much above the atmospheric boundary layer using the surface geostrophic wind calculated from sea level pressures. Furthermore, since vertical motion up to 5 km must be incorporated, a simple derivation of divergence from temporally interpolated radiosonde winds will be totally unsatisfactory. The revised design, therefore, incorporates an isentropic analysis of upper air data to ensure that divergence and vertical motion are properly interpolated for the wind field: Frontal features are a prime consideration in the design.

ii) Steps (15(a) and 21(a)): The technique of Goodin et al (1980), relies on a very dense network of wind observations,

if vertical motion for the revised design requirements is to be properly determined from observations using their technique. Instead, surface divergence has been estimated by parameterization and divergence at the top of the atmospheric boundary layer has been matched with that from the synoptic scale upper air analysis. For mesoscale regions where a dense network of observations is available, these observations are incorporated into the surface wind field.

iii) Steps (21 and 21(a)): Since horizontal wind divergence will be a feature of the revised diffusion model requirements, divergence reduction and elimination are not required. Instead, Endlich (1967) is used to adjust the layer average horizontal winds to give a mass consistent wind field with prescribed interpolated divergence: Only noise in the divergence due to temporal interpolation of winds is eliminated for both the mesoscale and long-range wind field models.

These are the changes in the originally proposed design concept which have been made to reflect the recommendations of the Peer Review Committee. Another modification which is proposed but which does not alter the overall design concept is as follows:

i) Steps (15) and (18): In the original design concept it was proposed to use a simple power-law to interpolate between the surface layer winds and the surface geostrophic wind with the surface layer winds determined using the drag law relationships of Agnew (1977) or Nieuwstadt (1981). This originally proposed method does not ensure continuity of the wind speed gradient within the boundary layer and is somewhat arbitrary. As an alternative proposal, a interpolation procedure which ensures continuity of wind speed and shear stress is given in this design document. The drag law similarity functions which result from the matching procedure are in very good agreement with those of Arya (1975) and Zilitinkevich (1975) for unstable conditions and with Arya(1975) and Yamada (1976) for stable conditions: The determination of surface layer winds is therefore essentially the same as those derived using drag law similarity functions as originally proposed and it is only the power law interpolation procedure which it is proposed to change.

3.1.3.2 Summary of Proposed Design

Figure 3.3 is a diagrammatic summary of the long-range and mesoscale wind field models together with data requirements. Three distinct steps are involved in the modeling procedure: (i) upper air analysis, (ii) atmospheric boundary layer analysis and (iii) reduction of the wind field to mass consistent components on the Eulerian grid.

The modeling procedure has been designed to ensure that the vertical wind component retains its significance and is properly reflected in the final wind field. This is achieved by identifying and quantifying sources of horizontal wind divergence which lead to vertical motion: These divergent components are preserved through the various interpolation steps and any additional divergence introduced by the process of analysis is eliminated.

In the upper air, on a scale of several tens of kilometers, vertical motion is determined by phenomena on a synoptic scale. Upper air divergence is impressed on the atmospheric boundary layer through 'steering' of the boundary layer flow by the divergent winds at its upper edge. Vertical motion relative to the terrain decreases to zero at the surface. Another source of vertical motion in the upper-air on the mesoscale, is convective storm activity: This convection cannot be reasonably modeled deterministically and is not included in the wind field model.

Figure 3.3

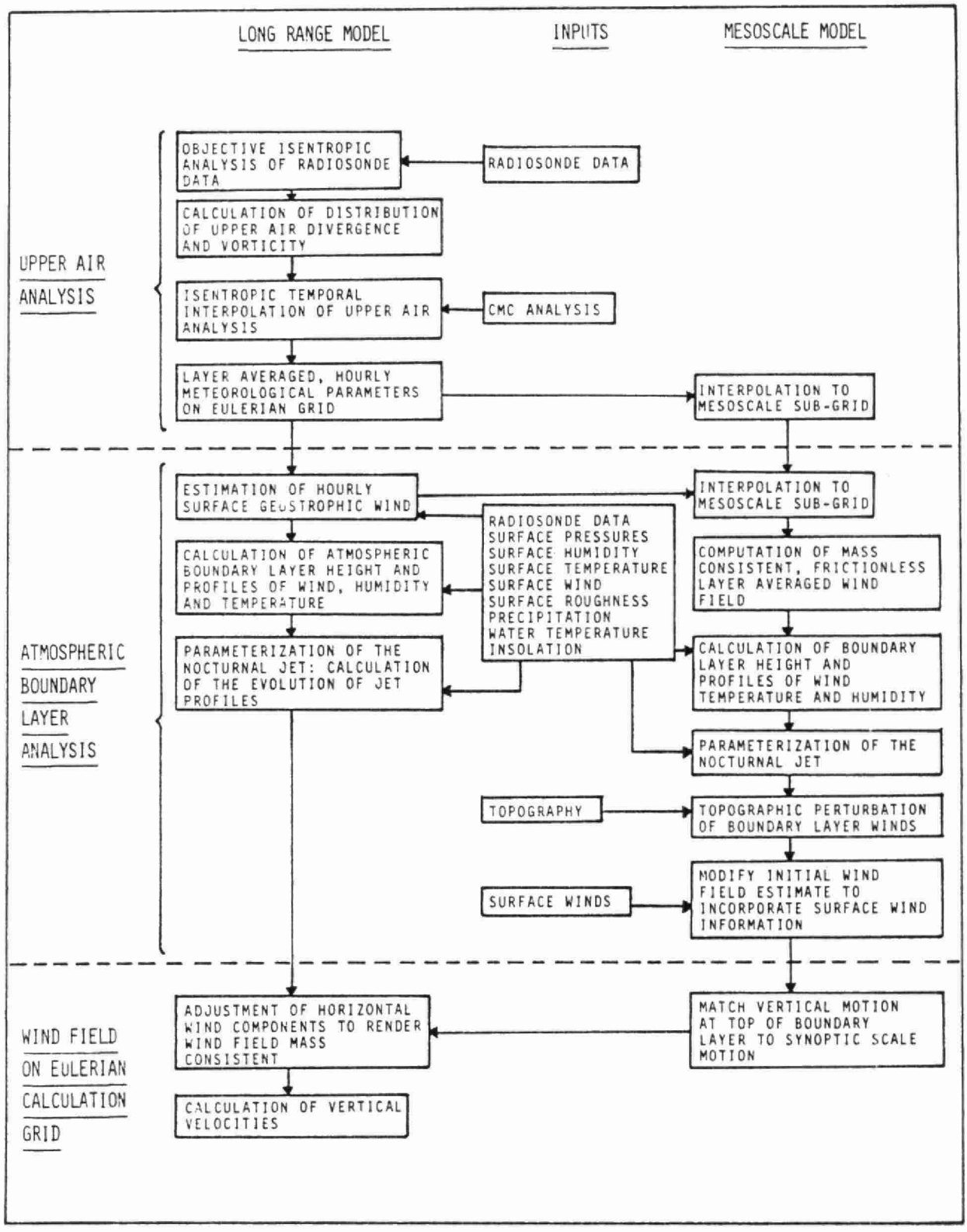
LONG RANGE MODEL
INPUTS
MESOSCALE MODEL
UPPER AIR ANALYSIS
OBJECTIVE ISENTROPIC ANALYSIS OF RADIOSONDE DATA
RADIOSONDE DATA
CALCULATION OF DISTRIBUTION OF UPPER AIR DIVERGENCE AND VORTICITY
ISENTROPIC TEMPORAL INTERPOLATION OF UPPER AIR ANALYSIS
CMC ANALYSIS
LAYER AVERAGED, HOURLY METEOROLOGICAL PARAMETERS ON EULERIAN GRID
INTERPOLATION TO MESOSCALE SUB-GRID
ATMOSPHERIC BOUNDARY LAYER ANALYSIS
ESTIMATION OF HOURLY SURFACE GEOSTROPHIC WIND
INTERPOLATION TO MESOSCALE SUB-GRID
RADIOSONDE DATA
SURFACE PRESSURES
SURFACE HUMIDITY
SURFACE TEMPERATURE
SURFACE WIND
SURFACE ROUGHNESS
PRECIPITATION
WATER TEMPERATURE
INSOLATION
CALCULATION OF ATMOSPHERIC BOUNDARY LAYER HEIGHT AND PROFILES OF WIND, HUMIDITY AND TEMPERATURE
COMPUTATION OF MASS CONSISTENT, FRICTIONLESS LAYER AVERAGED WIND FIELD
PARAMETERIZATION OF THE NOCTURNAL JET: CALCULATION OF THE EVOLUTION OF JET PROFILES
CALCULATION OF BOUNDARY LAYER HEIGHT AND PROFILES OF WIND TEMPERATURE AND HUMIDITY
PARAMETERIZATION OF THE NOCTURNAL JET
TOPOGRAPHY
TOPOGRAPHIC PERTURBATION OF BOUNDARY LAYER WINDS
SURFACE WINDS
MODIFY INITIAL WIND FIELD ESTIMATE TO INCORPORATE SURFACE WIND INFORMATION
WIND FIELD ON EULERIAN CALCULATION GRID
ADJUSTMENT OF HORIZONTAL WIND COMPONENTS TO RENDER WIND FIELD MASS CONSISTENT
MATCH VERTICAL MOTION AT TOP OF BOUNDARY LAYER TO SYNOPTIC SCALE MOTION
CALCULATION OF VERTICAL VELOCITIES

Within the atmospheric boundary layer, several sources of vertical motion can be identified, such as topographic effects, horizontal wind divergence due to spatial changes in surface roughness, type and stability, and local circulations. These effects are mainly visible on the mesoscale and are not resolved by the long-range grid: The atmospheric boundary layer for the long-range model will therefore reflect only the divergence and vertical motion impressed upon it by the synoptic scale flow. On the mesoscale, however, local divergence will influence the boundary layer flow, but except in cases of gross topographic relief, these mesoscale perturbations will decrease to insignificant levels at the top of the ABL where the vertical motion is again determined by the synoptic scale motion. While the long-range and mesoscale modeling procedures are in essence similar, the treatment of divergence within the ABL is slightly different as is shown in Figure 3.3 .

3.1.3.3 Upper Air Analysis

Upper air analysis to 250 mb is based on radiosonde data and CMC analysis products. The problems to be confronted for the upper air analysis are those associated with spatial and temporal interpolation of cbservational data. Spatial interpolation at observational hours is accomplished using the isentropic

technique of Mancuso, Endlich and Ehernberger (1981) . This technique recognizes the importance of vertical motion. Temporal interpolation between 12-hourly radiosoundings is also done isentropically with the assistance of 6-hourly CMC analyses. To preserve the significance of parameters, (such as stability, vorticity and wind divergence derived from the observational data), through the temporal interpolation, the derived values are interpolated rather than deriving them at each step from the interpolated primary data. Divergence estimates are examined at each step and are adjusted to conform to boundary constraints using the variational technique of O'Brien (1970) . The meso-scale sub-grid, if required, is included as a sub-set for interpolation at this stage.

3.1.3.4 Atmospheric Boundary Layer Analysis

Surface pressure data and 850 mb temperatures are analysed to permit the estimation of an hourly surface geostrophic wind. For the mesoscale model, the upper air wind field and frictionless surface wind are rendered mass consistent using Endlich (1967) retaining only those components of divergence derived from the synoptic scale motion.

Boundary-layer profiles of wind, temperature and humidity are obtained by interpolating between the top of the surface layer similarity profile and the free flow at the top of atmospheric boundary layer using an Ekman/Taylor layer profile. Land and water surfaces are considered.

A model which requires some further development is proposed for inclusion of the nocturnal jet. For the mesoscale model, the boundary layer which at this stage contains divergence due to the upper air motion and due to spatial changes in surface roughness, type and stability, is further perturbed by topography using the technique of Anderson (1971) . Finally, on the mesoscale, information contained in the surface winds is incorporated into the boundary layer flow using the technique of Cressman (1960). In areas where surface wind data are very sparse, it may be necessary to omit this step. The divergence in the several layers of the mesoscale ABL is then calculated and these estimates are adjusted using a variational technique to match with the vertical motion of the synoptic scale analysis at the top of the ABL .

The final steps in the modeling procedure are to adjust the horizontal wind components to render the wind fields mass consistent using Endlich (1967) and to calculate vertical components at each grid point of the Eulerian grid (vertical wind components which are determined from interpolated divergence estimates, are not altered).

3.2 Upper Air Analysis

3.2.1 Objectives and Overview

The purpose of carrying out an analysis of the upper air meteorological observations is to provide gridded values of wind, stability and mixing ratio with good spatial and temporal resolution for use in the dispersion model. The analysis described in this section deals only with the meteorology above the atmospheric boundary layer which under super-adiabatic conditions can extend to 1 or 2 km . For purposes of the dispersion model, the modeling domain extends to 5 km above the surface.

In view of the relative sparseness of observational data when compared to the density of the calculating grid, it is necessary to enhance the density of the information contained in the data using interpolation methods which are consistent with the prevailing meteorology. Under ideal conditions with a barotropic atmosphere, the heights of pressure surfaces are constant and parallel to isentropic (constant potential temperature) surfaces: Air motion is horizontal and vertical motion is absent. This meteorological condition is virtually featureless and horizontal interpolation of observational data to a regular grid may be carried out independently at fixed levels. (i.e. barotropically).

Under most meteorological conditions the atmosphere departs from the barotropic condition and is baroclinic: Large baroclinic effects are features of frontal systems. Under these circumstances, isobaric surfaces are spatially variable in height and not necessary parallel to isentropic surfaces which may intersect the

1000 mb level and have large slopes particularly near a frontal system. Air motion is not everywhere parallel to the earth's surface and considerable horizontal wind divergence is evident in the wind field: This divergence results in vertical air movement which cannot be neglected with respect to vertical diffusion in the dispersion model. Barotropic interpolation is not appropriate for a strongly baroclinic atmosphere since such interpolation, incorrectly implies that at a grid point, meteorological parameters such as wind, stability and mixing ratio are always directly related to their values at adjacent grid points on the same level. The free atmosphere however, may be described as quasi-isentropic and air tends to move along isentropic surfaces: Meteorological variables on isentropic surfaces are more continuous and tend to vary more linearly along these surfaces than on isobaric or constant height surfaces.

Mancuso, Endlich and Ehernberger (1981) have discussed the advantages of performing analyses on isentropic surfaces and have formulated and tested a objective technique for carrying out such upper air analysis. The objective scheme described in the following section is largely based on their method although we have extended the method to permit temporal interpolation of the meteorological

fields between twice daily station soundings.

The results of the objective scheme give hourly winds (including vertical motion) stability and mixing ratio at all nodes of the calculation grid above the atmospheric boundary layer.

3.2.2 Objective Scheme for Upper Air Analyses at 12-Hourly Observational Intervals

This stage of the analysis is summarized in Figure 3.4 . Following Mancuso et al (1981) the upper air analysis is generated for the observation hours of 0000Z and 1200Z using isentropic interpolation of radiosonde information.

The radiosonde pressures are reduced to geo-potential meters (or heights) using the usual relationship (Hess, (1959) .

$$\Delta z_i = - \frac{R\bar{T}_i^*}{g} \ln \frac{p_i}{p_{i-1}} \qquad (3.2.1)$$

where Δz_i is the vertical distance interval corresponding to a pressure decrease from p_{i-1} to p_i (equals 50 mb for standard pressure levels), R is the gas constant, g is the gravitational constant and the average virtual temperature, $\bar{T}^*$, is given in terms of the mixing ratio, r, and temperature T by

OBJECTIVE ANALYSIS OF RADIOSONDE

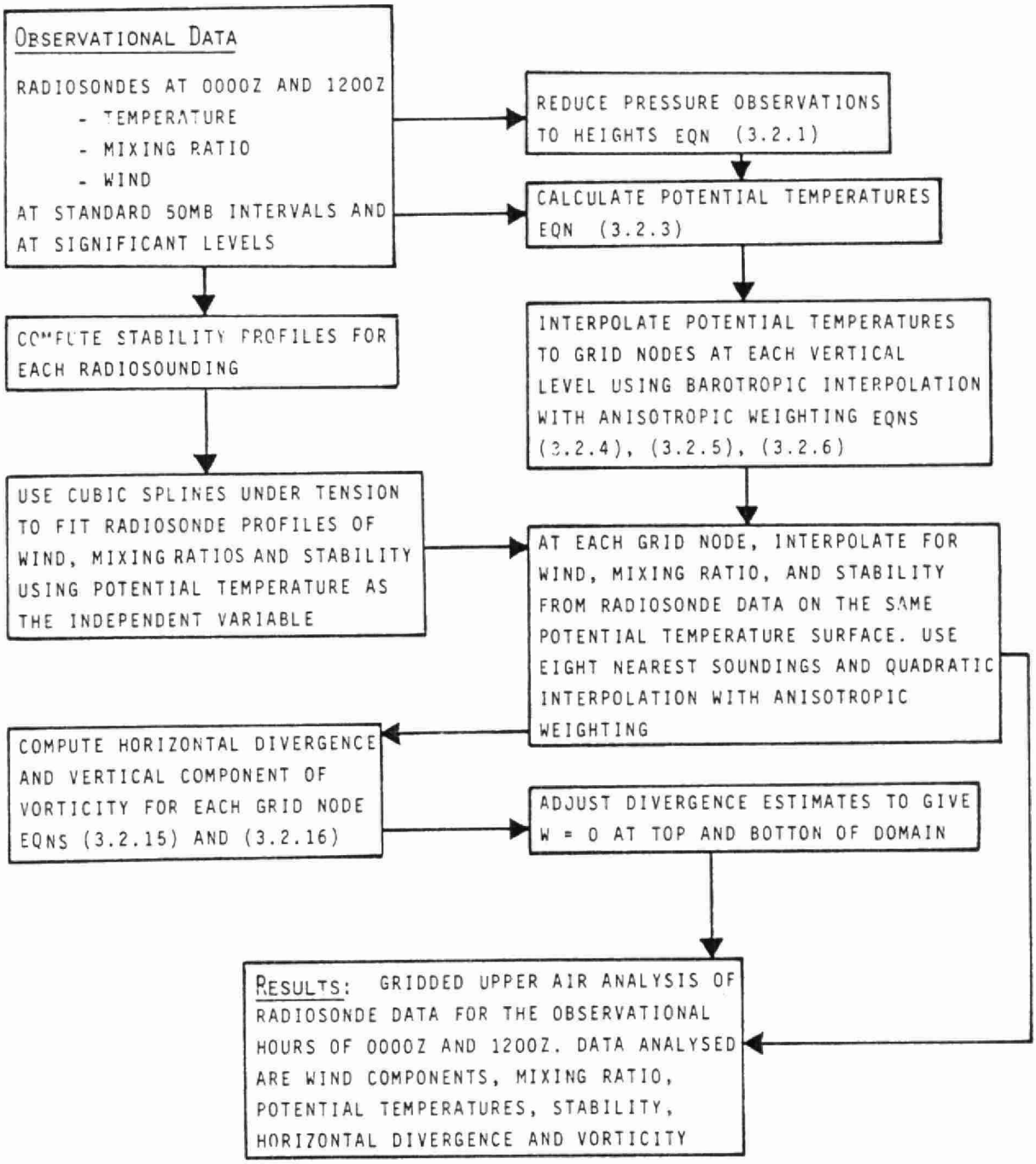

Fig. 3.4

$$\bar{T}^* = \left(\frac{1 + 1.609r}{1 + r} \right) \overline{T} \doteq \left(\frac{T^*_i + T^*_{i-1}}{2} \right) \qquad (3.2.2)$$

The observed temperatures are converted to potential temperature, θ, (proportional to entropy) using

$$\theta = T \left(\frac{1000}{p} \right)^{\kappa} \qquad (3.2.3)$$

where κ is R/C_p for air (=0.286 for dry air) .

3.2.2.1 Choice of Grid for Objective Analysis

The calculating grid for the dispersion model extends to 5000 m and has a maximum of twelve layers, many of which will be in the atmospheric boundary layer below 1500 m . In order to compute the distributions of divergence and vorticity from the objective analysis above 1500 m , it is necessary to have a grid of better vertical resolution that that required for the Eulerian model and to extend the analysis to 10 km . In the presence of a frontal system, the isentropic surfaces can be steeply inclined and a surface at a height of 10 km can intersect the underlying terrain at distances of the order of 2000 km .

For the objective analysis, the vertical grid spacings given in Table 3.1 will be used.

Table 3.1

Calculation Grid for Upper Air Analysis

Level	Pressure	Approximate Height	Approximate Thickness
	mb	m	m
1	850	1500	500
2	800	2000	500
3	750	2500	500
4	700	3000	600
5	650	3600	700
6	600	4300	700
7	550	5000	700
8	500	5700	700
9	450	6400	700
10	400	7100	1000
11	350	8100	1000
12	300	9100	1200
13	250	10300	

The horizontal grid coincides with the Eulerian grid which has 1° intervals in latitude and longitude for the long-range and 0.1° for the mesoscale model.

It would be economical, although not essential, if each upper level of the Eulerian grid coincides with one of the levels for objective analysis.

3.2.2.2 Isentropic Interpolation of Radiosonde Data to Grid

Isentropic interpolation involves calculating the potential temperature at each grid point and then interpolating meteorological variables from surrounding observations on the same potential temperature surface.

The potential temperature at each grid point is obtained using barotropic (or constant height) interpolation: A second-order polynomial surface fitted to the data at the nearest eight radiosonde observations will be used for interpolation.

$$\hat{q} = c_1 + c_2x + c_3y + c_4x^2 + c_5y^2 + c_6xy \qquad (3.2.4)$$

Minimizing the residuals gives the set of normal equations

$$\frac{\partial}{\partial c_k} \left[\sum_i w_i (q_i - \hat{q}_i)^2 \right] = 0 \qquad (3.2.5)$$

$k = 1$ to 6

$i = 1$ to 8

The weighting factor, w_i, is anisotropic in that it gives more weight to observations along the wind direction, than to those normal to the wind. Mancuso et al (1981) used

$$w_i = \frac{C^2}{\left[C^2 + R^2 + (\alpha s)^2\right]} \qquad (3.2.6)$$

where $C = 157$ km

$\alpha = \sqrt{2}$

R = distance from grid point

and $$S = \frac{\vec{k} \cdot \vec{R} \times \vec{V}}{|\vec{V}|} \qquad (3.2.7)$$

Solution of the set of linear normal equation (Equations (3.2.5) for the coefficients in Equation (3.2.4) is routine.

Once the potential temperature at each grid point, θ_g, has been calculated, the meteorological data at the levels corresponding to $\theta = \theta_g$ (i.e. on the same potential temperature surface) for the eight closest soundings, are determined from the sounding data by vertical interpolation using cubic splines under tension (Cline (1974) . These data together with weighting factors calculated from Equation (3.2.6) are used for the interpolation to the grid point in question. The meteorological parameters interpolated in this

manner are:

- u and v wind components
- mixing ratio
- stability

The stability

$$\left(\frac{1}{\theta}\right)\left(\frac{\partial\theta}{\partial z}\right) \qquad (3.2.8)$$

is calculated from the sounding data.

It is preferred for reasons of accuracy to calculate stability from data before interpolation rather than from the θ - profiles after interpolation to the grid.

This completes the interpolation of radiosonde observations yielding gridded winds, temperatures, mixing ratios and stability at 0000Z and 1200Z .

3.2.2.3 Calculation of Upper Air Divergence and Vorticity

Using curvilinear co-ordinates of latitude, ϕ, longtitude λ and elevation, z, the horizontal wind divergence and vertical component of vorticity may be written

$$\text{Divergence} = \nabla.\vec{V} = \mu_\lambda \frac{\partial \mu}{\partial \lambda} + \mu_\phi \left[\frac{\partial v}{\partial \phi} - v \tan \phi \right] \tag{3.2.9}$$

$$\text{Vorticity } \zeta_z = \mu_\lambda \frac{\partial v}{\partial \lambda} - \mu_\phi \left[\frac{\partial u}{\partial \phi} - u \tan \phi \right] \tag{3.2.10}$$

where $$\mu_\lambda = \frac{1}{R\cos\phi} \tag{3.2.11}$$

$$\mu_\phi = \frac{1}{R} \tag{3.2.12}$$

Neglecting the relatively small terms $-(v \tan \phi)/R$ in the divergence and $(u \tan \phi)/R$ in the vorticity one obtains

$$D = \mu_\lambda \frac{\partial u}{\partial \lambda} + \mu_\phi \frac{\partial v}{\partial \phi} \tag{3.2.13}$$

and

$$\zeta_z = \mu_\lambda \frac{\partial v}{\partial \lambda} - \mu_\phi \frac{\partial u}{\partial \phi} \tag{3.2.14}$$

or in central difference form, at a grid point (i, j, k)

$$D_{ijk} = \frac{\mu_\lambda \left[u_{i+1} - u_{i-1} \right]_{jk}}{2\Delta\lambda} + \frac{\mu_\phi \left[v_{j+1} - v_{j-1} \right]_{ik}}{2\Delta\phi} \quad (3.2.15)$$

$$\text{and} \quad \zeta_{ijk} = \mu_\lambda \frac{\left[v_{i+1} - v_{i-1} \right]_{jk}}{2\Delta\lambda} - \frac{\mu_\phi \left[u_{j+1} - u_{j-1} \right]_{ik}}{2\Delta\phi} \quad (3.2.16)$$

Using the above finite difference forms, the horizontal divergence and vertical component of vorticity are calculated at each grid point from the interpolated radiosonde data for 0000Z and 1200Z .

Mancuso et al have applied this objective technique to three test cases and present one case in their paper involving a cold front system. The results of the objective technique are compared qualitatively with subjective hand analysis of the same data. The computer generated results show good agreement with the subjective analysis, and are found to depict the baroclinic features of both the temperature and wind fields. The objective analyses of stability and divergence are very satisfactory, giving results which are compatible with the frontal surface.

3.2.2.4 Variational Scheme for Adjustment of Divergence Estimates

At each level the divergence estimated from equation (3.2.15) is subject to error and when vertical velocity is calculated by vertical summation of the divergence contributions, the error propagates and can lead to erroneous estimates of the vertical velocity at the upper levels. O'Brien (1970) has proposed a variational technique for adjusting the divergence contributions in each level so that realistic boundary values of vertical velocity are obtained.

The equation of continuity in pressure co-ordinates may be written

$$\frac{\partial \omega}{\partial p} + \frac{\partial u}{\partial x} + \frac{\partial v}{\partial y} = 0 \qquad (3.2.17)$$

where $\omega = -pgw$ for a steady barotropic atmosphere.

Integrating over a slice of the atmosphere Δp, gives

$$\omega_k = \omega_{k-1} + D_k \qquad (3.2.18)$$

where D_k is the horizontal wind divergence estimate in the k-th layer.

Hence, an initial estimate of the ω - profile may be made from the divergence estimates.

Assuming that the error of divergence estimate is proportional to the wind speed, adjustments to the divergence estimates are made using

$$D_k^1 = D_k - \frac{V_k}{Q_K} (\omega_k - \omega_T) \qquad (3.2.19)$$

where D_k^1 is the adjusted divergence, V_k is the layer wind speed and

$$Q_k = \sum_{n=1}^{k} V_n \qquad (3.2.20)$$

The values of ω at the surface and at the top of the domain ($k = K$) are assumed to be zero. The adjusted omega values are given by

$$\omega_k^1 = \omega_k - \frac{Q_k}{Q_K} (\omega_K - \omega_T) \qquad (3.2.21)$$

where ω_K is the desired value at the top of the domain (=0) and ω_T is the initial estimate of ω at the top of the domain.

In order to implement O'Brien's technique, the average divergence over each 50 mb layer is calculated and an initial estimate of ω_T is obtained using Equation (3.2.18) . The vertical wind speed at each pressure level is computed and the divergence estimates at each level are adjusted by applying Equations (3.2.19) and (3.2.21) with $\omega_K = 0$.

The adjusted divergences are then calculated at each grid by linear interpolation from the layer average values.

3.2.3 Objective Scheme for Temporal Interpolation of Upper Air Analysis

Section 3.2.2 describes an objective scheme for upper air analysis which is firmly based on observational data and which is of spatial resolution consistent with the resolution of the upper layers of the Eulerian calculation grid. The frequency with which such detailed upper air analysis may be performed is limited to the twice-daily soundings at the synoptic hours of 0000Z and 1200Z . The temporal resolution of the Eulerian model, which uses a time step of one hour for meteorological fields, is much finer than the temporal detail provided by 12-hourly upper air analyses : An objective scheme has been developed to carry out temporal interpolation between upper air analyses to give the one hour resolution required by the Eulerian model.

When the atmosphere in the modeling domain is reasonable quiescent over a 12-hour period, temporal interpolation using a relatively simple scheme will likely be satisfactory. However, as with spatial interpolation, in the presence of a frontal system, temporal interpolation is much more difficult and must be carried out in a manner which is consistent with the meteorology prevailing during the period : Simple time interpolation on barotropic surfaces will not be satisfactory.

Again, use is made of the quasi-isentropic nature of the free atmosphere for time interpolation. The objective technique is assisted by the use of 6-hourly analyses which are available on tape as a standard product from the Canadian Meteorological Centre (CMC) . These analyses are based on a hemispherical, primitive equation model run diagnostically using observational data available at the synoptic hours of 0000Z and 1200Z . Archived results are kept for two years plus the current year. Analysed parameters which are available on a 381 km polar stereographic grid, are wind, height, temperature and dew point on the 1000 mb, 850, 700, 500, 400, 300, 250, 200, 150, 100 isobaric surfaces. The vertical resolution of these analyses is somewhat less than that provided by radiosonde data (which report at 50 mb intervals and at significant levels), however, these analyses greatly enhance the temporal interpolation of upper air data.

The possibility exists of using the CMC model to generate hourly hemispherical analyses which would further improve the accuracy of the temporal interpolation. However, for purposes of this present design document only currently available meteorological products are relied upon.

3.2.3.1 Temporal Interpolation of Isentropic Surfaces and Associated Meteorological Parameters

In order to trace the motion of isentropic surfaces it is first necessary to define these surfaces on the analysis grid at the two synoptic observation times as well as at the intermediate CMC analysis times of 0600Z and 1800Z .

The CMC analyses at 0600Z and 1800Z require preprocessing to reduce the data to the λ, ϕ, z co-ordinate system from the 381 km polar-stereographic CMC grid on which the analyses are reported. Figure 3.5 summarizes the processing of CMC analyses.

Once the co-ordinate transformation has been done, the CMC analysis results are interpolated to 50 mb intervals and are then treated in the same manner as the radiosonde data to produce gridded values of wind, mixing ratio, potential temperature, stability,

REDUCTION OF CMC ANALYSES TO
UPPER-AIR ANALYSIS GRID

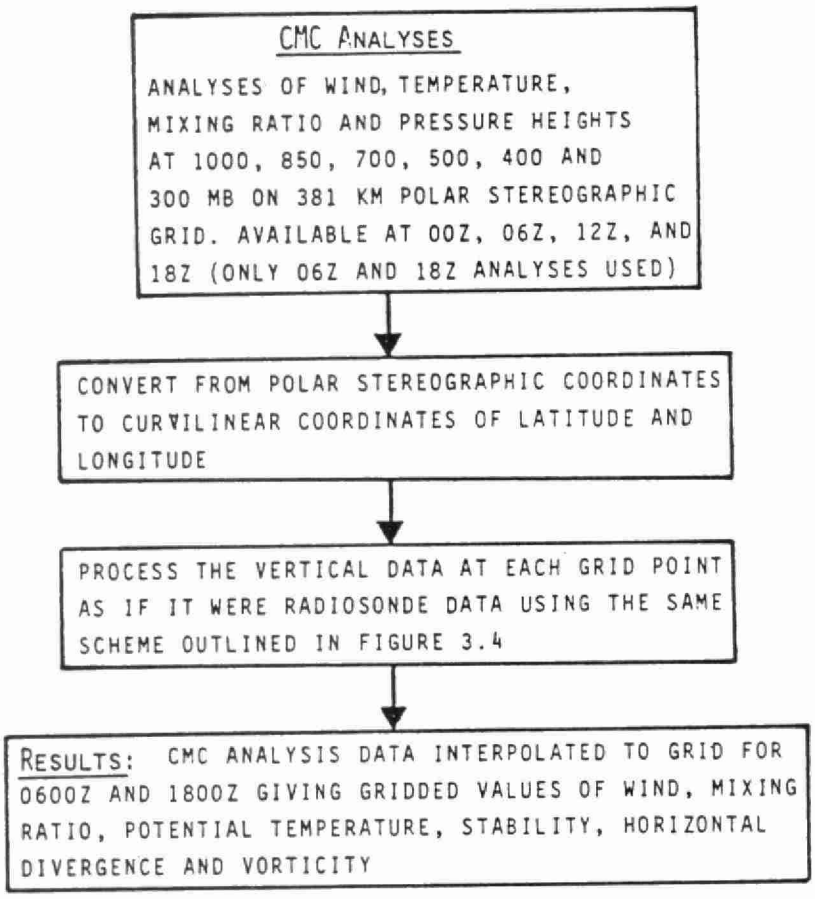

Fig. 3.5

horizontal divergence and vorticity on the same grid as the upper air analysis of radiosonde data.

It may seem tedious to interpolate from the CMC grid points to the objective analysis grid, but this is necessary for the next step of the temporal interpolation which is summarized in Figure 3.6 .

Starting with the gridded upper air analysis of radiosonde data and the CMC analysis at intermediate times, the heights at 2^{o} potential temperature intervals are determined by spline interpolation in the vertical and the associated values of wind, mixing ratio, vorticity, divergence and stability on each isentropic surface are determined by interpolation for each horizontal grid point.

Isentropic temporal interpolation is achieved by using a set of orthoganol polynomials to fit the isentropic surfaces in space and time (Sykes and Hatton (1976)). From experience with the objective interpolation of pressure fields, ninth-order polynomials in space and fourth-order in time should adequately fit the isentropic surfaces using the five upper air analyses which have been generated at 6-hour intervals over a 24-hour period.

TEMPORAL ISENTROPIC INTERPOLATION OF METEOROLOGICAL PARAMETERS

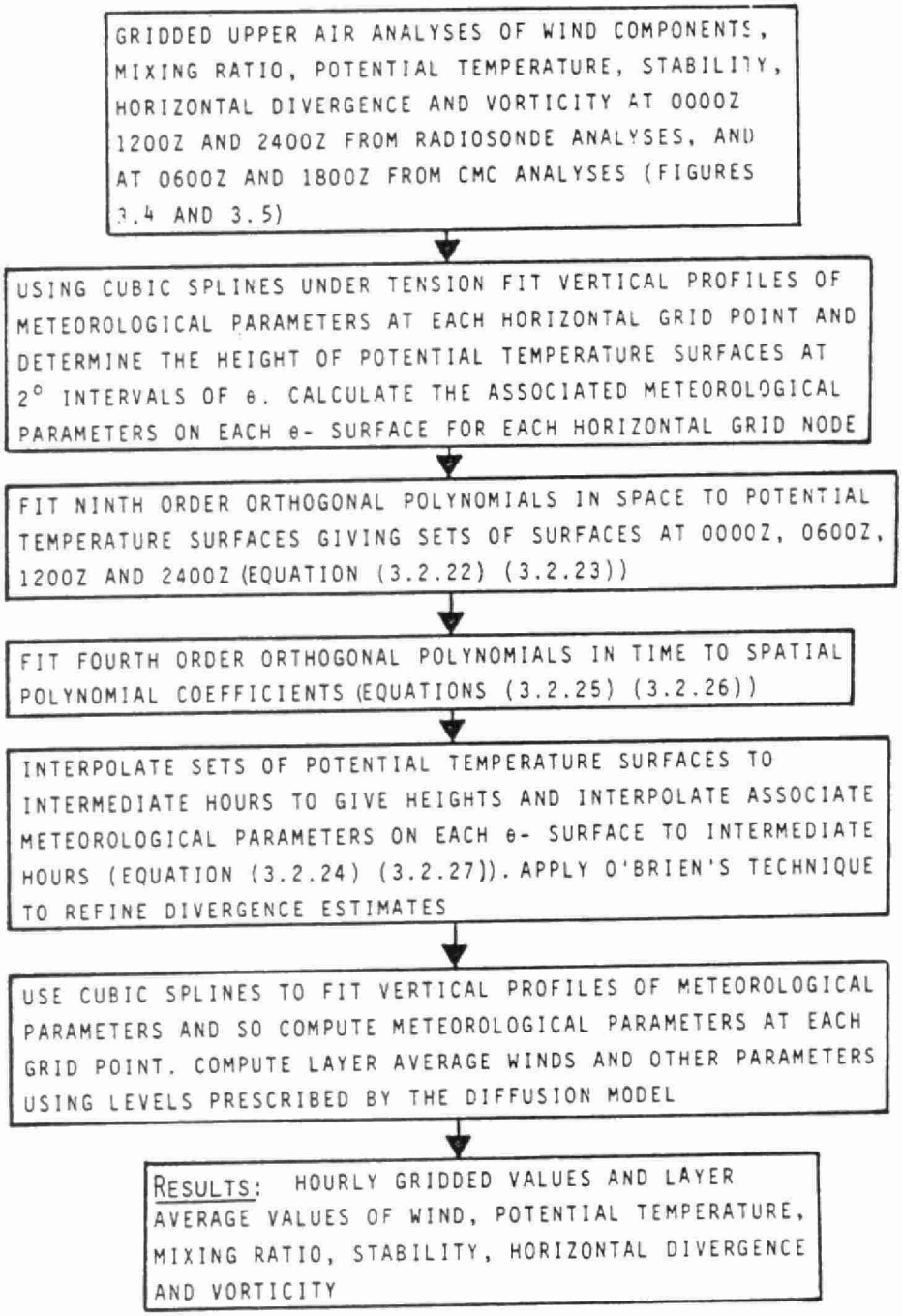

Fig. 3.6

Briefly, a fitted isentropic surface is given at t_o = 00Z, 06Z, 12Z, 18Z or 24Z by :

$$z_\theta (x,y,t_o) = \sum_{i=o}^{M} \sum_{j=o}^{i} a_{ij} \phi_{ij} (x,y) \qquad (3.2.22)$$

$$\text{and} \quad a_{ij}(t_o) = \sum_{n=1}^{N} z_\theta (x_n, y_n, t_o) \phi_{ij} (x_n, y_n) \qquad (3.2.23)$$

For interpolation at time t

$$z_\theta(x,y,t) = \sum_{i=o}^{M} \sum_{j=o}^{i} b_{ij}(t)\phi_{ij}(x,y) \qquad (3.2.24)$$

where

$$b_{ij}(t) = \sum_{k=o}^{L} C_k \theta_k(t) \qquad (3.2.25)$$

and

$$C_k = \sum_{p=1}^{K} a_{ij} (t_o)_p \theta_k (t_o)_p \qquad (3.2.26)$$

where M = 9 (order of spatial polynomials)
N = number of horizontal grid points
L = 4 (order of temporal polynomial)
K = number of time analyses = 5

Considerable computation is involved in computing the ϕ_{ij} and θ_k but since their values depend only on the grid co-ordinates and time interval between observations, they need be computed only once.

Equation (3.2.24) gives the time interpolated isentropic surface heights at each grid point. The meteorological parameters (including vorticity and divergence) are then interpolated isentropically using

$$f(t) = \sum_{k=o}^{L} d_k \, \phi_k \, (t) \qquad (3.2.27)$$

where

$$d_k = \sum_{p=1}^{K} f(t_o)_p \, \phi_k \, (t_o)_p \qquad (3.2.28)$$

and t is the time to which interpolation is required. For the interpolation of divergence, density variations must be allowed for by interpolating mass divergence (ρD) .

In this scheme, the vorticity and mass divergence are interpolated from the analysis times rather than calculating their values at each time from interpolated winds: This should preserve the significance of vorticity and divergence through the interpolation process as they are very sensitive to small errors in interpolating the wind components.

The interpolation process for divergence will introduce errors leading to possibly erroneous estimates of vertical velocity in the upper layers. O'Brien's technique for adjusting divergence is again applied to constrain the vertical velocity at the top of the domain to zero. (See Section 3.2.2.4) . Since the wind components are interpolated separately from ζ_z and D , the wind components at each interpolated time will not, at this stage of wind field development, be entirely consistent with the interpolated vorticity and divergence.

Rendering the wind field mass consistent will be done after the boundary layer profiles have been computed and the whole wind field has been reduced to layer averages for the Eulerian diffusion computations.

3.2.3.2 Calculation of Layer-Averaged Parameters From the Upper-Air Analysis

The final wind field in a layer averaged form must satisfy the continuity equation. The layer averaging procedure for wind components should therefore produce a mass averaged velocity or

$$\int_{z_i}^{z+\Delta z_i} (\rho u)\, dz = \bar{\rho}_i\, \bar{u}_i\, \Delta z_i \qquad (3.2.29)$$

where

$$\bar{\rho}\ \Delta z_i = \int_{z}^{z+\Delta z_i} \rho\ dz \qquad (3.2.30)$$

The integrals may be readily evaluated using splines fit to the vertical profiles of (ρu) and ρ or simple quadrature may be sufficiently accurate.

The layers over which the averages are determined are prescribed by the Eulerian grid for the diffusion model.

Other variables which must be reduced to layer-averages are horizontal divergence, vorticity, temperature and mixing ratio. Simple averaging such as that used for density (Equation 3.2.30) may be used for these parameters except the divergence which should be a density weighted average, i.e. .

$$\bar{D}_i = \frac{1}{\Delta\rho_i} \int_{\rho}^{\rho-\Delta\rho i} D\ d\rho \qquad (3.2.31)$$

3.3 Analysis of Winds in The Atmospheric Boundary Layer

3.3.1 Objectives and Overview

The objective upper air analysis and temporal interpolation scheme described in Section 3.2 , provides the wind field and mixing ratio profiles in the free atmosphere above the atmospheric boundary layer (ABL) which under super-adiabatic conditions may extend to 1 or 2 km above the terrain. The purpose of the upper air analysis is to determine the advection in the upper levels for the dispersion model and to define the vertical motion which can result in subsidence or convection through the top of the model at 5 km above the terrain.

From the point of view of dispersion, the highest pollutant concentration and the greatest variability of these concentrations in space and time, occurswithin the atmospheric boundary layer and hence the necessity for a larger number of vertical levels within the ABL for dispersion calculations. In order to reliably model the dispersion within the ABL it is therefore necessary to describe the wind field with good spatial and temporal resolution in the lower layers. The dependence of wind profiles within the ABL, as well as the dependence of boundary layer height, on atmospheric stability and surface roughness, must be included in the model.

As with the upper air analysis, vertical profile observations within the ABL are available only at 12-hourly intervals from radiosoundings at 0000Z and 1200Z and the main problem which has to be addressed in deriving hourly wind fields, is temporal interpolation. The only relevant data which are available hourly from routinely reporting stations are surface wind, surface pressure (reduced to mean sea level (MSL)), and the temperature.

Surface wind observations are greatly influenced by mesoscale effects such as local topography, drainage flows and other mesoscale circulations: Their use for the long-range wind field model has therefore been rejected since they are not generally representative of the regional surface flow. MSL surface pressures, which are not subject to the same mesoscale influences, are more representative of regional air movement and will be used in the analysis of the wind field in the ABL for the long-range model.

The objective scheme to be used to determine hourly wind field data within the atmospheric boundary layer is summarized in Figure 3.7 . Briefly, the distribution of surface pressure (MSL) is used to calculate the surface geostrophic wind, V_{gp} , which for a barotropic atmosphere, gives the flow of air over the terrain at the top

CALCULATION OF GRIDDED, LAYER-AVERAGED
WINDS IN THE ABL

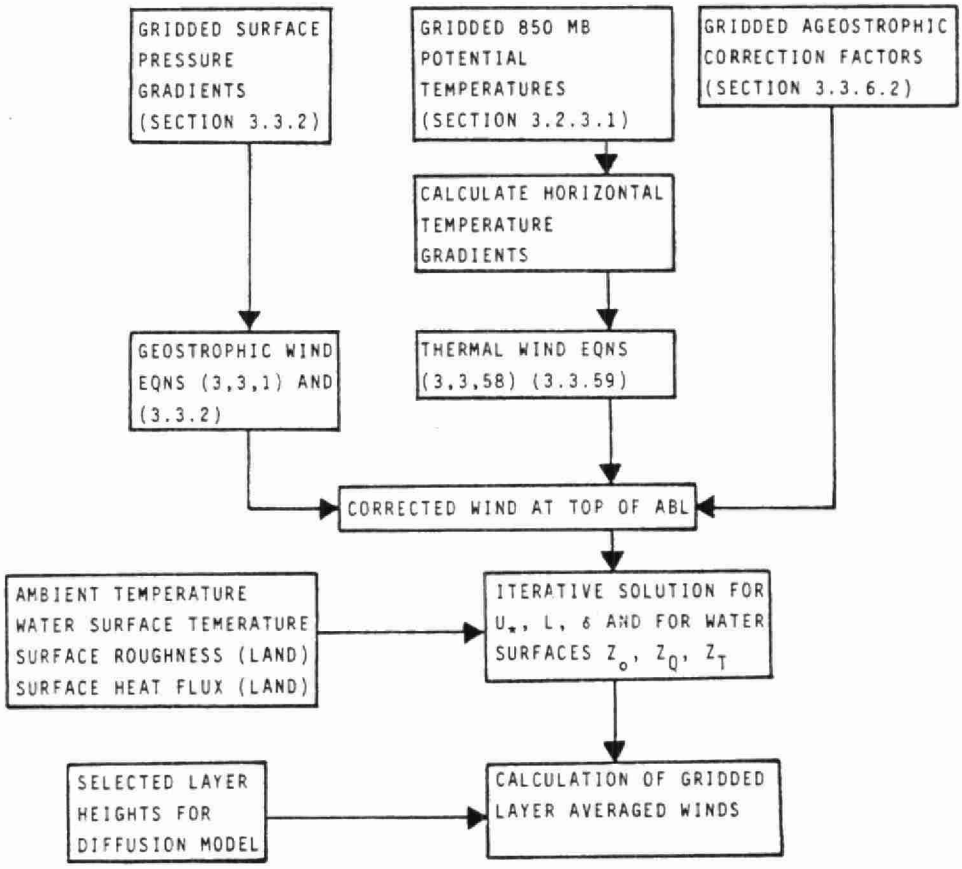

Fig. 3.7

of the ABL where frictional effects due to surface drag are small. In a baroclinic atmosphere, however, the geostropic wind at the top of the ABL is perturbed by ageostrophic wind components which are impressed on the surface flow by the baroclinity of the upper air. By comparing the wind observations from the 0000Z and 1200Z radiosoundings with the calculated surface geostrophic wind, the ageostrophic components of the wind at the top of the ABL can be estimated for each sounding station. By interpolating only the ageostrophic wind components in space and time, the hourly surface pressure observations may be used to 'steer' the flow at the top of the ABL through the hourly derived surface geostrophic wind. This technique of deriving ageostrophic correction factors from observations has been used by Mancuso et al for correcting pressure derived geostrophic winds.

Once the upper boundary winds have been determined for the ABL, the final step in the analysis involves calculation of the wind speed and direction profiles within the boundary layer.

The flow in the boundary layer may be divided into two layers: a surface frictional layer (usually of the order of 50 m thick) and an Ekman/Taylor layer through which the wind speed and direction changes with height and approaches the free flow at the top of the ABL . The wind profiles in the whole ABL can be obtained by matching the velocity profile in the upper layer with the surface-

layer profile. This matching procedure leads to the so-called resistance or drag laws which describe the transmission of surface generated shear stress through the ABL . Proper attention must be given to the difference between flow over water surfaces and solid terrain.

3.3.2 Interpolation of Surface Pressures to the Grid and Calculation of Surface Geostrophic Wind

Surface pressures are reported as equivalent mean sea-level pressures so that the effect of the altitude of the observing station is removed from the pressure observation. In order to calculate the surface geostrophic wind, it is necessary to analyse the surface pressure distribution and to obtain horizontal pressure gradients.

The surface geostrophic wind is given by

$$U_g = - \frac{1}{\rho f} \left[\mu_\phi \frac{\partial p}{\partial y} + \frac{\mu_\lambda}{f} \frac{\partial}{\partial x} \left(\frac{\partial p}{\partial t} \right) \right] \qquad (3.3.1)$$

and

$$V_g = \frac{1}{\rho f} \left[\mu_\lambda \frac{\partial p}{\partial x} - \frac{\mu_\phi}{f} \frac{\partial}{\partial y} \left(\frac{\partial p}{\partial t} \right) \right] \qquad (3.3.2)$$

The pressure tendency terms with respect to time include some of the ageostrophic effects of a baroclinic atmosphere but do not allow for the more marked effects of large thermal gradients and vorticity advection.

The spatial and temporal gradients of pressure are computed by fitting ninth-order orthogonal polynomials in space and fourth-order in time to the hourly observational data (Sykes and Hatton (1976)). The procedure is identical to that described in Section 3.2.3.1 for fitting isentropic surfaces:

$$p(x,y,t_o) = \sum_{i=o}^{M} \sum_{j=o}^{i} a_{ij}(t_o)\, \phi_{ij}(x,y) \qquad (3.3.3)$$

where $$a_{ij}(t_o) = \sum_{n=1}^{N} p(x_n,y_n,t_o)\ \phi_{ij}(x_n,y_n) \qquad (3.3.4)$$

and $$p(x,y,t) = \sum_{i=o}^{M} \sum_{j=o} b_{ij}(t)\ \phi_{ij}(x,y) \qquad (3.3.5)$$

where $$b_{ij}(t) = \sum_{k=o}^{L} c_k\, \theta_k(t) \qquad (3.3.6)$$

and $$C_k = \sum_{p=1}^{K} a_{ij}(t_o)_p\, \theta_k(t_o)_p \qquad (3.3.7)$$

where M = 9 (order of spatial interpolation)
N = number of observing stations
L = 4 (order of temporal polynomial)
K = number of time observations

Again with fixed grid and observing station co-ordinates, the ϕ_{ij} and θ_k need be computed only once. Temporal and spatial derivatives of the pressure field may be computed from the series so permitting the calculation of the surface geostrophic wind using Equations (3.3.1) and (3.3.2) at each grid point and at the radiosounding stations at 0000Z and 1200Z .

3.3.3 Estimation of the Height of the Atmospheric Boundary Layer

The hydrodynamic thickness of the atmospheric boundary layer may be defined as the height at which frictional effects on the atmospheric motion become negligible and the air motion is determined by pressure forces, thermal gradients and the kinematic properties of the motion such as vorticity and divergence. Within the boundary layer, the shear stress is determined by the geostrophic flow as well as the roughness of terrain and stability of the atmosphere.

The well known Ekman solution of the steady equation of motion for a homogeneous atmosphere yields the so-called Ekman spiral. The boundary layer height from this solution which assumes a constant

eddy viscosity with height, is

$$h = c\sqrt{\frac{K}{f}} \tag{3.3.8}$$

where K is the eddy viscosity and f the coriolis parameter.

Stable Stratification:

Assuming that this relationship still holds for a variable K, Nieuwstadt (1981) showed that for a stable atmosphere

$$\frac{h}{L} = \frac{0.3 \left(\frac{u_*}{fL} \right)}{\left[1 + 1.9 \left(\frac{h}{L} \right) \right]} \tag{3.3.9}$$

where u_* is the friction velocity $(=(\tau_{o/\rho})^{\frac{1}{2}})$ and L is the Monin-Obukhov length defined as

$$L = - \frac{\rho c_p u_*^3}{k \beta H} \tag{3.3.10}$$

where τ_o and H are the turbulent fluxes of heat and momentum at the surface, ρ is density, c_p specific heat, k is the von Karman constant (= 0.35) and β is a buoyancy parameter defined as the ratio of temperature, T, to gravitational acceleration, g .

For a neutral atmosphere, $L \to \infty$, and

$$h = 0.3 \frac{u_*}{f} \tag{3.3.11}$$

which is the expression proposed by Tennekes (1973) . For a very stable atmosphere, $L \to 0$, and

$$h = 0.4 \left(\frac{u_* L}{f} \right)^{\frac{1}{2}} \tag{3.3.12}$$

This expression is similar to that given by Zilitinkevich (1972) and Businger and Arya (1974) except that the proportionality constant was found to be close to 0.7 . Using linear regression Arya (1981) proposes the following diagnostic expressions for h .

$$h = 113.5 + 0.34 \left(\frac{L u_*}{f} \right)^{\frac{1}{2}} \tag{3.3.13}$$

or

$$h = 85.1 + 0.089 \left(\frac{u_*}{f} \right) \tag{3.3.14}$$

valid for near neutral or stable boundary layers.

Brown (1981) proposes the following length scale for characterizing boundary layer thickness

$$\delta = \frac{2 u_* k \lambda}{f\left[1 + \lambda \frac{\partial \psi}{\partial (z/\delta)}\right]} \quad ; z = \lambda\delta \tag{3.3.15}$$

For stable conditions, this expression with k=0.35 λ=0.15 , approaches,

$$\delta = 0.39 \left(\frac{u_* L}{f} \right)^{\frac{1}{2}} \tag{3.3.16}$$

which is essentially the same as Tennekes (1973) (Equation (3.3.12)) .

Prognostic models of the dynamic height of the stable boundary layer are available which predict the growth of the nocturnal stable layer (Nieuwstadt and Tennekes (1981)) . These authors derive the rate equation

$$\frac{dh}{dt} = \frac{(h_e - h)}{T} \tag{3.3.17}$$

where $$T = -\frac{3}{4}\frac{(\theta_h - \theta_o)}{\left(\frac{\partial\theta_o}{\partial t}\right)} \qquad (3.3.18)$$

and the equilibrium height is given by

$$h_e = 0.15\,\frac{f\,G^2 \sin\alpha \cos\alpha}{\frac{g}{T}\left|\frac{\partial\theta_o}{\partial t}\right|} \qquad (3.3.19)$$

G is the geostrophic wind speed, α the cross-isobar angle of the surface flow, θ_h and θ_o are the potential temperatures at the top of the boundary layer and at the surface respectively. The prognostic rate equation results and the diagnostic equation (Equation (3.3.12)) were compared with data and a far better agreement with the prognostic model was obtained.

While the prognostic model does seem superior to diagnostic models of the stable boundary layer height, the former model is not only more complex but relies on relatively detailed information regarding temperature profiles and surface cooling rates. Bearing in mind that the boundary layer depth at this stage is only required to determine the height at which to measure the free atmosphere flow from the radiosound observations, it is more appropriate to use the simpler diagnostic model given by Equation (3.3.12) or (3.3.15) .

Nieuwstadt (1982) recommends that these diagnostic equations are only applicable 2 hours after sunset and that the boundary layer height for transitional hours should be obtained by interpolation from daytime mixing heights.

Unstable Stratification:

Holzworth (1964) has given a technique for determining the depth of the mixed layer using the 1200Z radiosounding temperature profile and hourly surface temperature observations. The method involves extending a dry adiabat vertically from the surface temperature, to intersect the radiosonde temperature profile. With a fully developed mixed layer trapped beneath a stable layer (such as might exist towards noon), Holzworth's technique probably gives a good estimate of the thickness of the atmospheric boundary layer.

Brown suggests that his diagnostic Equation (3.3.15) is applicable to unstable conditions. For large L from Equation (3.3.15)

$$\delta = \frac{2u_* \, k \, \lambda}{f} \qquad (3.3.20)$$

Using Brown's definition of boundary layer thickness

$$h = \pi\sqrt{\frac{2K}{f}} \quad = \quad \pi\,\delta$$

one obtains for neutral conditions

$$h = 0.33\left(\frac{u_*}{f}\right) \tag{3.3.21}$$

which is in reasonable agreement with Equation (3.3.11) . Equation (3.3.20) was used by Brown (1981) and Brown and Liu (1982) with considerable success for modeling the planetary boundary layer over Arctic seas.

Generally speaking, diagnostic equations are not very successful for estimating the daytime boundary layer thickness and several prognostic modles have been proposed (Deardorff (1974), Maul (1980)) . The latter model gives the hourly development of the convective boundary layer as

$$h(t+\Delta t) = \left[h^2(t) + \frac{2H(1+A)\,\Delta t}{\gamma\rho C_p} - \frac{2\Delta\theta(t)h(t)}{\gamma}\right]^{\frac{1}{2}} + \frac{\Delta\theta(t+\Delta t)}{\gamma}$$

where

$$\Delta\theta(t+\Delta t) = \left[\frac{2\gamma\,A\,H\,\Delta t}{\rho C_p}\right]^{\frac{1}{2}} \tag{3.3.22}$$

and γ is the lapse rate above the mixing height, Δ is a constant (0.15), $\Delta\theta$ is the temperature discontinuity at the top of the mixed layer, and H is the surface heat flux.

In view of the level of detailed information required by Equation (3.3.22), and the uncertainties of this detail introduced by temporal interpolation, it may be difficult to apply this prognostic equation. It is therefore proposed to use Holzworth's technique together with a temporally interpolated 850 mb lapse rate between soundings. The use of a prognostic equation such as (3.3.22) may be used to assist with the interpolation.

3.3.4 Wind Profiles in the Atmospheric Boundary Layer

Assuming that the boundary layer thickness and the free air wind at the top of the boundary layer are known, the wind profile in the ABL can be estimated by considering the flux of momentum through the boundary layer. Separate solutions for the flow in the surface layer (or inner layer) and the outer or Ekman/Taylor layer are available. The problem of interpolating from the top of the surface layer to the geostrophic flow is one of matching inner and outer solutions in such a manner that boundary conditions at the surface and top of the ABL are satisfied while ensuring that shear stress and wind velocity are continuous through the boundary layer. The matching can be achieved by simple matching of boundary conditions for each solution or through the use of dimensional analysis and dynamic similarity arguments.

3.3.4.1 Wind Profile in the Surface Layer

The surface layer is characterized as a layer through which the shear stress, τ_o , is approximately constant. The actual value of the shear stress (or flux of momentum) is dependent on the wind speed, surface type and roughness as well as on the stability of the surface air. The stability in turn depends on the surface heat flux, and over a water surface, on the mass

flux of water vapour as well. For a water surface the surface roughness is also a function of shear stress. Hence, in order to get a description of the wind profile in the surface layer, it is necessary to consider the simultaneous transfer of momentum, heat and water vapour. Over a land surface, the effects of water vapour transfer are generally small. However, in the following development a general surface is considered, i.e. land or water.

In the surface layer the profiles of wind speed, humidity and potential temperature may be written (Businger (1973))

$$\frac{T(z)-T_s}{T_*} = \left[\ell n \left(\frac{z}{z_T} \right) - \psi_T (\zeta) \right] \frac{1}{(\alpha_H k)} \qquad (3.3.23)$$

$$\frac{Q(z)-Q_s}{Q_*} = \left[\ell n \left(\frac{z}{z_Q} \right) - \psi_Q (\zeta) \right] \frac{1}{(\alpha_E k)} \qquad (3.3.24)$$

$$\frac{u(z)-u_s}{u_*} = \left[\ell n \left(\frac{z}{z_0} \right) - \psi_U (\zeta) \right] \frac{1}{k} \qquad (3.3.25)$$

where the characteristic scales of velocity, temperature and humidity are given by

$$u_* = \left(\frac{\tau_o}{\rho} \right)^{\frac{1}{2}} \tag{3.3.26}$$

$$T_* = - \left(\frac{H_o}{c_p \rho u_*} \right) \tag{3.3.27}$$

$$Q_* = \left(\frac{E}{\rho u_*} \right) \tag{3.3.28}$$

where H_o and E are the surface fluxes of heat and water vapour and L is the Monin-Obukhov length given by

$$L = \frac{- T_v u_*^2}{gk T_{V_*}} \tag{3.3.29}$$

$$\zeta = \frac{z}{L} \tag{3.3.30}$$

$$T_v = T(1+0.61Q) \tag{3.3.31}$$

$$T_{v_*} = T_*(1 - 0.61 Q) + 0.61 TQ_* \tag{3.3.32}$$

The values of T and Q are taken at some reference height (say 10 m): This definition of L allows for the effect of humidity fluctuations on stability. The ratios α_T and α_E are the ratios of eddy thermal diffusivity and eddy mass diffusivity to eddy momentum diffusivity. Subscript s refers to the surface value and the values of z_o, z_Q and z_T are related to surface roughness: Over a water surface they will depend on the molecular processes at the air/water interface.

The stability effects on the profiles are given by the functions $\psi(\zeta)$ which may be expressed for unstable conditions by

$$\psi_T = 2 \ln \left(\frac{1+Y}{2} \right) \tag{3.3.33}$$

$$\psi_E = 2 \ln \left(\frac{1+Y^1}{2} \right) \tag{3.3.34}$$

$$\psi_u = 2 \ln \left(\frac{1+X}{2} \right) + \ln \left(\frac{X^2+1}{2} \right) - 2 \tan^{-1}(X) + \frac{\pi}{2} \tag{3.3.35}$$

where

$$X = (1 + a_u|\zeta|)^{\frac{1}{4}} \tag{3.3.36}$$

$$Y = (1 + a_T|\zeta|)^{\frac{1}{2}} \tag{3.3.37}$$

$$Y^1 = (1 + a_E|\zeta|)^{\frac{1}{2}} \tag{3.3.38}$$

and for stable conditions

$$\psi_T = -b_T\zeta \tag{3.3.39}$$

$$\psi_E = -b_E\zeta \tag{3.3.40}$$

$$\psi_u = -b_u\zeta \tag{3.3.41}$$

Following Liu et al (1979) $\alpha_H = \alpha_E = 1.14$; $a_u = a_E = 16$ and $b_u = b_T = b_E = 7$ (Paulson (1970); Monin and Yaglom (1971)) .

The value of z_o is dependent on the shear stress for a water surface and Kondo (1975) gives the following empirical expressions for the surface drag coefficient based on the 10 m wind under neutral conditions.

u(10)	$C_D(10)$
0.3 - 2.2	$1.08\ U^{-0.15}$
2.2 - 5.0	$0.771 + 0.0858\ U$
5.0 - 8.0	$0.867 + 0.025\ U$
8.0 -25.0	$1.2 + 0.025\ U$
25 - 50	$0.073\ U$

The drag coefficient is given by

$$C_D = \left(\frac{u_*}{u}\right)^2 \tag{3.3.42}$$

For neutral conditions $\psi_u(\zeta)=0$ and z_o can be estimated from Equation (3.3.25) giving

$$z_o = \exp\left[\ell n(10) - k\, C_D^{-\frac{1}{2}} \right] \tag{3.3.43}$$

Over a land surface z_o may be estimated from the type of terrain and vegetative cover. The values of z_T and z_E over a water surface depend on the molecular processes at the interface and may be estimated from Liu et al (1979) .

$$\frac{z_T u_*}{\nu} = a_1 \left(\frac{z_o u_*}{\nu} \right)^{b_1} \tag{3.3.44}$$

$$\frac{z_E u_*}{\nu} = a_2 \left(\frac{z_o u_*}{\nu} \right)^{b_2} \tag{3.3.45}$$

where the coefficients and exponents depend on the roughness Reynolds number ($= z_o u_*/\nu$) .

$\left(\frac{z_o u_*}{\nu}\right)$	a_1	b_1	a_2	b_2
0 - 0.11	0.177	0	0.292	0
0.11 - 0.825	1.376	0.929	1.808	0.826
0.825 - 3.0	1.026	-0.599	1.393	-0.528
3.0 - 10.0	1.625	-1.018	1.956	-0.870
10.0 - 30	4.661	-1.475	4.994	-1.297
30 - 100	39.904	-2.067	30.79	-1.845

For a land surface, the roughness lengths for heat, mass and momentum transfer are approximately equal.

For a water surface, the surface water temperature can be estimated from the bulk water temperature, T_w, (Liu et al (1979)) by

$$T_s = T_w - ST_{*_w} \tag{3.3.46}$$

where

$$T_{*_w} = - \frac{H_w}{c_{p_w} \rho_w u_{*_w}} \tag{3.3.47}$$

$$H_w = -(H + L_v E + R) \tag{3.3.48}$$

R is the net radiation (Geiger 1965)

$$R = \sigma_s T_s^4 - \sigma_s T_a^4 \ (0.82-0.250 \times 10^{-0.094 e_a}) \qquad (3.3.49)$$

and S is given by

$$\begin{aligned} S &= 9.3\ Pr^{\frac{1}{2}}\ Rr^{\frac{1}{4}} && Rr \leq 0.85 \\ &= 16\ Pr^{\frac{1}{2}} && Rr > 0.85 \end{aligned} \qquad (3.3.50)$$

Pr is the Prandtl number and Rr is the roughness Reynolds number, L_v latent heat of vaporization and e_a the partial pressure of water vapour in the air.

This section has summarized the surface layer equation for a general surface type: In order to interpolate to the geostrophic flow, these relationships must be matched with the Ekman/Taylor upper boundary layer.

3.3.4.2 Wind Profiles in the Ekman/Taylor Layer

Brown (1974) gives a solution of the steady equation of motion for constant eddy diffusivity, K

$$\frac{1}{\rho}\frac{\partial p}{\partial x} - fv - K\frac{\partial^2 u}{\partial z^2} = 0 \qquad (3.3.51)$$

$$\frac{1}{\rho}\frac{\partial p}{\partial y} + fu - K\frac{\partial^2 v}{\partial z^2} = 0 \qquad (3.3.52)$$

with the boundary conditions

$$u \to U_g \qquad z \to \infty$$

$$v \to V_g$$

and

$$u \to u(h) \qquad z \to 0$$

$$v \to 0$$

giving

$$\frac{u(z)}{G} = \cos\alpha - \exp\left(-\frac{z}{\delta}\right)\left\{\cos\left(\alpha+\frac{z}{\delta}\right) - \frac{u}{G}(h)\cos\left(\frac{z}{\delta}\right)\right\} \quad (3.3.53)$$

$$\frac{v(z)}{G} = \sin\alpha - \exp\left(-\frac{z}{\delta}\right)\left\{\sin\left(\alpha+\frac{z}{\delta}\right) - \frac{u}{G}(h)\sin\left(\frac{z}{\delta}\right)\right\} \quad (3.3.54)$$

where the co-ordinate system is chosen so that the x-co-ordinate is in the direction of $u(h)$ and α becomes the angle between the geostrophic flow, G, and the surface flow, $u(h)$. The scaling length for the outer layer, δ , is given by

$$\delta = \left(\frac{2K}{f}\right)^{\frac{1}{2}} \quad (3.3.55)$$

This solution has an advantage over the classical Ekman solution in that the lower boundary condition, $u \to u(h)$, is satisfied which is appropriate for the upper layer.

Brown has used this solution and a matching procedure with the surface layer equation, to describe the flow through the whole ABL .

Brown also modeled the effect of thermal wind and secondary flow on the outer velocity profile: Equations (3.3.53 and 3.3.54) are modified to

$$\frac{u(z)}{G} = \cos\alpha + \frac{u_T z}{G\delta} - e^{-\frac{z}{\delta}}\left\{\left[\cos\left(\frac{z}{\delta}\right) - \sin\left(\frac{z}{\delta}\right)\right]\sin\alpha + \frac{v_T}{G}\cos\left(\frac{z}{\delta}\right)\right\} + \frac{u_2}{G} \tag{3.3.56}$$

$$\frac{v(z)}{G} = \sin\alpha + \frac{v_T z}{G\delta} - e^{-\frac{z}{\delta}}\left\{\left[\cos\left(\frac{z}{\delta}\right) + \sin\left(\frac{z}{\delta}\right)\right]\sin\alpha + \frac{v_T}{G}\sin\left(\frac{z}{\delta}\right)\right\} + \frac{v_2}{G} \tag{3.3.57}$$

where $$u_T \doteq \frac{-g}{fT_o}\frac{\partial T}{\partial y} \tag{3.3.58}$$

$$v_T \doteq \frac{g}{fT_o}\frac{\partial T}{\partial x} \tag{3.3.59}$$

and u_2, v_2 are secondary flows (Brown (1970)) .

3.3.5 Matching of Surface Boundary Layer Flow to the Geostrophic Flow

Kajanskii and Monin (1960) used consideration of dynamic similarity and dimensional analysis to match an outer viscous-Coriolis force balance to the inner logarithmic profile giving

$$\frac{kG \cos \alpha}{u_*} = \ln \left(\frac{u_*}{fz_o} \right) - A \qquad (3.3.60)$$

$$\frac{kG \sin \alpha}{u_*} = - B \qquad (3.3.61)$$

Clark (1970) considered the effects of stratification on the ABL adding a third relationship

$$\frac{k\theta}{\theta_*} = \ln \frac{u_*}{fz_o} - C \qquad (3.3.62)$$

Various empirical values and expressions have been proposed for A, B and C which depend on stability. With suitable values of these constants, the above equations permit the estimation of u_* , θ_* and α from the geostrophic flow, so permitting the calculation of surface winds.

Brown (1981) and Brown and Liu (1982) carried out a matching of the outer Ekman/Taylor solution (Equation (3.3.56 and 3.3.57)) with the surface layer profiles. The matching procedure and boundary conditions lead to the expressions

$$\frac{kG}{u_*}(\sin\alpha + \beta) = -B = -\left(\frac{1}{2\lambda}\right)\left[1 - \lambda\left(\frac{\partial\psi}{\partial(z/\delta)}\right)\right]_{z=\lambda\delta} \tag{3.3.63}$$

$$\frac{kG}{u_*}(\cos\alpha + \gamma) = -A = \ell n\left(\frac{\lambda\delta}{z_o}\right) - \psi\left(\frac{\lambda\delta}{L}\right) + B \tag{3.3.64}$$

The solutions are matched at $z = \lambda\delta$ where δ is a length scale.

$$\delta = \frac{2k\lambda u_*}{f\left[1 - \lambda\left(\frac{\partial\psi}{\partial(z/\delta)}\right)\right]} \tag{3.3.65}$$

$$\beta = \left(\frac{v_T - u_T}{2}\right) + \left(\frac{v_2 - u_2}{2}\right)_{z=\lambda\delta} \tag{3.3.66}$$

$$\gamma = \left(\frac{v_T + u_T}{2}\right) + \left(\frac{v_2 + u_2}{2}\right)_{z=\lambda\delta} \tag{3.3.67}$$

From the discussion in Section 3.3.3, it appears that this scaling length, δ , is only appropriate for stable conditions and the mixed layer thickness should be used for unstable conditions.

Solving for u_* from Equations (3.3.56),(3.3.57)and (3.3.25) gives

$$\frac{u_*}{kG} = \frac{-\gamma A - \beta B + \left[B^2 + A^2 - (\gamma B - \beta A)^2\right]^{\frac{1}{2}}}{A^2 + B^2} \qquad (3.3.68)$$

An iterative solutions of the equations is necessary since they are implicit in u_* . One of the advantages of the Brown technique is that in principle, the constants A and B are easily obtained from the geostrophic flow and boundary layer parameters enabling the complete ABL wind profile to be calculated.

Brown and Liu (1982) have proposed a computational scheme which combines the boundary layer parameterizations of Liu, Katsaros and Businger (1979), Kondo (1975), (as described in Section 3.3.4.1), with the planetary boundary layer model of Brown (1981) . The combined model was tested on GOASEX and JASIN data sets for a marine environment from the Gulf of Alaska Experiment and the Joint Air-Sea Interaction Experiment. Very good agreement with surface wind observations were obtained and deviation were generally less than 1 m/s for wind speed and less than 10^{o} for

direction except near a frontal system where the inherent smoothing of pressure and temperature fields due to interpolation, led to deviations within 3 m/s and 30^{o} .

Du Vachat and Musson-Genon (1982) have proposed a similar matched surface/Ekman boundary layer profile solution for describing the ABL . The Ekman layer profile assumes a constant diffusivity which is a function of the stability parameter, μ ,

$$\mu = \frac{ku_*}{fL} \tag{3.3.69}$$

The solution for the velocity defect is given by

$$F(\mu,z) = \frac{(i-1)}{\sqrt{2K_H}} \exp\left[\frac{-(1+i)(Z-H_s)}{\sqrt{2K_H}}\right] Z \geq H_s$$

$$= \ell n\left(\frac{Z}{H_s}\right) - \left[\psi(\mu Z)-\psi(\mu H_s)\right] + \frac{(i-1)}{\sqrt{2K_H}} Z < H_s \tag{3.3.70}$$

where $F = F_u + iF_v$ (3.3.71)

$$F_u = k\left(\frac{u - u_g}{u_*}\right) \; ; \; F_v = k\left(\frac{v - v_g}{u_*}\right)$$

$$Z = \frac{zf}{ku_*}$$

$$K_H = \frac{H_s}{\phi(\mu H_s)}$$

H_s is the value of Z at which the surface layer and Ekman layer solutions are matched and ϕ is the non-dimensional shear profile given by Businger et al (1971) . H_s is a function of μ :

$$\begin{aligned} H_s &= 0.01\sqrt{-\mu} && \mu \leq -9 \\ &= 0.03 && -9 < \mu \leq 9 \\ &= 0.27/\mu && \mu > 9 \end{aligned} \qquad (3.3.72)$$

The solution is also extended to the more general baroclinic atmosphere. Wind profiles calculated from the model are compared with velocity defect profiles from the Wangara data (Yamada (1976)) and good agreement with the data was found. The similarity functions $A(\mu)$ and $B(\mu)$ are given by

$$A(\mu) = \left(\frac{1}{2K_H} \right)^{\frac{1}{2}}$$

$$B(\mu) = -\ell n(kH_s) - A(\mu) + \psi(\mu H_s)$$

Using the expression in Equations (3.3.71) for K_H one obtains the following values for $A(\mu)$ and $B(\mu)$.

μ	$A(\mu)$	$B(\mu)$
-100	1.13	4.53
- 50	2.07	3.21
- 10	3.80	1.12
0	4.08	0.476
20	9.16	- 5.07
50	14.5	- 9.50
80	18.3	-12.8

Figure 3.8, taken from du Vachat and Musson-Genon, shows the variation of the similarity parameters according to Arya (1975), Zilitinkevich (1975) and Yamada (1976) . The above tabulated values are in very good agreement with those of Arya and Yamada. Hence, the surface layer wind profiles and geostrophic departure angles obtained using a matched surface layer/Ekman layer technique are similar to those obtained using the similarity functions of the drag laws. A similar conclusion is reached using the relationships of Brown.

In view of the suitability of the Brown and Liu model to both water and land surfaces, and in view of the good results obtained when

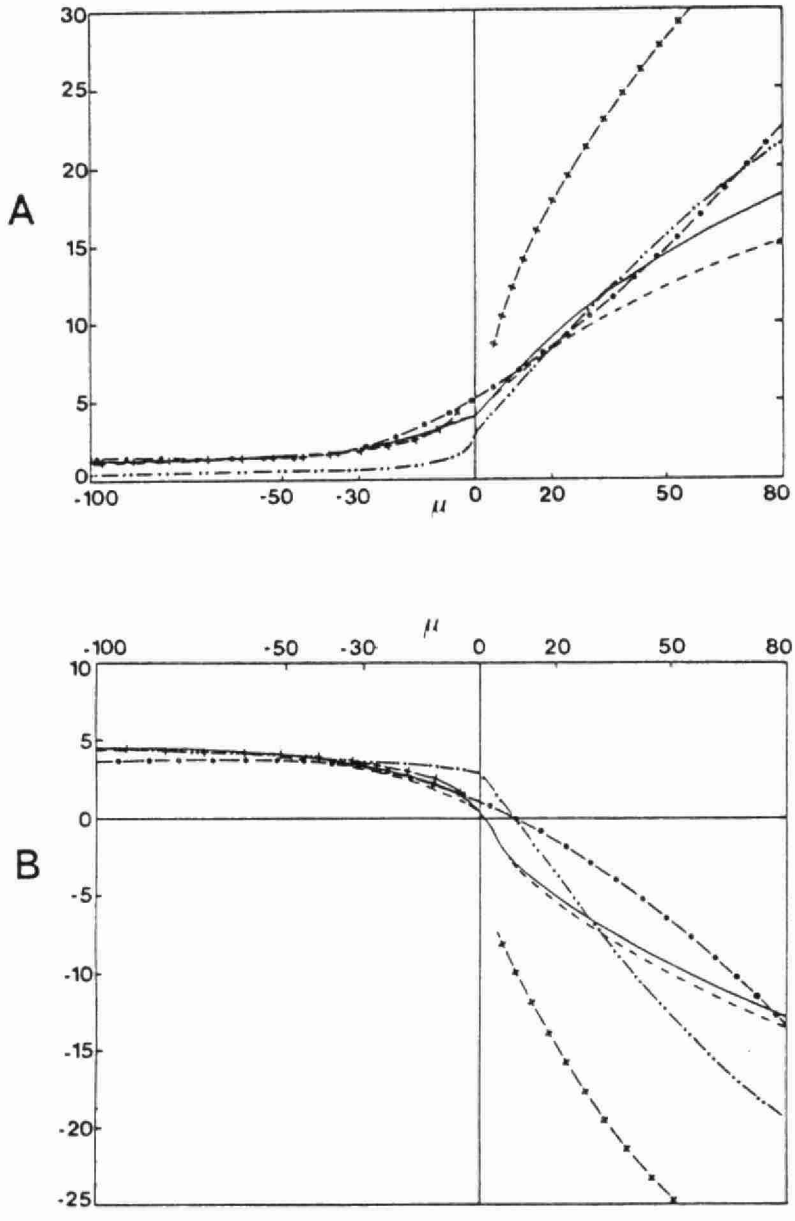

Figure 3.8 Functions A(μ) and B(μ) with the Prandtl's Formulation (solid line) and with the turbulent energy scheme (dashed line); formulation deduced with measurements by Arya (•—•), Yamada (••— ••), Zilitinkevich (+— +).

(Reproduced from Vachat and Musson-Genon (1982))

tested against observations, it is recommended that this modeling procedure be used for wind profiles in the ABL .

It is recognized that at the time of implementing the proposed design, it may be necessary to evaluate other modeling procedures such as that of du Vachat and Musson-Genon (1982) . The proposed scheme is not restricted to using Brown's model which is currently recommended.

The following section details the computational scheme which has been adapted to utilize the results of the presently recommended upper air analysis.

3.3.6 Computational Scheme for Calculation of Wind Profiles in the Atmospheric Boundary Layer

Figure 3.9 summarizes the general scheme for computing wind profiles in the ABL over either a land or water surface. In order to execute the procedure, the following information and data are required:

- Geostrophic wind speed and direction including thermal wind and ageostrophic correction factors.
- Surface heat flux and roughness length for land surfaces.
- Bulk water surface temperature.
- Ambient air temperature.

ITERATIVE PROCEDURE FOR COMPUTING WIND PROFILES
IN THE ABL FROM THE GEOSTROPHIC WIND

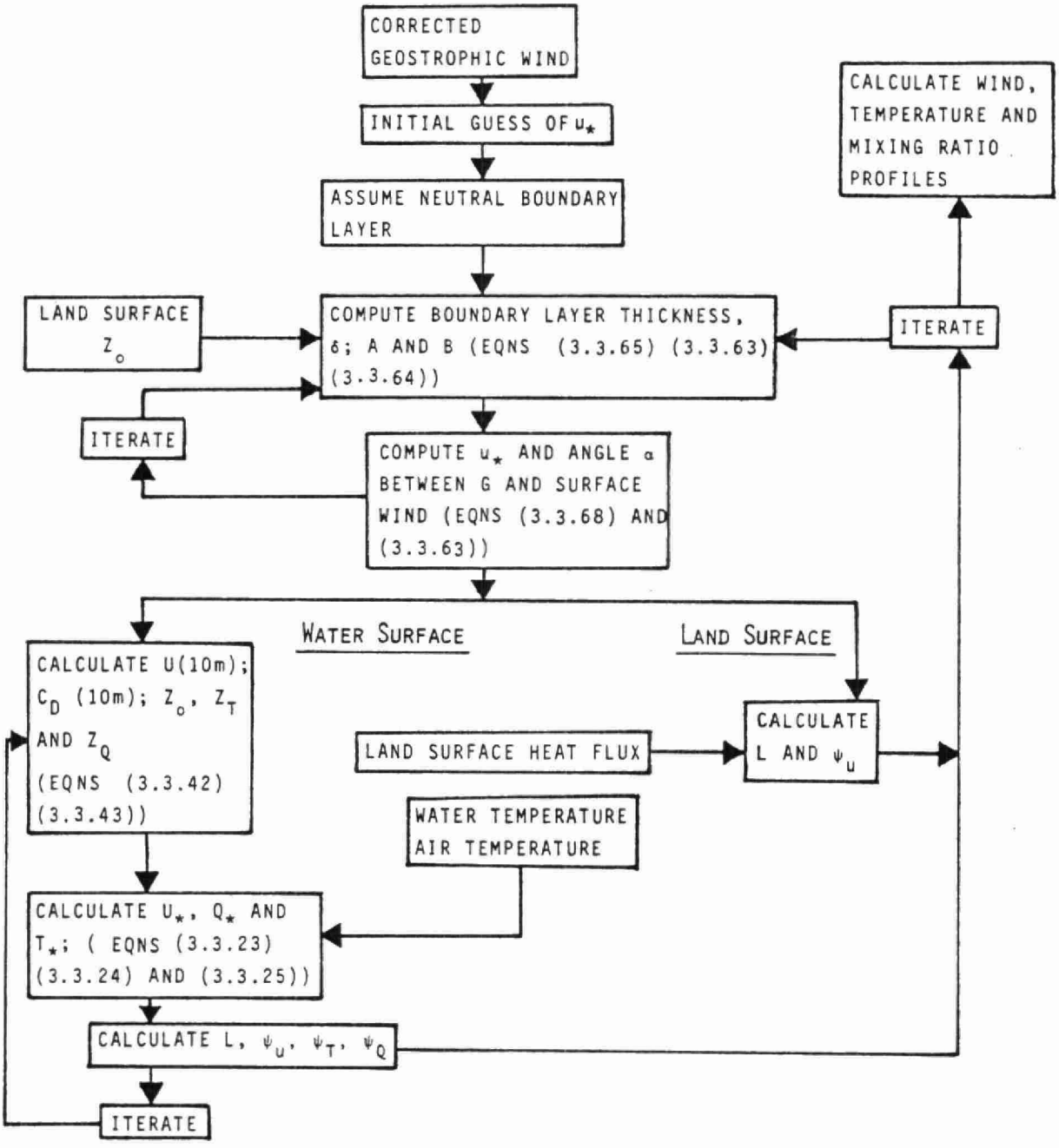

Fig. 3.9

Since the ABL equation described in Section 3.3.5 are implicit in u_* , δ and L , it is necessary to carry out the computations iteratively. Starting with an assumed u_* and neutral conditions, the boundary layer scale, δ, and functions A and B in Equations (3.3.63), (3.3.64) and (3.3.65) are computed ($\psi = 0$) . Using Equation (3.3.68) a revised estimate of u_* is obtained and the estimates of δ and u_* are refined through iteration. For unstable conditions, the mixing height will be used instead of Equation (3.3.65) .

For a land surface, using the estimated heat flux and current u_* value, the Monin-Obukhov stability length, L , from Equation (3.3.29) and the value of ψ_u ($\frac{\lambda\delta}{L}$) from Equation (3.3.35) are computed. Through iteration for δ , A and B, the final values of u_* , α and δ are obtained permitting the wind profile in the ABL to be computed from Equations (3.3.25), (3.3.56) and (3.3.57) .

For a water surface, the value of the roughness length, z_o, may be estimated from the drag coefficient using Equations (3.3.42) and (3.3.43) . The roughness lengths z_Q and z_T may then be estimated from Equations (3.3.44) and (3.3.45) and so the values of u_*, Q_* and T_* may be calculated from Equations (3.3.23), (3.3.24) and (3.3.25) recalling that $\psi_u = \psi_T = \psi_Q = 0$ for the first iteration.

The value of Q_s is taken to be the saturation value at the water temperature and Q is calculated for a relative humidity of 70% . The value of L may then be calculated from Equation (3.3.29) and the ψ - functions from Equations (3.3.33 to 3.3.41) . The procedure for a water surface is then the same as for a land surface; the final values of u_*, α and δ are obtained iteratively, and so the wind profiles from Equations (3.3.25), (3.3.56) and (3.3.57) .

3.3.6.1 Estimation of Surface Heat Flux over Land

The surface heat flux over a water surface is computed in Figure 3.9 as part of the process of matching the surface and upper boundary layer profiles. Over a land surface an independent estimate of the heat flux must be made.

Berkowicz and Prahm (1982) have given a method of estimating the surface flux of sensible heat from routine meteorological data using a resistance method. The technique has been tested on three data sets and gave a very satisfactory comparison with experimental data. The method is applicable only to land surfaces free of snow.

The technique is dependent on the estimation of u_*, θ_* and L . These boundary layer parameters may be computed using the geostrophic flow with apriori knowledge of the surface heat flux as in Figure 3.9 . In the Berkowicz and Prahm method of estimating, H, the values of u_* and θ_* are obtained from surface observations of wind, humidity and temperature. In the best of circumstances, these separate estimates of u_*, θ_* and L should be the same and a comparison between the two estimates will form part of the model development and validation. Initially, however, the estimates of these parameters for the heat flux calculation will be based on surface observations whereas for the profile calculations they will be based on the geostrophic flow as in Figure 3.9 .

The surface heat flux is given by

$$H = \frac{R_n(r_a + r_s) - Dq\ (\rho C_p/\gamma)}{r_s + (1 + \Delta/\gamma)\ r_a + \alpha_g\ (r_a + r_s)} \qquad (3.3.73)$$

where r_a and r_s are the aerodynamic and surface resistances, γ is the psychometric constant, Δ is the rate of change of saturation vapour pressure with respect to temperature at the ambient temperature and $\alpha_g \approx 1/3$.

The net radiation, R_n , is computed from cloud cover and solar elevation (Nielsen et al (1981)) . The aerodynamic resistance is calculated from the similarity profiles for momentum and mass transfer as

$$r_a = \frac{0.74}{k^2 u(z_u)} \left[\ell n \left(\frac{z_u}{z_o} \right) - \psi_m \left(\frac{z_u}{L} \right) + \psi_m \left(\frac{z_o}{L} \right) \right] \cdot$$

$$\cdot \left[\ell n \left(\frac{z_t}{z_o} \right) - \psi_h \left(\frac{z_t}{L} \right) + \psi_h \left(\frac{z_o}{L} \right) \right] \qquad (3.3.74)$$

where z_u and z_t are the heights of wind and temperature observations respectively. The functional forms of ψ_m and ψ_h are slightly different from those in Equations (3.3.33 to 3.3.55) and the forms used by Berkowicz et al should be used in Equation (3.3.74) for consistency with their model. The surface resistance is given by

$$r_s = \frac{\rho C_p D_q}{\gamma F} \qquad (3.3.75)$$

where the humidity deficit is given by

$$D_q = q_s(T) - q \qquad (3.3.76)$$

$q_s(T)$ is the saturation vapour pressure at screen temperature T , q is the observed vapour pressure.

The factor F is computed from the accumulated hourly net radiation since the last precipitation event

$$F = AR_n + D \tag{3.3.77}$$

where

$$A = 0.6 - 0.48 \sum R_n \times 2 \times 10^{-4} \qquad \Sigma R_n < 2 \times 10^4$$

$$= 0.12 \qquad \Sigma R_n \geq 2 \times 10^4 \tag{3.3.78}$$

$$D = \text{minimum of} \left[67 \text{ W/m}^2; \; 221 \exp (\Sigma R_n \times 2 \times 10^{-4}) \right] \tag{3.3.79}$$

The value of H is dependent on the stability length, **L** , and must be calculated iteratively starting with neutral conditions ($L=\infty$) . The computational scheme for estimating heat flux is shown in Figure 3.10.

ESTIMATION OF SENSIBLE HEAT FLUX AT SURFACE

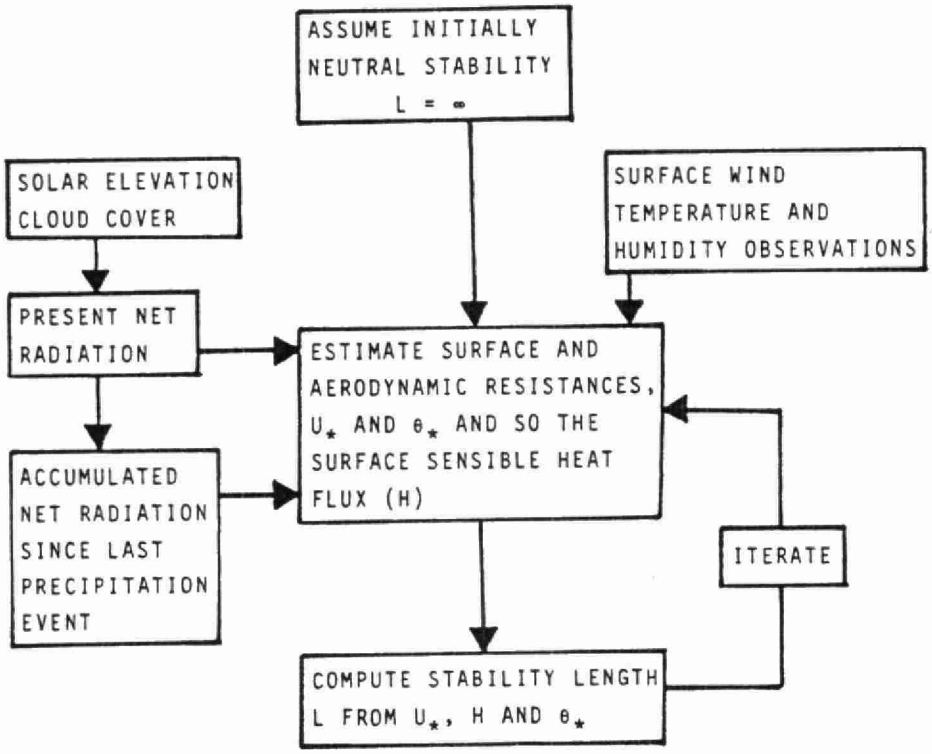

Fig. 3.10

3.3.6.2 Determination of Ageostrophic Correction Factors From Radiosonde Data

The ageostrophic correction factors represent those components of the calculated geostrophic wind which are not resolved by the surface pressure gradient and the 850 mb temperature gradients. The correction factors can be calculated by comparing the computed geostrophic wind with winds from radiosoundings at the observational hours of 00Z and 12Z . Spatial interpolation to all grid points and temporal interpolation to intermediate hours is then used to provide hourly values of the correction factors at each grid point. Except for locations close to a frontal system, the ageostrophic correction factor will be small.

Figure 3.11summarizes the computations required to determine the ageostrophic correction factors from radiosonde and surface pressure data as well as the analysed upper air temperature data.

From the surface pressure gradients and 850 mb temperature gradients, the surface geostrophic and thermal wind components are calculated from Equations (3.3.1), (3.3.2), (3.3.58) and (3.3.59) . Using this first estimate of the flow at the top of the ABL , the boundary layer thickness, δ , is determined using the iterative procedure described in Section 3.3.6, (Figure 3.9) . By comparing the radiosonde wind components at $z = \delta$, the values

CALCULATION OF AGEOSTROPHIC CORRECTION FACTORS FROM RADIOSONDE DATA

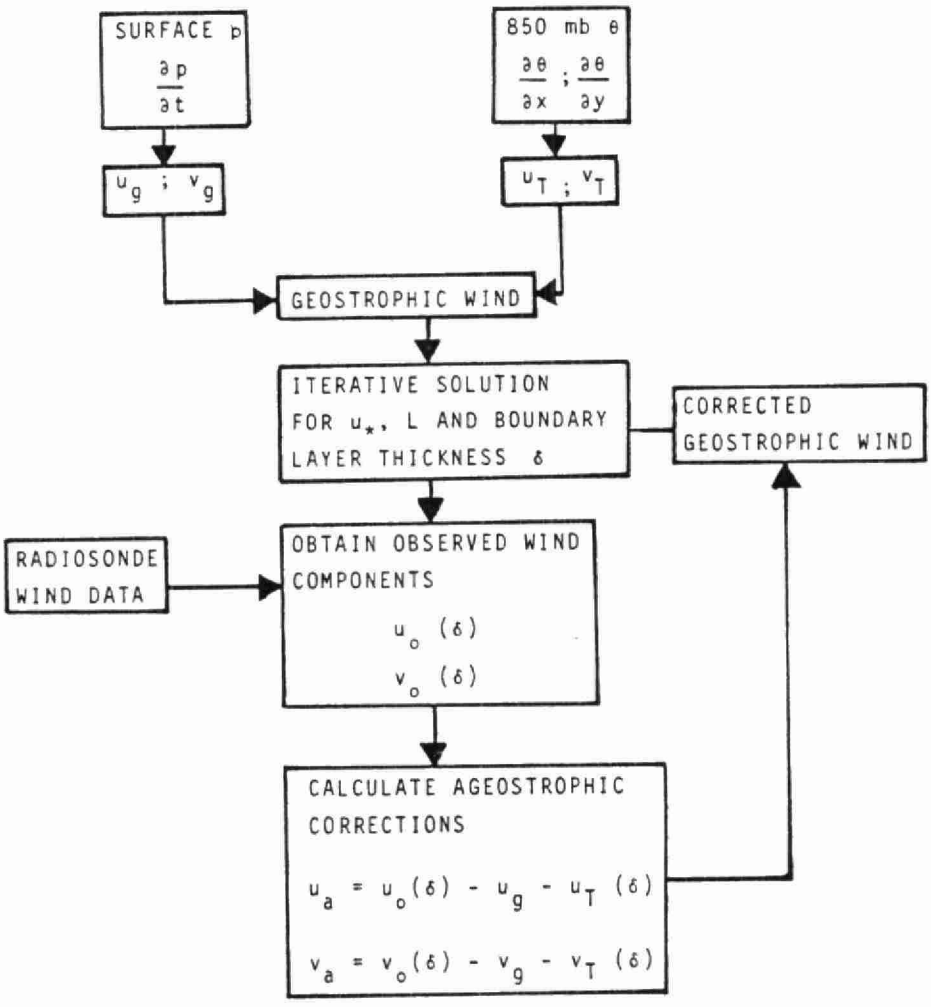

Fig. 3.11

of u_a and v_a are obtained by difference. The estimate of δ can then be refined using the corrected geostrophic wind if u_a and v_a are significant. For unstable conditions the mixing height replaces δ .

Once the correction factors are determined in this manner at the radiosounding stations, they are interpolated to the grid using the second-order interpolation procedure described in Section 3.2.2.2 , Equations (3.2.4) and (3.2.6) . Using values of u_a and v_a determined at three consecutive observation hours, for example 00Z, 12Z and 24Z , the values are interpolated to intermediate hours using orghogonal polynomials, Section 3.3.2 , Equation (3.3.5) .

3.3.6.3 Calculation of Layer Averaged Winds in the ABL

In the preceeding sections all the required input information and computational procedures have been developed which enable the calculation of wind profiles in the ABL as shown in Figure 3.9 .

Layer averaged winds could be determined by integrating the wind profile equation, (Equations (3.3.25), (3.3.56) and (3.3.57)), however it will probably be more economical and adequate to use

simple quadrature such as Simpson's Rule. The number of layers and their thicknesses will be prescribed by the dispersion calculations. The lowest level for the upper-air analysis is 1500 m . Layer averages will be calculated from the ABL profiles up to a height of $z = \delta$. If $\delta < 1500$ m , winds between δ and 1500 m will be linearly interpolated between the top of the ABL and the 1500 m level of the upper air analysis. If $\delta > 1500$ m, then ABL winds will be used for computing averages up to 1500 m and the winds derived from the upper air analysis for layers above 1500 m .

3.3.7 Parameterization of the Nocturnal Jet

3.3.7.1 Review of Available Models

The parameterizations of the ABL wind profiles described in Section 3.3.6 assume that steady conditions prevail in the boundary layer. The steady state assumption is reasonable where vertical mixing (or transmission of shear stress) is relatively rapid and a balance between pressure forces, shear stress and Corioli s force is quickly approached in the Ekman/Taylor layer: This condition is relevant to unstable or moderately stable conditions.

Under very stable conditions, such as those which may develop during the night hours under clear skies, turbulence in the lower part of the ABL is rapidly damped out except close to the surface, and the shear stress decreases rapidly with height to a very small residual value. Under these conditions, the upper ABL , which prior to the onset of strong stability, was in motion under a balance between shear stress, pressure forces and Coriolis force, is suddenly forced into a state imbalance by the removal of the shear stress. The subsequent process of adjustment to the new conditions has a time scale of the order of 12 hours and leads to the formation of the nocturnal jet. At the same time, the surface layer is coupled to the geostrophic flow only through the pressure gradient and its structure evolves with a similar time scale to the upper layer in response to the changing wind conditions at the upper boundary.

Clearly, the steady state assumptions are not applicable to very stable nocturnal conditions. A review of the literature has not revealed a well validated model of the processes described above. However, the nocturnal jet is far too important a feature of the wind field to neglect and a parameterization of this flow will

be developed based on information and models which are reported in the literature.

Blackadar (1957) examined the occurrence of wind maxima in the wind profiles which are observed at night under conditions of strong stability. Assuming steady day time conditions the motion in the ABL is described by

$$\frac{\partial u}{\partial t} = f(v - v_g) + \frac{\partial}{\partial z}\left(K_z \frac{\partial u}{\partial z}\right) = 0 \qquad (3.3.80)$$

$$\frac{\partial v}{\partial t} = -f(u - u_g) + \frac{\partial}{\partial z}\left(K_z \frac{\partial u}{\partial z}\right) = 0 \qquad (3.3.81)$$

When the shear stress in the upper part of the ABL is rapidly removed, the flow undergoes an adjustment process described by

$$\frac{\partial u}{\partial t} = f(v - v_g) \qquad (3.3.82)$$

and $$\frac{\partial v}{\partial t} = -f(u - u_g) \qquad (3.3.83)$$

Defining $W = u + iv$, the solution of these equations is

$$W = W_o e^{-ift} \tag{3.3.84}$$

Where W_o is the deviation vector from the geostrophic vector at sunset. The temporal behavior of W is in good qualitative agreement with observation.

Delage (1974) solved Equations (3.3.80) and (3.3.81) as well as the thermal transport equation

$$\frac{\partial \theta}{\partial t} = \frac{\partial}{\partial z}\left(K \frac{\partial \theta}{\partial z} \right) \tag{3.3.85}$$

By postulating a time and height variation for K and a surface cooling rate, the model equations were solved numerically showing the formation of the nocturnal jet and the temporal change in directional shear through the ABL . The shear stress tends to very low values with height and Delage's model reduces to that of Blackadar for the upper most layers. Again good qualitative agreement with observation was obtained: Proper validation was not possible due to a lack of sufficient observational data.

Thorpe and Guymer (1977) considered a two-layer model for the average wind components. The two layers are defined as being the top of the stable nocturnal boundary layer with a upper layer extending to the top of the boundary layer during the preceeding daylight hours. At sunset, the two layers are suddenly decoupled. The solution for the upper layer is identical to that of Blackadar. The lower layer model is Equation (3.3.80) and (3.3.81) where a linear parameterization of shear stress is assumed giving

$$\frac{\partial u}{\partial t} = fv - \frac{k_s u}{h} \tag{3.3.86}$$

and

$$\frac{\partial v}{\partial t} = -f(u - u_g) - \frac{k_s v}{h} \tag{3.3.87}$$

Hodographs of the solutions of these equations were compared with data from the Wangara experiment (Clarke et al (1971)) . The temporal behavior as well as the super-geostrophic wind components were in good qualitative agreement with the data. Again proper validation was inhibited by the lack of adequate data.

On the basis of these three studies, it appears that the model of the nocturnal jet embodied in Equations (3.3.80) to and (3.3.84) gives a reasonable description of the nocturnal jet despite the lack of proper validation, It is recommended that a parameterization of the nocturnal jet be developed, based on these models. The following section gives the development of a model which is suitable for the presently proposed wind field model.

3.3.7.2 Proposed Modeling Scheme for the Nocturnal Jet

The final results of the upper air and ABL analyses of Sections 3.2.3.2 and 3.3.6.3 are expressed as layer-averaged wind components suitable for use by the diffusion model. The model of Thorpe and Guymer (1977) is a two-layer, averaged wind component model. Since greater vertical resolution is required by the diffusion model than that given by the Thorpe and Guymer model, it is proposed to extend their method to several layers to correspond with the layers defined by the Eulerian diffusion model grid.

Averaging Equation 3.3.80 over a layer of thickness Δh gives

$$\frac{\partial \bar{u}}{\partial t} = f(\bar{v} - v_g) + \left(\frac{\tau_{z+\Delta n} - \tau_z}{\rho \, \Delta h} \right) \tag{3.3.88}$$

Thorpe et al uses a linear parameterization of shear stress,

$$\vec{\tau} = \rho k_s \vec{V} \tag{3.3.89}$$

and shows that the resulting hodograph is not very different from that using the quadratic law suggested by similarity theory.

The p-simultaneous differential equations given by Equation (3.3.88) for p-layers can be solved numerically; however, since the solution must be carried out for each hour at each grid point, such a solution would involve considerable computer effort: An approximate method of solving the set of equations might be more appropriate. Since the evolution of the nocturnal jet flow takes several hours, without great loss of accuracy, the interlayer shear stresses may be approximated by their average value over the time step.

$$\bar{\tau}_i = \rho k \left(\vec{v}_i - \overline{\vec{v}}_{i-\frac{1}{2}} \right) \tag{3.3.90}$$

With this approximation, Equation (3.3.88) has the solution

$$W_p = \left[W_p(0) - A_p \right] \exp \left[-\left(if + \frac{k_{j-1}}{\Delta h} + \frac{k_j}{\Delta h} \right) t \right] + A_p \qquad (3.3.91)$$

where

$$W_p = (u_p - u_g) + i\,(v_p - v_g) \qquad (3.3.92)$$

$$W_p(0) = (u_o - u_g)_p + i\,(v_o - v_g)_p \qquad (3.3.93)$$

$$A_p = \left(\frac{k_{j-1}\,\overline{W}_{j-1} + k_j\,\overline{W}_{j+1}}{if\Delta h + k_{j-1} + k_j} \right) \qquad (3.3.94)$$

t = time since sunset

and the overbars indicate average values over the interval.

The solution then reduces to the solution of p-algebraic linear equations of the form

$$W_p = a_p W_{p-1} + d_p \qquad (3.3.95)$$

$$W_{p-1} = a_{p-1} W_{p-2} + b_{p-1} W_p + d_{p-1}$$

$$\vdots$$

$$W_1 = b_1 W_2 + d_1,$$

Using $\bar{W}_p = W_p(0)$ as an initial guess, application of the solution iteratively to refine $\bar{W}_p$ gives an approximate solution for the $W_p(t)$. Clearly there are other approximate methods which should be tested in the development. The distribution of k with height must be specified. The components of the geostrophic flow are the hourly values determined in Section 3.3.6.2 (See Figure 3.6) .

Implementing this nocturnal jet model will require some development work and a technique for diagnosing the presence of a nocturnal jet must also be developed. During the winter months, the 1200Z sounding could be used to show the nocturnal jet before sunrise in the central North American continent. During the summer months a technique which does not rely on soundings must be developed since the nocturnal jet disappears rapidly at sunrise.

Figure 3.12gives the computational scheme whereby the nocturnal jet may be included in the wind field model. If the nocturnal jet is diagnosed to be present during the hours after sunset, then the layer averaged boundary layer profile which pertains to one hour before sunset is taken as the initial condition for the first hour of the nocturnal jet solutions and the equations are solved for the wind components in each layer. By repeatedly applying the

IMPLEMENTATION OF NOCTURNAL JET MODEL

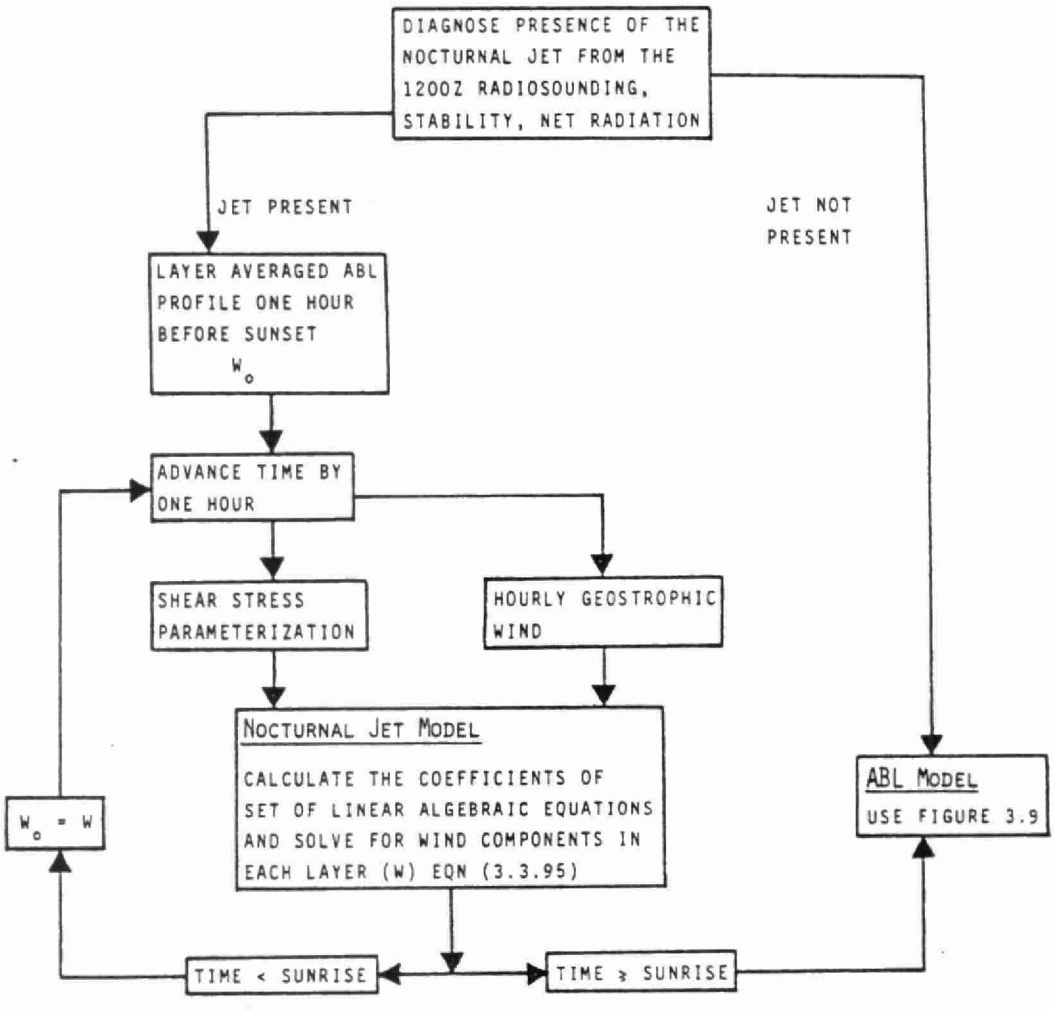

Fig. 3.12

solution, using the appropriate hourly geostrophic wind components, the wind field in the ABL is computed until sunrise or until the stability or net radiation no longer will support the nocturnal jet. After sunrise, the ABL computation scheme of Figure 3.9 is used.

3.3.8 Rendering the Wind Field Mass Consistent

The results of the wind field analysis generated in the previous section, are in the form of layer averaged winds and for those layers above 1500 m , layer averaged horizontal divergence and vorticity have also been calculated. Since in the upper air analysis, the divergence and vorticity have been interpolated separately from the wind components, the layer average wind components will not necessarily be consistent with the interpolated divergence and vorticity.

3.3.8.1 Divergence in the ABL

Other than near a frontal system, divergence in the ABL will be small and mainly due to cross-isobar flow caused by surface drag. Similarly, in the absence of a frontal system, the divergence above 1500 m determined from the upper-air analysis, will also be small.

The divergence in the ABL can be estimated by extrapolating from that at 1500 m given by the upper air analysis, to zero divergence at the surface. For the extrapolation, a linear variation of divergence with height will be assumed although other functional forms for the variation which depend on the stability of the boundary layer could be used.

For linear extrapolation

$$D_i = \frac{1}{\Delta h_i}\left[w_{z_i+\Delta h_i} - w_{z_i} \right] = \frac{\left(z_i + \frac{\Delta h_i}{z}\right)}{1500} D_{1500} \qquad (3.3.96)$$

3.3.8.2 Adjustment of the Layer Average Wind Components to Be Consistent with the Prescribed Vorticity and Divergence Distributions

The kinematic properties of wind fields may be adjusted iteratively to be mass consistent with a prescribed vorticity distribution using a technique due to Endlich (1967) .

Subscripts 'o' are used to denote interpolated layer averaged wind components and 'RD' to denote changes in the wind components required to make the horizontal divergence equal to the interpolated layer averaged value, $D_o(ijk)$. For any level k , Equation (3.2.15)

may be written (omitting the k subscript) as

$$\mu_\lambda \left\{ \left[u_o\,(i+1,j) + u_{RD}(i,j) \right] - \left[u_o(i-1,j) - u_{RD}(i,j) \right] \right\} + \frac{}{2\Delta\lambda}$$

$$\mu_\phi \left\{ \left[v_o\,(i,j+1) + v_{RD}(i,j) \right] - \left[v_o(i,j-1) - v_{RD}(i,j) \right] \right\} = \frac{}{2\Delta\phi}$$

$$= D_o(i,j) \qquad (3.3.97)$$

Let the divergence calculated from the interpolated winds be $D_t(i,j)$, (i.e. the divergence from Equation (3.3.97) with $u_{RD}(i,j) = v_{RD}(i,j) = 0$) , then it is required that

$$\mu_\lambda \frac{u_{RD}(i,j)}{\Delta\lambda} + \mu_\phi \frac{v_{RD}}{\Delta\phi} = \left[D_o(i,j) - D_t(i,j) \right]$$

$$= \Delta D(i,j)$$

$$= 0 \qquad (3.3.98)$$

If both u_{RD} and v_{RD} contribute equally to the divergence then

$$u_{RD}(i,j) = -\tfrac{1}{2}\,\frac{\Delta\lambda}{\mu_\lambda}\,\Delta D(i,j) \qquad (3.3.99)$$

and

$$v_{RD}(i,j) = -\tfrac{1}{2}\,\frac{\Delta\phi}{\mu_\phi}\,\Delta D(i,j) \qquad (3.3.100)$$

The new estimates of wind components are now

$$u_o^1(i+1,j) = u_o(i+1,j) + u_{RD}(i,j) \qquad (3.3.101)$$

$$u_o^1(i-1,j) = u_o(i-1,j) - u_{RD}(i,j)$$

$$v_o^1(i,j+1) = v_o(i,j+1) + v_{RD}(i,j)$$

$$v_o^1(i,j-1) = v_o(i,j-1) - v_{RD}(i,j)$$

Using the new estimates of u^1 and v^1 , another alteration is made so that the vorticity derived from the winds, ζ_t is consistent with the interpolated value, ζ_o giving

$$u_{RR}(i,j) = -\tfrac{1}{2}\,\frac{\Delta\phi}{\mu_\phi}\,\Delta\zeta(i,j) \tag{3.3.102}$$

$$v_{RR}(i,j) = \tfrac{1}{2}\,\frac{\Delta\lambda}{\mu_\lambda}\,\Delta\zeta(i,j) \tag{3.3.103}$$

where

$$\Delta\zeta(i,j) = \zeta_o(i,j) - \zeta_t(i,j) \tag{3.3.104}$$

and

$$u''_o(i,j+1) = u'_o(i,j+1) - u_{RR}(i,j) \tag{3.3.105}$$

$$u''_o(i,j-1) = u'_o(i,j-1) + u_{RR}(i,j)$$

$$v''_o(i+1,j) = v'_o(i+1,j) - v_{RR}(i,j)$$

$$v''_o(i-1,j) = v'_o(i-1,j) + v_{RR}(i,j)$$

By applying iteratively, first the divergence correction to the grid followd by the vorticity correction procedure, Endlich found that ΔD and $\Delta\zeta$ decrease quite rapidly and 10 to 15 iterations produced residuals of the order of 10^{-6} sec.$^{-1}$.

Finally, in order to ensure that the corrected wind field retains the average wind speed of the interpolated winds over the domain, the final wind components are adjusted by a constant value given by

$$\Delta u = \left[\sum_i \sum_j u_o(i,j) - \sum_i \sum_j u''_o(i,j) \right] / N \qquad (3.3.106)$$

$$\Delta v = \left[\sum_i \sum_j v_o(i,j) - \sum_i \sum_j v''_o(i,j) \right] / N \qquad (3.3.107)$$

when N is the number of grid points in layer k .

After applying this procedure to all layers, the derived wind field will be mass consistent and have the vorticity and divergence distribution determined by the upper air analysis.

3.3.8.3 Calculation of Vertical Velocities

The final step in the wind field analysis is the calculation of vertical velocities for each grid point. For a layer average, the horizontal divergence (the density weighted average) is given by

$$\mu_\lambda \frac{\partial \bar{u}_i}{\partial \lambda} + \mu_\phi \frac{\partial \bar{v}_i}{\partial \phi} = -\frac{1}{\Delta z}\left[w_i - w_{i-1}\left(\frac{\bar{\rho}_{i-1}}{\bar{\rho}_i}\right)\right]$$

$$= \bar{D}_i \qquad (3.3.108)$$

starting at the surface, $w_o = o$, the vertical velocity at each grid point can be calculated for all layers from

$$w_i = \left(\frac{\bar{\rho}_{i-1}}{\bar{\rho}_i}\right) w_{i-1} - \bar{D}_i \, \Delta z_i \qquad (3.3.109)$$

3.4 Wind Field Analysis For the Mesoscale Model

3.4.1 Objectives and Overview

In Sections 3.2 and 3.3 all wind field analysis has been carried out on a grid with a horizontal interval of 1^{o} in latitude and longtitude. For the mesoscale model a grid interval of 0.1^{o} is to be used so that the spatial variability of the winds in the ABL will be better resolved. For the long-range model, the topographically induced horizontal wind divergence will not be resolved by the 1^{o} grid interval and topographic effects have been neglected. For the mesoscale model, topographic effects can be resolved by the 0.1^{o} grid interval and the induced horizontal wind divergence must be included, particularly under stable conditions.

Other parameters which contribute to the greater variability of surface winds on the mesoscale are surface heat flux and roughness changes as well as mesoscale circulations such as land/water thermal circulations and urban heat islands. These local circulations will be reflected in surface wind observations if these data are sufficiently dense. For the mesoscale model, surface wind observations, which were rejected for use by the long-range model as not being regionally representative on a

1^{o} grid interval, will be used to refine the ABL winds on the 0.1^{o} grid interval of the mesoscale model.

The computational scheme for computing the mesoscale ABL winds is given in Figures 3.13 to 3.15. The upper air winds which are less spatially variable than the ABL winds are obtained by interpolation from the synoptic scale analysis on 1^{o} grid intervals. If for a specific area, more detailed upper air information is available, this information can be incorporated into the interpolation scheme: As a generality, however, it is presently assumed that no further upper air data are available.

To ensure that mesoscale divergence contributions due to spatial changes in surface heat flux, roughness and stability and topography are reflected in the final analysis of surface winds, it is necessary to adjust the upper air and surface geostrophic wind components to give a mass consistent wind field, free of surface drag, with the divergence and vorticity prescribed by the upper air synoptic scale analysis. The mesoscale perturbations of the divergence are then added to the wind field.

COMPUTATION OF MASS CONSISTENT
FRICTIONLESS WIND FIELD

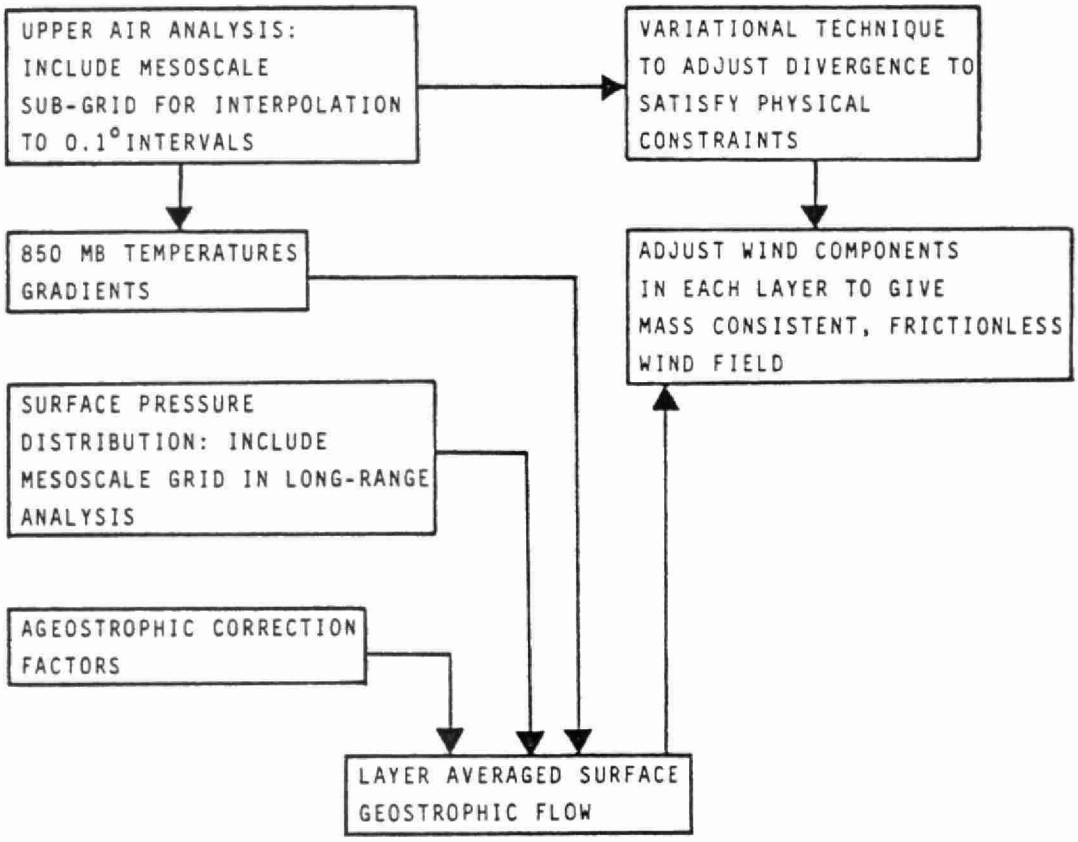

Fig. 3.13

INCORPORATION OF SURFACE DRAG AND
TOPOGRAPHIC PERTURBATIONS INTO WIND FIELD

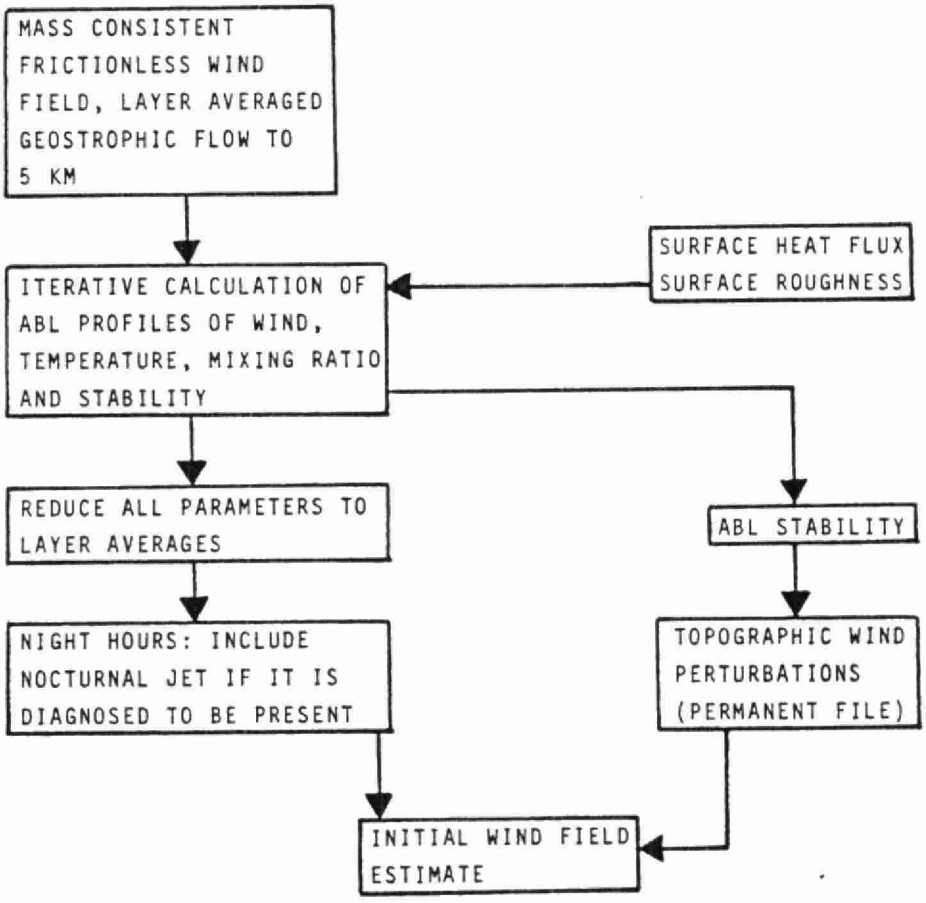

Fig. 3.14

INCORPORATION OF SURFACE WIND OBSERVATIONS
INTO WIND FIELD AND COMPUTATION OF FINAL
MASS CONSISTENT WINDS

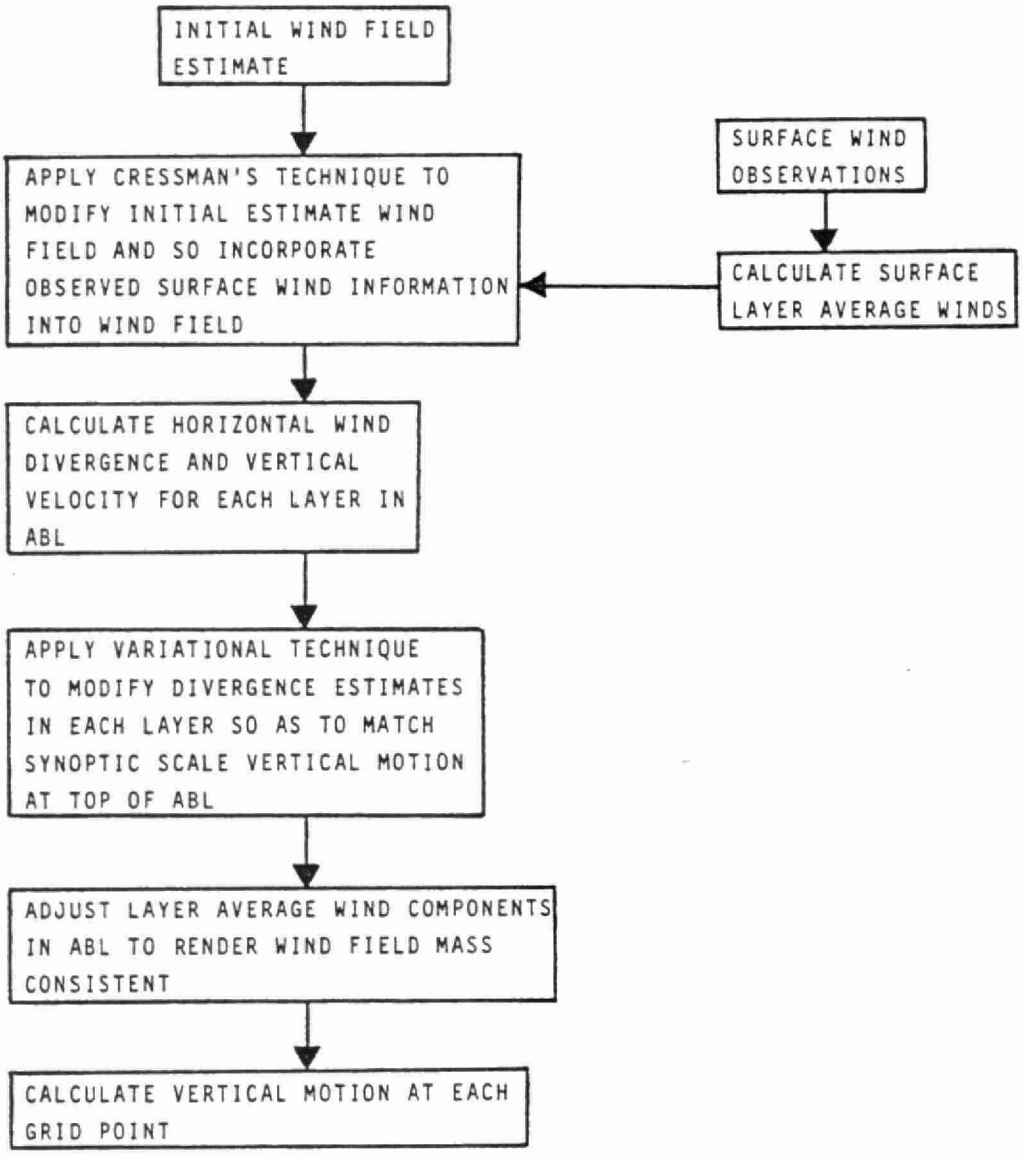

Fig. 3.15

The vertical resolution of the mesoscale model is similar to that of the long-range model. However, on the mesoscale grid, the topography must be incorporated into the model either through the use of a terrain following co-ordinate system (McRae et al (1982)) or through the use of variable layer thicknesses which would allow the topography to penetrate into the layers. Since, the diffusion model is restricted in application to constant layer thicknesses, a terrain following co-ordinate system will be used.

3.4.2 Interpolation of the Upper Air Analysis to the Mesoscale Grid

Except when a frontal system is present, the variability of the flow above the ABL over angular distances of the order of 1^{o} is far less than that in the ABL . Assuming that all available upper air information has been utilized in the analysis described in Section 3.2 , the interpolation to the sub-grid mesoscale cannot further enhance the information on the mesoscale.

Referring to Figure 3.13, interpolation to the 0.1^{o} mesoscale grid of the upper air analysis is achieved by including the mesoscale sub-grid in the isentropic temporal analysis described in Section 3.2.3 (Figure 3.6) : This ensures that there is no further filtering of information in the reduction to the mesoscale grid.

For periods and regions where the meteorology is relatively simple, a straight-forward second order interpolation of the upper air analysis results on the 1^{o} scale to the 0.1^{o} scale may yield acceptable accuracy. However, for the mesoscale wind field the upper air analysis must in any case be carried out on a larger domain before interpolation to the 0.1^{o} scale; It is therefore preferred to use the former method and to include the mesoscale grid as a sub-set for the interpolation described in Section 3.2.3 (Figure 3.6) . In this manner, layer averaged winds, temperature, mixing ratio, vorticity and horizontal divergence on the mesoscale grid are derived.

The horizontal layer averaged divergence estimates are then corrected using O'Brien's variational technique (Section 3.2.2.4) .

3.4.3 Divergence in ABL Winds for the Mesoscale Model

The mesoscale grid gives far higher resolution of the spatial distribution of surface roughness, type and heat flux as well as better definition of land/water boundaries. It is therefore not acceptable to merely interpolate the ABL winds derived on the 1^{o} grid interval to the 0.1^{o} sub-grid. Instead it is necessary to compute the ABL profiles at each mesoscale grid point.

On a synoptic scale, the horizontal wind divergence which is derived from an analysis of the upper air flow, will be impressed on the mesoscale wind field. Mesoscale perturbations of the ABL winds will not contribute significantly to the regional divergence when the whole mesoscale domain is considered. On the mesoscale, however, spatial changes in surface roughness, type and heat flux as well as topographic effects and local circulations will cause localized perturbations of the wind field with corresponding departures from the large scale divergence. Hence, before the local effects are considered, the upper air geostrophic flow, and surface geostrophic flow, free of surface drag, are adjusted to have the divergence prescribed by the upper air analysis.

Referring to Figure 3.13, a surface geostrophic wind is calculated, as for the long-range model, from the surface pressure distribution and 850 mb temperature distribution (Sections 3.3.2 and 3.3.6.3; Figure 3-7). Again, interpolation of surface pressure data to the mesoscale grid is achieved by including the 0.1^{o} grid as a sub-set for the interpolation on the long-range grid. The ageostrophic correction factors determined in Section 3.3.6.2 (Figure 3.11) are also interpolated to the mesoscale grid and the corrected surface geostrophic wind is calcualted. The surface geostrophic

flow is then reduced to layer averages for model layers below 850 mb . In the absence of thermal gradients, the surface geostrophic flow will be invariant with height.

Using a linear variation of divergence from 850 mb to the surface, the geostrophic wind components in each layer are adjusted to render the wind field mass consistent with prescribed divergence as described in Section 3.3.8 .

Referring to Figure 3.14 , boundary layer profiles are then calculated at each grid point using the iterative scheme described in Section 3.3.6 (Figure 3.9) . The ABL winds calculated in this manner will reflect mesoscale perterbations of the regional divergence due to spatial changes in surface characteristics. During the night hours, if a nocturnal jet is diagnosed to be present, layer averaged winds are modeled using the scheme described in Section 3.3.7.2 (Figure 3.12) . The ABL winds at this stage will reflect the horizontal wind divergence due to synoptic scale effects as well as due to non-uniformities of surface drag on the mesoscale.

3.4.4 Topographically Induced Horizontal Wind Divergence

For the mesoscale model a terrain following vertical co-ordinate is defined by

$$\rho = \left[z(x,y) - h(x,y) \right] \qquad (3.4.1)$$

where $z(x,y)$ is the MSL height and $h(x,y)$ is the MSL topographic height. Before the topographic height can be determined, the topography must be smoothed on a scale which is consistent with the resolution of the mesoscale grid so that gradients and heights are representative of the grid interval.

Simple smoothing algorithms such as four-point smoothing can be used, however, it is preferable to use a smoothing technique which filters the topography by excluding only those frequencies higher than those resolvable by the grid. This can be achieved through the use of bi-cubic splines which are fit to the topographic data by least squares (Ahlberg et al (1967)) . By choosing the 'knot' points of the splines to coincide with the grid, a filtering is achieved which has a sharp cut-off at wave lenghts shorter than the grid interval. Once the filtering has been done, the heights and gradients determined from the filtered surface will be consistent with the grid resolution.

Using the terrain following vertical co-ordinate, the vertical air velocity is given by

$$W = w - \vec{V}.\nabla h \qquad (3.4.2)$$

where w is the vertical motion relative to MSL . The second term in Equation (3.4.2) represents the vertical motion of the co-ordinate system relative to MSL . Under extremely stable low wind speed conditions, $w \to 0$ and

$$W = -\vec{V}.\nabla h \qquad (3.4.3)$$

under unstable low wind conditions, the flow follows the terrain,

$$w = \vec{V}.\nabla h \qquad (3.4.4)$$

and accordingly

$$W = 0$$

The interaction between topography and air motion is therefore dependent on stability.

Anderson (1971) has given a method for estimating the induced horizontal wind divergence in a layer average wind with flow between the topography and an elevated material surface (such as an inversion). Lui et al (1980) have used Anderson's method with some success for perturbing interpolated wind observations with topographically induced divergence: The effects of stability were not included in their analysis.

For the presently proposed mesoscale wind field model, it is proposed to adapt Anderson's technique to the multi-level mesoscale wind field and to incorporate variable stability.

Using for the moment, a conventional MSL based vertical co-ordinate, the continuity equation may be written

$$\frac{\partial \bar{u}}{\partial x} + \frac{\partial \bar{v}}{\partial y} = - \frac{1}{\Delta z} \left[w(z_2) - w(z_1) \right] \qquad (3.4.6)$$

Anderson chooses $z_2 >> z_1$ and sets $w(z_2) = 0$

giving

$$\nabla \vec{V} = - \frac{1}{H} \vec{V} \nabla h \qquad (3.4.7)$$

where H is the height of the material surface and $\vec{V}_H$ is the layer averaged horizontal wind .

Restricting the development to small perturbations,

$$\vec{V} \approx \vec{U} \tag{3.4.8}$$

where $\vec{U}$ is the layer averaged, non-divergent unperturbed wind vector giving

$$\nabla^2\phi' = \frac{1}{H}\ \vec{U}\cdot\nabla h \tag{3.4.9}$$

where ϕ' is the potential function of the topographic wind disturbance. By solving this linear equation for separate unit west and unit south unperturbed winds, the perturbation of any wind vector can be obtained by summation.

For the present multi-layered meso-scale model, it is necessary to quantify the topographically induced horizontal wind divergence in each vertical layer. Starting from Equation (3.4.6), the vertical velocity may be parameterized by

$$w = w_o e^{-k(z-h)} \tag{3.4.10}$$

where w_o is the vertical motion for $z = h$

or

$$w_o = \vec{U} \cdot \nabla h \tag{3.4.11}$$

substituting in Equation (3.4.6) gives

$$\nabla \vec{V}' = - \frac{\vec{U} \cdot \nabla h}{\Delta \rho} \left[e^{-k\rho_2} - e^{-k\rho_1} \right] \tag{3.4.12}$$

The constant k, depends on atmospheric stability. For $k \to o$, the flow follows the terrain, $\vec{V}' = o$ and $\vec{V} = \vec{U}$. For very stable flow, k is large and from Equation (3.4.10), the vertical motion is rapidly damped with increasing height above the terrain. For the lowest layer

$$\nabla \vec{V}' = - \frac{\vec{U} \cdot \nabla h}{\Delta \rho} \left(e^{-k\rho_2} - 1 \right) \tag{3.4.13}$$

and the flow disturbance is large. The dependence of k on stability must be determined from observations.

In terrain following co-ordinates.

$$W = \vec{V} \cdot \nabla h \left(e^{-k\rho} - 1 \right) \tag{3.4.14}$$

and the terrain induced divergence is given by Equation (3.4.12) which can be solved very efficiently using the ADI method of Peaceman and Rachford (1955) (Scholtz and Brouckaert (1978)) . Since the equation is linear, the perturbation for any unperturbed vector may be obtained by summation of two unit solutions as for Anderson's technique. The unit solution needs be carried out only once for a particular topographic region.

The topographic perturbation model is implemented as shown in Figure 3.14 by noting that the regional divergence of the unperturbed ABL winds is small compared to the locally induced divergence due to topography. The vector $\vec{U}$ is given by the local unperturbed ABL wind and the layer averaged divergence is calculated from Equation (3.4.12) . The components of the perturbed velocity are given by

$$u = U \cos \theta + u' \tag{3.4.15}$$

$$v = U \sin \theta + v'$$

where u' and v' are the solution of Equation (3.4.12) .

3.4.5 Incorporation of Surface Wind Observations into The Mesoscale Wind Field Model

Incorporating the surface wind observations into the wind field is not merely a problem of reconciling the model with observation: In areas where the surface observations are not greatly influenced by local circulations, the deviations of the model from observation would be attributed to short comings in the model as well as the inherent noise component of wind observations especially when short averaging times or no averaging is used. On the other hand, in some areas, the surface wind observations will contain information regarding local circulations and other mesoscale perturbations which are not included in the model; Again this information is corrupted by a noise component. Hence, it would not be correct to accept the surface wind observations as fixed points of reference for adjustment of the modeled wind field.

Cressman (1960), has proposed a technique for incorporating observational data into a field of initial estimates. This technique has gained acceptance and is currently used by the Atmospheric Environment Service of Environment Canada for incorporating surface meteorological data into prognostic model results. The Cressman technique recognizes the uncertainties in a single observation without rejecting consistent departures

of the model results from observation. The success of the method depends on the density of observations and in data sparse areas, the incorporation of surface wind observations into the wind field model may serve to corrupt rather than refine the wind field estimate.

Using the wind field derived in Section 3.4.4 as a starting estimate, deviations of the model result from observation at each observing station are calculated. Simple interpolation to the reporting station from gridded model results is used. Considering a particular grid point, a weighting factor is calculated

$$W = \frac{q^2 - d^2}{q^2 + d^2} \qquad W \geq 0 \qquad (3.4.1)$$

where q is the radius of influence and d is the distance from the observation. The adjustment to be made to the grid point model result is given by

$$C = \frac{\sum_{i}^{N} W_i E_i}{N} \qquad (3.4.2)$$

where E is the deviation at the observing station and N is the number of observations within distance q of the grid point.

By repeatedly correcting the initial wind field estimate using successively smaller values of q , a spectrum of scales of information contained in the observations is incorporated into the wind field. The smallest value of q which is usable is determined by N which should not be less than 3 or 4 depending on the averaging time and reliability of the data. If the density of observations is high, then a great deal of observational information may be incorporated into the wind field model using this technique. If the density is low, then at the best, an averaged regional correction to the modeled wind field will result.

In applying the Cressman technique to the mesoscale wind field, (See Figure 3.15) the surface wind observations must be converted to surface layer averaged winds using the appropriate stability and surface characteristics from Section 3.3.6 . Only the surface layer is adjusted using surface wind observations: The adjustments in other layers is determined with the constraint that the pertubation introduced at the surface vanishes at the top of the ABL .

3.4.6 Rendering the Mesoscale Wind Field Mass Consistent

As an intermediate step, the geostrophic wind field, before the introduction of surface drag and ABL modifications, was adjusted

to satisfy the continuity equation (Figure 3.13). The horizontal divergence of this drag-free flow was determined from the upper-air analysis. With the inclusion of surface drag, topography and surface wind observations, the distribution of divergence in the ABL has been modified; At the top of the boundary layer these divergence perturbations should reduce to zero leaving the residual synoptic scale divergence and vertical motion at the top of the ABL : The computational scheme for achieving this is included in Figure 3.15 .

In Section 3.4.2 , vertical motion for the unperturbed geostrophic flow is determined in using O'Briens technique (Figure 3.13) . The condition to be satisfied in the ABL through the adjustment of wind components, is that the vertical motion at the top of the ABL match that determined in Section 3.4.2 . This is achieved by computing the horizontal wind divergence for each layer in the ABL and then using O'Brien's technique to match the vertical motion at the boundary layer top leaving the surface layer divergence unchanged. The wind components in each layer of the ABL are adjusted to conform to the corrected divergence giving a mass consistent wind field. Finally, the vertical motion at each grid point is computed.

REFERENCES

Agnew, T., 1977: Prediction of Representative Surface Winds in the Beaufort Sea Computerized Support System, Fisheries and Environment Canada, Atmospheric Environment Service.

Agnew, T. and Diehl, L. 1978: Prediction of Representative Surface Winds in the Beaufort Sea Computerized Support System, Presented at the Weather Forecasting and Analysis and Aviation Meteorology Conference, October 16-19, Silver Spring, Md.

Ahlberg, J. H., Nielson, E.N., and Walsh, J.L., 1967: The Theory of Splines and Their Application, Academic Press, New York.

Anderson, G.E., 1971: Mesoscale Influences on Wind Fields, Journal of Applied Meteorology, 10, 377-386.

Anthes, R.A., 1976: Initialization of Mesoscale Models with Real Data, Sixth Conf. Weather Forecasting and Analysis, Amer. Meteor. Soc., 156-160.

Anthes, R.A., and Keyser, D., 1979: Tests of a Fine-Mesh Model Over Europe and the United States, Mon. Wea. Rev., 107, 963-984.

Anthes, R.A., and Warner, T.T., 1978: Development of Hydrodynamic Models Suitable for Air Pollution and Other Mesometeorological Studies, Mon. Wea. Rev., 106, 1045-1078.

Arya, S.P.S., 1975: Geostrophic Drag and Heat Transfer Relations for the Atmospheric Boundary Layer, J.Roy. Met. Soc., 101, 147-161.

Arya, S.P.S., 1978: Comparative Effects of Stability, Baroclinity and the Scale-Height Ratio on Drag Laws for the Atmospheric Boundary Layer, Journal Atmospheric Sciences, 35, 40-46.

Arya, S.P.S., 1981: Parameterizing the Height of the Stable Atmospheric Boundary Layer, Journal Applied Meteorology, 20, 1192-1202.

Bass, A., 1981: Modeling Long-Range Transport and Diffusion, Report Prepared Under A Co-operative Agreement With The Environmental Protection Agency.

Benkovitz, C.M., 1982: Compilation of an Inventory of Anthropogenic Emissions in the United States and Canada, Atmos. Environ. 16, 1551.

Berkowicz, R., and Prahm, L.P., 1982: Sensible Heat Flux Estimated from Routine Meteorological Data by the Resistance Method, National Agency of Environmental Protection Air Poll. Lab. MST LUFT A-56.

Bhumralkar, C.M., Endlich, R.M., Nitz, K., Brodzinski, R., Martinez, J.R., and Johnson,W.B., 1981: Refined Air Pollution Model For Calculating Daily Regional Patterns and Transfrontier Exchanges of Airborne Sulfur in Central and Western Europe, Proc. 12th International Tech. Meeting on Air Pollution Modeling and its Application, NATO-CCMS, California, August 25-28.

Billard, C., Andre, J.C., Du Vachat, R., 1981: On the Similarity Functions A and B as Determined from the 'VOVES' Experiment, Boundary Layer Met., 21, 495-507.

Blackadar, A.K., 1957: Boundary Layer Wind Maxima and their

Significance for the Growth of the Nocturnal Inversion, Bull. Am. Met. Soc. 38, 283-290.

Blackadar, A.K., 1962: The Vertical Distribution of Wind and Turbulent Exchange in a Neutral Atmosphere, J. Geophys. Res., 67, 3095-3101.

Blackadar, A.K., and Tennekes, H., 1968: Asymptotic Similarity in Neutral Barotropic Planetary Boundary Layers, J. Atmos. Sciences, 25, 1015-1020.

Bleck, R., 1975: An Economical Approach to the Use of Wind Data in the Optimum Interpolation of Geo- and Montgomery Potential Fields, Mon. Wea. Rev., 103, 807-816.

Borghi, S., 1981: Atmospheric Circulation on the Regional Scale and Isentropic Trajectories as Support to the Long-Range Transport of Air Pollutants, 11th Int. Techn. Mtg. on Air Pollution Modelling and Its Application, Amsterdam, The Netherlands.

Bornstein, R.D., and Runca, E., 1977: Preliminary Investigations of SO_2 Patterns in Venice, Italy Using Linked PBL and K-Models, Including Removal Processes, in Joint Conference on Applications of Air Pollution Meteorology, AMS, Salt Lake City, Utah.

Bosch, J.C.,1982: Emission Inventories for Acid Rain Studies (unpublished) NADB report, US. EPA .

Briggs, G.A., 1975: Plume Rise Predictions, AMS Workshop on Meteorology and Environmental Assessment, Boston, Mass.

Brost, R.A. and Wyngaard, J.C., 1978: A Model of the Stably Stratified Planetary Boundary Layer, J. Atmospheric Sciences, 35, 1427 .

Brown, R.A., 1970: A Secondary Flow Model for the Planetary Boundary Layer, J. Atmospheric Sciences, 27, 742 .

Brown, R.A., 1974a: Matching Classical Boundary-Layer Solutions Toward a Geostrophic Drag Coefficient Relation, Boundary Layer Met. 7, 489-500 .

Brown, R.A., 1974b: Analytical Methods in Planetary-Layer Modeling, John Wiley, New York, 148 pp.

Brown, R.A., 1981: Modeling the Geostrophic Drag Coefficient for AIDJEX, J. Geophysical Research, 86, 1989-1994 .

Brown, R.A., and Liu, W.T., 1982: An Operational Large-Scale Marine Planetary Boundary Layer Model, J. App. Met., 21, (3), 261 .

Businger, J.A., 1973: Turbulent Transfer in the Atmospheric Surface Layer, Workshop on Micrometeorology, Amer. Met. Soc. 67-100 .

Businger, J.A., and Arya, S.P.S., 1974: Height of the Mixed Layer in the Stably Stratified Planetary Boundary Layer, Advances in Geophysics, 18A, Academic Press, pp. 73-92 .

Businger, J.A., Wyngaard, J.C., Izumi, Y., Bradley, E.F., 1971: Flux-Profile Relationships in the Atmospheric Surface Layer, J. Atmos. Sciences, 28, 181 .

Butson, K.D. and Hatch, W.L., 1975: Selective Guide to Climatic Data Sources, National Climatic Center NOAA .

Carmichael, G.R., and Peters, L.K., 1981: Application of The Sulfur Transport Eulerian Model (STEM) To A SURE Data Set, Proc. 12th International Technical Meeting on Air Pollution

Modeling and its Application, NATO-CCMS, California, August 25-28.

Cats, G.J., 1980: Analysis of Surface Wind and Its Gradient in a Mesoscale Wind Observation Network. Monthly Weather Review, 108, 1100-1107 .

Chang, C.B., Perkey, D.J., Kreitzberg, C.W., 1981: A Numerical Case Study of the Squall Line of 6 May 1975, J. Atmospheric Sciences, 38, 1601 .

Clark, T.L., 1980: Annual Anthropogenic Pollutant Emissions in the United States and Southern Canada East of the Rocky Mountains, Atmos. Environ. 14, 961 .

Clarke, R.H., 1970: Observational Studies in the Atmospheric Boundary Layer, Quart. J. Roy. Met. Soc., 96, 91-114 .

Clarke, R.H., Dyer, A.J., Brook, R.P., Reid, D.G., and Troup, A.J., 1971: The Wangara Experiment: Boundary Layer Data, CSIRO, Div. of Met. Phys. Tech. Paper No. 19 .

Cline, A.K., 1974: Scalar- and Planar- Valued Curve Fitting Using Splines Under Tension, Commun. ACM, 17, 218-220 .

Cressman, G.P., 1960: An Operational Objective Analysis System, Monthly Weather Review, 87, 367 .

Danard, M., 1977: A Simple Model for Mesoscale Effects of Topography on Surface Winds, Monthly Weather Review, 105, 572-581 .

Deardorff, J.W., 1972: Parameterization of the Planetary Boundary Layer for Use in General Circulation Models, Monthly Weather Review, 100, 93 .

Deardorff, J.W., 1974: Three-Dimensional Numerical Study of the Height and Mean Structure of a Heated Planetary Boundary Layer, Boundary-Layer Met., 7, 81-106 .

De Boor, C., 1962: Bicubic Spline Interpolation, J. Math. Phys. 41, 212-218 .

Delage, Y., 1974: A Numerical Study of the Nocturnal Atmospheric Boundary Layer, Quart. J. Roy. Met. Soc., 100, 351-364 .

Dickerson, M.H., 1978: MASCON - A Mass Consistent Atmospheric Flux Model for Regions with Complex Terrain, J. Appl. Meteor., 17, 241-253 .

Ditto, F.H., Gutierrez, L.T., and Bosch Jr., J.C., 1976: Weighted Sensitivity Analysis of Emissions Inventory Data, J.A.P.C.A., 26, 875 .

Draxler, R.R., 1977: A Mesoscale Transport and Diffusion Model, Joint Conf. on Applications of Air Pollution Met., AMS/APCA, Nov. 29 - Dec. 2, Salt Lake City, Utah.

Draxler, R.R., 1979: Modeling The Results of Two Recent Mesoscale Dispersion Experiments, Atmospheric Environment 13, 1523-1533.

Du Vachat, R. and Musson-Genon, L., 1982: Rossby Similarity and Turbulent Formulations, Boundary Layer Met., 23, 47-68 .

Eliassen, A., 1980: A Review of Long-Range Transport Modeling, J. Appl. Met., 19. 231-240.

Endlich, R.M., 1967: An Iterative Method for Altering the Kinematic Properties of Wind Fields, Journal of Applied Meteorology, 6, 837-844 .

EPA, 1976: AEROS Manual Series, Vol 1, EPA-450/2-76/001, US EPA, Research Triangle Park.

Fankhauser, J.C., 1974: The Derivation of Consistent Fields of Wind and Geopotential Height from Mesoscale Rawinsonde Data, J. Appl. Meteor., 13, 637-646 .

Gandin, L.S., 1963: Objective Analysis of Meteorological Fields, Translated from Russian by the Israel Program for Scientific Translations, 1965 .

Geiger, R., 1965: The Climate Near the Ground, Harvard University Press, 611 pp.

Goodin, W.R., McRae, Gregory J., and Seinfeld, John, H., 1979: A Comparison of Interpolation Methods for Sparse Data: Application to Wind and Concentration Fields, J. Applied Met., 18, 762-771 .

Goodin, W.R., McRae, G.J., and Seinfeld, J.H., 1980: An Objective Analysis Technique for Constructing Three-Dimensional Urban-Scale Wind Fields, Journal Applied Meteorology, 19, 98-108 .

Hanna, S.R., 1969: The Thickness of The Planetary Boundary Layer, Atmospheric Environment 3, 519-536 .

Hardy, D.M.,and Walton, J.J., 1978: Principal Components Analysis of Vector Wind Measurements, J. Applied Met., 17, 1153 .

Heald, R.C. and Mahrt, L., 1981: The Dependence of Boundary-Layer Shear on Diurnal Variation of Stability, Journal Applied Meteorology, 20, 859-867 .

Heffter, J.L., 1980: Air Resources Laboratories Atmospheric Transport and Dispersion Model (ARL-ATAD), NOAA Technical

Memorandum ERL ARL-81 .

Henderson, L. and Clare, F., (Eds), 1980: NCAR Graphics Software, Boulder, Colorado.

Henderson-Sellers, A., 1980: A Simple Numerical Simulation of Urban Mixing Depths, Journal Applied Meteorology, 19, 215-218.

Henry, T.J.G., 1973a: Approximations for Boundary-Layer Parameters in Numerical Prediction Models, Paper for Presentation at the Forecast Research Symposium, May 3, AES Headquarters, Downsview.

Henry, T.J.G., 1973b: Estimation of Boundary-Layer Parameters from Free-Atmosphere Predicted Values. Paper for Presentation at the Forecast Research Symposium, May 3, AES Headquarters, Downsview.

Hess, S.L., 1959: Introduction to Theoretical Meteorology, Henry Holt and Company, N.Y.

Hicks, B.B., 1976: Wind Profile Relationships from the 'Wangara' Experiment. Quart. J. Roy. Met. Soc. 102, 535-551.

Hoke, J.E., and Anthes, Richard A., 1976: The Initialization of Numerical Models by a Dynamic-Initialization Technique, Mon. Wea. Rev., 104, 1552-1556 .

Holzworth, G.C., 1964: Estimates of Mean Maximum Mixing Depths in the Contiguous United States, Monthly Weather Review, 92, 235-242.

Hoxit, L.R., 1973: Variability of Planetary Boundary Layer Winds, Atmospheric Science Paper No. 199, Colorado State University, Ft. Collins , Co.

Irwin, J.S., 1979: A Theoretical Variation of the Wind Profile Power Law Exponent as a Function of Surface Roughness and Stability, Atmos. Environ. 13, 191-194.

Jenne, Roy L., 1975: Data Sets for Meteorological Research, NCAR-TN/IA-111, National Centre for Atmospheric Research, Boulder, Colorado.

Kazinski, A.B., and Monin, A.S., 1960: A Turbulent Regime Above the Atmospheric Layer, Izv. Acad. Nauk, USSR, Geophys. Sci. No. 1, 110-112 (English ed.).

Keyser, D., 1978: An Initialization Procedure for Limited-Area Models for Numerical Weather Prediction. Technical Report, Naval Post-Graduate School, Monterey, California.

Klaspisz, C., and Weill, A., 1982: Mean Horizontal Wind in an Inversion-Capped Convective Boundary Layer, J. Applied Met., 21, 648.

Kondo, J., 1975: Air-Sea Bulk Transfer Coefficients in Diabetic Conditions, Boundary Layer Met., 9, 91-112.

Kuchler, A.W., 1970: Potential Natural Vegetation of the Coterminous U S., American Geographical Society, N.Y.

Lamb, R.G., 1981: A Regional Scale (1000 km) Model of Photochemical Air Pollution Part I: Theoretical Formulation, Met. & Ass. Div., Environmental Sciences Research Lab. Research Triangle Park, North Carolina.

Lee, R.J., 1975: Objective Determination of Surface Winds in Data Sparse Areas, Environment Canada, Atmospheric Environment Service, Technical Memorandum Series, TEC-823.

Lee, H.N., Kau, W.S. and Kao, S.K., 1981: A Model for Pollutant Concentration Prediction in Complex Terrain, Proc. 12th International Technical Meeting on Air Pollution Modeling and its Application. NATO-CCMS, California, August 25-28.

Lettau, H.H., 1962: Theoretical Wind Spirals in the Boundary Layer of a Barotropic Atmosphere, Beit. Phys. Atmos., 35, 195-212.

Liu, C.Y. and Goodin, W.R., 1976: An Iterative Algorithm for Objective Wind Field Analysis, Mon. Weat. Rev., 104, 784-792.

Liu, M.K., Yocke, M.A. and McElroy, J.L., 1978: Development and Validation of a Three-Dimensional Wind Model for Air Quality Analysis in Complex Terrain, Proc. 9th Int. Techn. Mtg. on Air Pollution Modeling and Its Application, Aug. 28-31, Toronto, Canada.

Liu, W.T., Katsaros, K.B., and Businger, J.A., 1979: Bulk Parameterization of Air-Sea Exchanges of Heat and Water Vapor Including the Molecular Constraints at the Interface, J. Atmos. Sci., 36, 1722.

Mancuso, R.L., Endlich, R.M., and Ehernberger, L.J., 1981: An Objective Isobaric/Isentropic Technique for Upper Air Analysis, Monthly Weath. Rev., 109, 1326.

Maul, P.R., 1980: Atmospheric Transport of Sulphur Compound Pollutants, Ph.D. Thesis submitted to the University of London.

McLain, D.H., 1974: Two Dimensional Interpolation from Random Data, Comput. J., 19, 178-181.

McNider, R.T., and Pielke, R.A., 1979: Application of the University of Virginia Mesoscale Model to Air Pollutant

Transport, in Fourth Symp. on Turbulence, Diffusion and Air Pollution, Reno, Nevada.

McRae, G.J., Goodin, W.R., and Seinfeld, J.H., 1982: Development of A Second-Generation Mathematical Model for Urban Air Pollution - I. Model Formulation, Atmos. Environ., 16, 679-696.

Monin, A.S. and Yaglom, A.M., 1971: Statistical Fluid Mechanics, Mechanics of Turbulence, Vol. 1, The MIT Press, 769 pp.

Mueller, P.K., et al., 1981: The Sulphate Regional Experiment: Report of Findings, Supplemental Volume, Report ER-1907, Electric Power Research Institute, Palo Alto, Ca.

National Air Pollution Surveillance, 1981: Surveillance Report, EPS 5-AP-81-13, Air Pollution Control Directorate, Environment Canada.

National Cartographic Information Center, 1981: Map Data Catalog, U.S. Dept. of the Interior, Geological Survey.

Nielsen, L.B., Prahm, L.P., Berkowicz, R., and Conradsen, K., 1981: Net Incoming Radiation Estimated from Hourly Global Radiation and/or Cloud Observations, J. Climatology, 1, 255-272.

Nieuwstadt, F.T.M., 1980: A Rate Equation for the Inversion Height in a Nocturnal Boundary Layer, J. Appl. Met., 19, 1445-1447.

Nieuwstadt, F.T.M., 1981: The Steady-State Height and Resistance Laws of the Nocturnal Boundary Layer: Theory Compared with Cabauw Observations, Boundary Layer Met., 20, 3-17.

Nieuwstadt, F.T.M.,and Tennekes, H., 1981: A Rate Equation for

the Nocturnal Boundary-Layer Height, J. Atmos. Sci., 38, 1418.

Nieuwstadt, F.T.M., 1982: Private Communication.

O'Brien, J.J., 1970: Alternative Solutions to the Classical Vertical Velocity Problem, J. Appl. Meteor., 9, 197-203.

Ontario Ministry of Environment, 1981: Air Quality Monitoring Reports 1980.

Pala, S., 1982: Private communication with chief scientist, OCRS.

Pandolfo, J.P. and Jacobs, C.A., 1973: Tests of an Urban Meteorological-Pollutant Model Using CO Validation Data in the Los Angeles Metropolitan Area, Vol. 1, No. R4-73-025A, U.S. EPA Research Triangle Park.

Paulson, C.A., 1970: The Mathematical Representation of Wind Speed and Temperature Profile in the Unstable Atmospheric Surface Layer, J. Appl. Meteor. 9, 857-861.

Peaceman, P.W. and Rachford, H.H., 1959: The Numerical Solution of Parabolic and Elliptic Differential Equations, J. Soc. Ind. and Appl. Math., 3 , 28-41.

Racher, P., Rosset, R., and Caneill, Y., 1980: A Mass Consistent Wind Field Model Over the Mid-Rhine Valley, Proc. 11th Int. Techn. Mtg. on Air Pollution Modeling and its Application, NATO-CCMS, Amsterdam, The Netherlands, Nov. 24-27.

Ropelewski, C., Predoehl, M., and Platto, M., 1980: The Interim Climate Data Inventory, NOAA-EDIS, Washington, D.C.

Rose, M.F., 1973: Objective Analysis of Local Wind Fields, Environment Canada, Atmospheric Environment Service, Techn.

Memo. Series, TEC 793.

Sasaki, Y., 1958: An Objective Analysis Based on the Variational Method, J. Meteor. Soc. of Japan, Ser. 2, 36, 77-88.

Sasaki, Y., 1970a: Some Basic Formalisms in Numerical Variational Analysis, Monthly Weather Review, 98, 875-883.

Sasaki, Y., 1970b: Numerical Variational Analysis Formulated Under the Constraints as Determined by Longwave Equations and a Low-Pass Filter, Monthly Weather Review, 98, 884-899.

Scholtz, M.T. and Brouckaert, C.J., 1978: Modeling of Stable Air Flow Over a Complex Region, J. Appl. Met., 17, 1249-1257.

Shapiro, R., 1973: A High-Order Interpolation Procedure for Use in Fine-Mesh Limited - Area Models, Air Force Cambridge Research Lab., Physical Sciences Research Papers, No. 560, AFCRL-TR-73-0543.

Sheih, C.M., Wesely, M.L., and Hicks, B.B., 1979: Estimated Dry Deposition Velocities of Sulfur over the Eastern United States and Surrounding Regions, Atmos. Env., 13, 1361.

Sherman, C.A., 1978: A Mass-Consistent Model for Wind Fields Over Complex Terrain, J. Appl. Met., 17, 312-319.

Stephens, J.J. and Johnson, K.W., 1978: Rotational and Divergent Wind Potentials, Monthly Weather Review, 106, 1452-1457.

Stolzenbach, K.D., Madsen, O.S., Adams, E.E., Pollack, A.M., and Cooper, C.K., 1977: A Review and Evaluation of Basic Techniques for Predicting the Behavior of Surface Oil Slicks, Marine Assessment Division, National Oceanic and Atmospheric Administration, U.S. Dept. of Commerce.

Sykes, R.J. and Hatton, L., 1976: Computation of Horizontal Trajectories Based on the Surface Geostrophic Wind, Atmos. Environ., 10, 925-934.

Tarbell, T.C., Warner, T.T., and Anthes, R.A., 1981: An Example of the Initialization of the Divergent Wind Component in a Mesoscale Numerical Weather Prediction Model, Mon. Wea. Rev., 109, 78-95.

Tennekes, H., 1973: A Model for the Dynamics of the Inversion Above a Convective Boundary Layer, J. Atmos. Sci., 30, 558-567.

Thorpe, A.J. and Guymer, T.H., 1977: The Nocturnal Jet, Quart. J. Roy. Met. Soc., 103, 633-653.

Tuerpe, D.R., Rodriguez, D.J., Gresho, P.M., and Sani, R.L., 1978: Mass-Consistent Wind Field Modeling: Finite Difference Vis-A-Vis Finite Element, Proc. 9th Int. Techn. Mtg. on Air Pollution Modeling and Its Application, Aug. 28-31, Toronto, Canada.

Voldner, E.C., Shah, Y., and Whelpdale, D.M., 1980: A Preliminary Canadian Emissions Inventory for Sulfur and Nitrogen Oxides, Atmos. Environ., 14, 419.

Van Dop, H., de Haan, B.J., and Cats, G.J., 1981: A Mesoscale Air Pollution Transport Model: Outline and Preliminary Results, Proc. 12th Int. Techn. Mtg. on Air Pollution Modeling and Its Application, NATO-CCMS, California, Aug. 25-28.

Walton, J.J., and Sherman, C.A., 1978: Objective Wind Field Pattern Characterization, Proc. 9th Int. Techn. Mtg. on Air Pollution Modeling and Its Application, Aug. 28-31, Toronto, Canada.

Warner, T.T., 1981: Verification of a Three-Dimensional Transport Model Using Tetroon Data from Project STATE, Atmos. Environ., 15, 2219-2222.

Wetzel, P.J., 1982: Toward Parameterization of the Stable Boundary Layer, J. Appl. Meteor., 21, 7.

Wieringa, J., 1980: Estimation of Mesoscale and Local-scale Roughness for Atmospheric Transport Modeling, 11th Int. Techn. Mtg. on Air Pollution Modeling and Its Application, Amsterdam, The Netherlands.

Wisniewski, J. and Kinsman, J.D., 1982: An Overview of Acid Rain Monitoring Activities in North America, Bulletin American Meteorological Society, 63, 598.

Wojcik, M.A., 1980: Sensitivity of a Regional Air Quality Model to Meteorological Parameters, 2nd Joint Conf. on Applications of Air Pollution Meteorology, American Meteorological Society, Air Pollution Control Association, Mar 24-27, New Orleans, La.

Wong, T.S., 1975: Ontario Pollutant Inventory Information, Air Resources Branch, OME.

Wyngaard, J.C., Arya, S.P.S., and Cote, O.R., 1974: Some Aspects of the Structure of Convective Planetary Boundary Layers, J. Atmos. Sci., 31, 747.

Yamada, T., 1976: On the Similarity Functions A, B and C of the Planetary Boundary Layer, J. Atmos. Sci., 33, 781-793.

Zilitinkevich, S.S., 1972: On the Determination of the Height of the Ekman Boundary Layer, Bound. Layer Meteor., 3, 144-145.

Zilitinkevich, S.S., 1975: Resistance Laws and Prediction

Equations for the Depth of the Planetary Boundary Layer, J. Atmos. Sci., 32, 742.